NISTIR 4723

Evaporator Performance Investigation for Residential Air-Conditioning Application Using Mixed Refrigerants

Maciej Chwalowski

United States Department of Commerce
National Institute of Standards and Technology

NISTIR 4723

Evaporator Performance Investigation for Residential Air-Conditioning Application Using Mixed Refrigerants

Maciej Chwalowski

November 1991

U.S. Department of Commerce
Robert A. Mosbacher, Secretary
National Institute of Standards and Technology
John W. Lyons, *Director*
Building and Fire Research Laboratory
Gaithersburg, MD 20899

EPRI *Leadership in Science and Technology*
Electric Power Research Institute

Prepared for:
Electric Power Research Institute
Dr. Powell Joyner, Project Manager
Exploratory Research Program
Nuclear Power Division
Office of Exploratory Research
Palo Alto, CA 94303

ABSTRACT

The design of the heat exchanger utilizing nonazeotropic refrigerant in an air conditioning application presents unique problems due to the phase change of the moist air and the variable specific heat of the evaporating refrigerant mixture. This study discusses the performance analysis and the design procedure of a cross counterflow heat exchanger working as an evaporator in an experimental system which simulated a residential air conditioning application.

The design of the heat exchanger, used for the experimental testing, consisted of several depth rows. Separated banks permitted the determination of the sensible and the latent heat loads for each bank and the heat profiles across the heat exchanger. The interaction between the refrigerant mixture and the moist air was quantified by determining the temperature profiles of both media and the moisture removal rate. The overall heat transfer coefficient for each bank of the heat exchanger was determined from the measured quantities. The effect of the change of the mixture composition on heat exchanger performance was evaluated.

The focus of the theoretical study was the development of the effectiveness/NTU (ϵ/NTU) relationships with the use of the experimentally derived quantities for moist air flowing across the heat exchanger. For moist air, the variable mixture specific heat, air and heat profiles obtained from the experimental results were utilized to obtain the expression for ϵ/NTU. The derived ϵ/NTU relations were verified and found to be in good agreement

with dry and moist air test results.

This study resulted an understanding of an application of a refrigerant mixture working fluid in an evaporator and provided tools to design such a heat exchanger.

CONTENTS

ILLUSTRATIONS

TABLES

NOMENCLATURE

English

a	tube wall thickness (m)
A	heat transfer area (m^2) or air heat profile coefficient
B	air temperature profile coefficient
C	composition (-) or flow stream capacity rate (kJ/s-K)
c_p	specific heat at constant pressure (kJ/kg K)
D	tube diameter (m)
E	error (-)
f	friction factor (-)
G	mass flux (kg/m^2 s)
g	acceleration due to gravity (m/s^2)
h	heat transfer coefficient (W/m^2K)
h_{fg}	latent heat of vaporization (kJ/kg)
i	enthalpy (kJ/kg) or (kJ/kmol)
K	pressure loss coefficient (-)
k	thermal conductivity (W/m^2-K)
L	tube length (m)
l	fin length from root to center (m)
M	mass flow rate of air (kg/s)
m	mass flow rate of refrigerant (kg/s) or fin effectiveness parameter (-)
NTU	number of transfer units (-)
P	power (kW)
p	pressure (kPa)
Pr	Prandtl number (-)

Q	heat (W)
q	heat flux (W/m^2)
R	gas constant (J/kg-K)
Re	Reynolds number (-)
St	Stanton number (-)
T	temperature (K or °C)
ΔT	temperature difference (K)
t	fin thickness (m)
U	heat transfer coefficient (W/m^2-K)
V	volume (m^3) or volumetric flow of air (m^3/s)
v	specific volume of moist air (m^3/kg)
W	humidity ratio (-)
X	liquid composition based on a mole (-)
X_M	liquid composition based on mass (-)
x	quality (-)
y	fin height (m)
Z	normalized enthalpy (-)
z	local conditions (-) or distance between adjacent fins (m)

Greek

α	ratio of total transfer area on one side of the exchanger to total volume of the exchanger (-)
δ	fin thickness (-)
ϵ	exchanger effectiveness (-)
η_f	fin temperature effectiveness (-)
η_o	total surface temperature effectiveness (-)
μ	viscosity coefficient

σ standard deviation (-) or ratio of free flow area to total area

Subscripts

a air

ar air to refrigerant

af air to fin

b bank

c entrance

e exit

eq equilibrium

fr fin to refrigerant

f fluid or fin

g glide

i inside

l latent or liquid

m mean

max maximum

min minimum

o outside or overall

p constant pressure

r refrigerant

s sensible

sat saturation

sup superheat

t total, temperature or tube

v vapor

w water or wall

ACKNOWLEDGEMENTS

This work, though being conducted at the National Institute of Standards and Technology, did also serve as my doctoral dissertation in the Mechanical Engineering Department of the Catholic University of America with Dr. David Didion serving as major professor. The author feels indebted to all members of the Thermal Machinery Group at NIST in Gaithersburg, MD for helping with many questions associated with bringing this study to completion. Special gratitude is extended to Drs. Didion, Domanski, and Kedzierski who provided guidance, offered insights, and gave helpful advice to make this report as best as possible. Sharon Smith was very helpful in explaining the intricacies of the WordPerfect. David Ward answered many questions concerning equipment and provided desired environmental conditions in chambers to run tests. The author also wishes to thank the Electric Power and Research Institute for sponsoring this project, with Dr. Powell Joyner as Project Manager.

Section 1

INTRODUCTION

BACKGROUND

During the past few decades there has been a research interest in the use of nonazeotropic binary mixtures as working fluids for refrigeration systems. There has been two main factors which gave the impetus to this research.

The first one dates back to the early 70's and the energy crisis which made the energy conservation one of the major concerns. A device which can make a significant contribution to the energy conservation is the heat pump. By raising low grade heat to a more useful heat, new sources of higher grade heat become available, for example, ambient air and waste heat which previously were considered unsuitable for recovery because of their relatively low temperature. The heat pump, therefore, can vastly increase the potential use of low grade energy.

As the heat pump technology improved, the demands on providing the adequate environmental conditions irrespective of the outdoor temperatures increased as well. This is where the heat pump technology could not fully satisfy this demand. A problem experienced with a heat pump operating according to a conventional vapor compression cycle is a loss of capacity at low evaporator temperatures. As a result, at near freezing temperatures, an electric heater has to be operated to meet the demand, thus lowering the heat pump seasonal efficiency. If a heat pump is sized to satisfy the load at the lowest outdoor design temperature (for the largest expected load), the efficiency of

the system during part-load operation will be low due to increased equipment cycling. A variable capacity system could provide capacity modulation during part-load operation, thus maintaining an improved efficiency over the entire operating range. The use of nonazeotropic refrigerant mixtures may allow for attaining capacity modulation.

The second reason for research into refrigerant mixtures occurred due to the increased concern over the presumed destructive influence of some refrigerants on the ozone layer. Those refrigerants, which are fully halogenated and which are eventually released into the atmosphere, decompose and their chlorine elements react with the ozone, contributing to its depletion.

Presently, it does not appear likely that new single component refrigerants can be developed, because of the limited number of elements available for combination to produce volatile, nonflammable, nonpoisonous, chemically stable compounds. Consequently, any improvement in refrigerant performance in the future is expected to result from the application of mixtures of known refrigerants. These nonazeotropic mixtures appear very promising, because elementary theoretical considerations suggest that considerable improvement should be realized. Among many advantages claimed for nonazeotropic mixtures in refrigeration systems are improved thermodynamic efficiency, ability for a refrigerant composition shift which alters the capacity of the working fluid to match load requirements, and lower pressure ratio across the compressor.

Previous work has shown, that a simple substitution of a mixture into a residential heat pump (with air-to-refrigerant heat exchangers) that was

designed for single component refrigerants, yields only minimal performance increases. For example, Mulroy et. al. [1] showed that, the capacity increase in the heating mode was 2 to 3 percent for heat pumps running with R13B1 and R152a over pure R22, while there was no improvement in the cooling mode. Similarly, Cooper et. al. [2] obtained 8 percent improvement for the same mixture in the heating mode and no improvement in the cooling mode. In tests involving a mixture of propane and butane over pure butane, Haselden et. al. [3] showed the improvement of 7 percent. For water-to-water heat pumps, the COP improved by 2 to 6 percent. For all experimental results examined, where mixtures were used, the improvement was only 0 percent to 11 percent for either the heating or the cooling mode, while theoretical considerations suggested an improvement of between 35% to 50%.

These results indicate, that system modifications are necessary when utilizing nonazeotropic mixtures. The earliest system modifications included placing a distillation column in the cycle to extract one of the mixture components at one point of the cycle and to add at another point. A variation of this method was to extract the high boiler refrigerant at low evaporator temperature to modulate the capacity. Another modification was to allow refrigerant coming out of the condenser to flow through the internal heat exchanger in the evaporator to lower the pressure differential across the compressor. These modifications, while technically feasible, add complexity to a system and decrease its reliability. The most promising and the simplest modification to a heat pump utilizing mixtures appears to be a counterflow heat exchanger. Mixtures, for reasons explained in [4], exhibit lower heat transfer coefficient and a counterflow heat exchanger enhances the heat transfer process.

The study by Kauffeld [5], of an experimental heat pump with counterflow water-to-refrigerant mixture heat exchangers demonstrated an increase in the coefficient of performance (COP) of up to 32% for an optimized mixed refrigerants as compared to the performance with pure R22. Such a significant increase in performance may be attributed to a favorable composition of the refrigerants, low temperature lift of the working fluid and counterflow heat exchangers. However, to apply such a system as a residential heat pump, poses a serious problem. If a refrigerant-to-water and a water-to-air heat exchangers are used in one system, then double inefficiency may render such system less attractive than a conventional heat pump. On the other hand, air-to-refrigerant counterflow heat exchangers may be cumbersome and difficult to apply in a residential heat pump because of limited space and aesthetic considerations. Therefore, an effort has to be made to design a counterflow air-to-refrigerant heat exchanger which will be practical and which will utilize the potential offered by mixtures.

THERMODYNAMIC PROPERTIES OF BINARY MIXTURES

In this study a reference to "binary mixture" describes a solution of two substances, each of which can be present in two phases, one liquid and the other gaseous. An illustration of such a solution is given in Fig. 1.1 where a two-phase, two component mixture is in equilibrium at constant temperature and pressure. Both components A and B are present in the liquid phase as a mixture, whose composition is dependent upon the thermodynamic state of the system. Similarly, the vapor phase contains both A and B in a gaseous state. Ideally, when two fluids are combined in a binary solution, the fluid

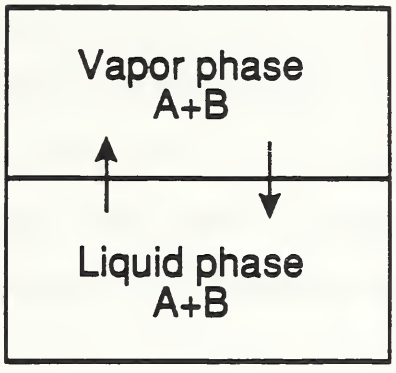

Figure 1.1 A binary mixture system in equilibrium.

properties will show a proportional relationship with the concentration of the mixture. The vapor pressure of each component in a liquid solution, for instance, called the partial pressure, is proportional to the mixture concentration for an ideal mixture (Raoult's law). At low pressures, the pressure of a mixture of gases is equal to the sum of the partial pressures of the constituents for an ideal mixture (Dalton's law). In general, however, the composition of the vapor in equilibrium with the liquid will be richer in the more volatile component than will the composition in the liquid phase. Exceptions are the two end points, representing the pure liquids, and certain other points in special cases. Depending on this different behavior, mixtures are called either azeotropic or nonazeotropic, respectively. For azeotropic mixtures, the deviation from Raoult's law becomes very large (because of polarity differences), causing the total vapor pressure curve to pass through a maximum or minimum. According to the theorem of Gibbs-Konovalov, the equilibrium vapor evolved by this liquid must have the same

composition as the liquid; that is, the curves of liquid and vapor composition must touch tangentially at the concentration of maximum or minimum pressure. This concentration is defined to be the azeotropic composition. The azeotropic composition is slightly temperature dependent (azeotropic stems from Greek, meaning no change in temperature during phase change).

The azeotropic point is a function of pressure such, that it moves toward less volatile one as pressure increases. At the azeotrope, the compositions of the liquid and the vapor phases are identical. To the left side of the azeotrope, the composition of the more volatile refrigerant in the vapor phase is greater than that of the liquid phase, which is similar to the characteristics of the nonazeotropic mixture. The reverse is true to the right side. The azeotrope behaves like a single component fluid, since the compositions in both phases are the same. Except for the azeotropic point, an evaporative process would exhibit a temperature glide, as it would for a nonazeotropic mixture. These azeotropic mixtures are, by far, less likely to be found and exist only under specific temperature and pressure conditions. This study is concerned only with nonazeotropic mixtures.

Mixture that do not form an azeotrope at any concentration, i.e., mixtures whose total pressure curve does not pass through an extreme value, are defined as nonazeotropic mixtures. In such instances, the composition of the two phases differs across the entire concentration range. A specification of the thermodynamic properties of a system, determines the compositions of the two phases. Gibbs phase rule, equation (1.1), determines the number of thermodynamic properties which must be specified to fix the equilibrium

thermodynamic state.

$$P + V = C + 2 \tag{1.1}$$

where P, V, and C are the number of phases present, the number of intensive thermodynamic properties, and the number of components present, respectively.

For the system given in Fig. 1.1 (P=2 and C=2), two intensive properties such as temperature and pressure are sufficient to fix the equilibrium state and thus the compositions of the two phases. The component with the higher vapor pressure (or lower boiling temperature at a given pressure) is more volatile and hence has a larger mole fraction in the vapor phase than the less volatile component. In this study, the mass fraction of the more volatile component is used as composition determinant unless otherwise specified.

Phase equilibrium diagrams are often used to visualize the relationship between the equilibrium temperature, pressure, and the compositions in the two-phase region. From these diagrams it is also convenient to describe the evaporative or condensing process of a binary mixture. Fig. 1.2 depicts the phase equilibrium diagram at constant pressure for an azeotropic R12/R152a mixture and Fig. 1.3 for a nonazeotropic R22/R114 mixture. Mole fractions of the more volatile component in the liquid and vapor phases are plotted on the horizontal axis. The vertical axis displays thermodynamic equilibrium temperature (i.e. saturation temperature). The extreme end points represent the boiling temperatures of the pure components. The bubble and dew lines divide the diagram into three regions. The bubble line represents the

saturated liquid line below which the liquid is subcooled. The dew line represents the saturated vapor line above which the vapor is superheated. Between the lines is the liquid-vapor region, where a mixture exists in two phases.

When a binary nonazeotropic mixture undergoes evaporation, the compositions of the two phases are different for a given overall composition. This can be illustrated by describing the evaporative process of a R22/R114 mixture in Fig. 1.3. For a given overall composition, C_o, a liquid phase alone exists with a composition of C_o at state 1. State 2 is on the saturated liquid line and has a liquid phase composition of C_o in equilibrium with a vapor of composition C_{v2}. As the evaporation process continues to state 3, the composition shifts to C_{l3} for the liquid phase and C_{v3} for the vapor phase. Reaching the saturated vapor line at state 4 gives a liquid composition of C_{l4} and vapor composition of C_o. Further heating evaporates all the liquid so that at state 5 a superheated vapor alone exists with a composition of C_o. There are several observations to consider from this diagram during the evaporation of a nonazeotropic mixture. As quality is increased, the liquid phase becomes richer in the less volatile component, while the vapor phase is richer in the more volatile component. This is expected intuitively, since the more volatile component is above its normal boiling point, while the reverse is true for the less volatile component in the two-phase region. In addition, the evaporation process at a constant pressure does not occur at a constant temperature but rather over the range of temperatures, referred to as the gliding temperature effect represented as D_{tg} in Fig. 1.3. For a fixed overall composition, as quality increases, so does the equilibrium

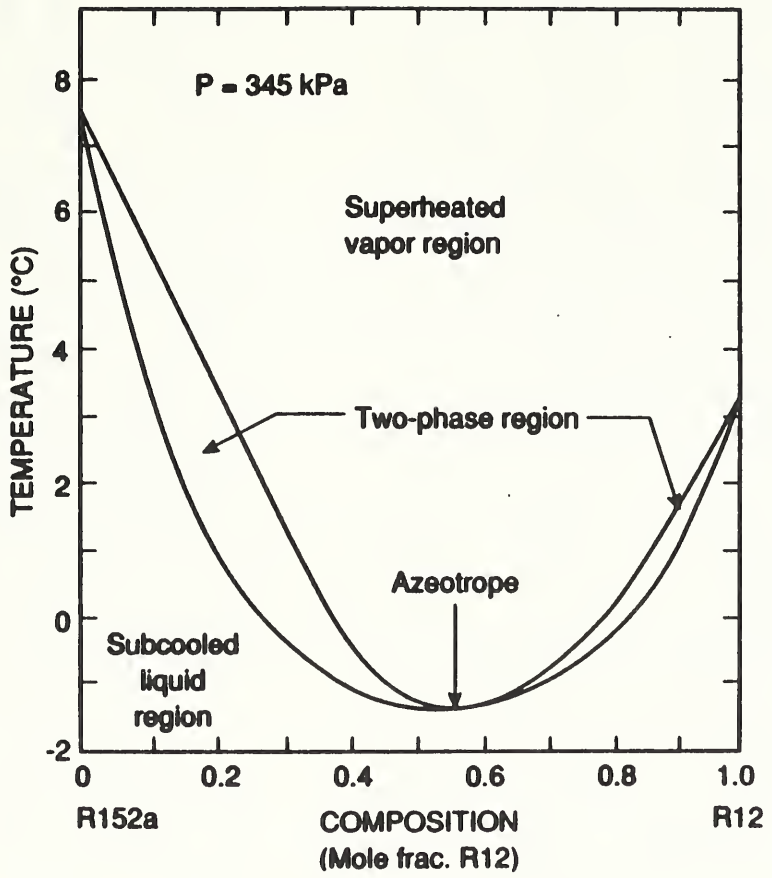

Figure 1.2 Temperature - composition diagram for azeotropic R12/R152a mixture.

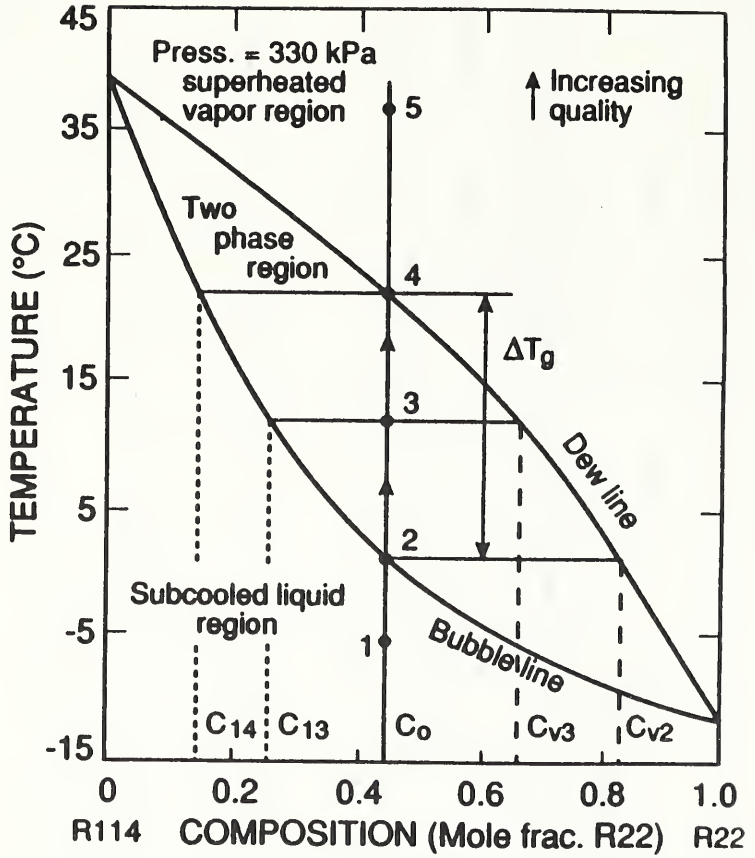

Figure 1.3 Temperature - composition diagram for nonazeotropic R22/R114 mixture.

temperature, T_{eq}.

Carnot versus Lorenz Cycle

A consequence of the nonazeotropic mixture behavior described above, is that there exists a two-phase region over a temperature range, instead of a single temperature as is the case for pure refrigerants. This feature allows the nonazeotropic mixture, flowing in counterflow with the heat exchange fluid, to approach the same temperature glide as is present in the heat sink and heat source of air conditioners, thus allowing a more uniform temperature difference between the refrigerant and the heat exchange fluid, which reduces thermal irreversibility.

A refrigeration cycle with changing temperatures of the refrigerant in the heat exchanger operates according to the Lorentz cycle. This cycle consists of two isentropes (s=const.) and two polytropes (pv^n=const), which is a rather general cycle, since the polytropes can be any of the several processes depending on the polytropic exponent n. The polytropic exponent could be for example equal to 1 (n=1), in which case the polytropes are isotherms. Therefore, the Carnot cycle would be just a special case of the Lorentz cycle.

The Carnot cycle with constant refrigerant temperatures in the heat exchangers is found for single component refrigerants. The Carnot principle, stating that the Carnot cycle efficiency can not be exceeded is limited to applications of constant temperature heat sinks and heat sources. An improvement in system efficiency for an air conditioner can be obtained by following a

cycle, which approaches the Lorenz cycle with changing temperatures of the refrigerant. The reason for this improvement can be found in the nature of the heat sink and the heat source. Since the heat exchange fluids are not changing phase while travelling through the heat exchanger, they have to change temperature in order to change their enthalpy. This means that a temperature glide will always exist at the heat source and the heat sink side.

In the Carnot cycle the temperatures of the refrigerant remain the same throughout the heat exchanger. As can be seen on the T-s diagram this mismatch in temperature requires an additional unnecessary work for the Carnot cycle (shaded area in Fig. 1.4). The amount of work which has to be supplied can be reduced by matching the temperature profiles of the refrigerant with those of the heat exchange fluids. Superimposing the two cycles shows the amount of work which can be saved, assuming an infinite heat exchanger. The work equal to the areas A and B in Fig. 1.4 is not required by the heat exchange fluids, but has to be supplied for the Carnot cycle. This work can be saved if the refrigerant follows a similar temperature glide as the heat sink and heat source, which results in improvement of system performance. Another way of looking at both cycles is to compare the temperature lift between evaporator and condenser. In the Carnot cycle, lift is determined between constant condenser and evaporator temperatures, while in the Lorentz cycle it is between the mid-points of both temperature profiles. Since in the Lorentz cycle, temperature in evaporator increases and in condenser decreases, then the temperature lift would be lower thus resulting in lower compressor work and higher coefficient of performance.

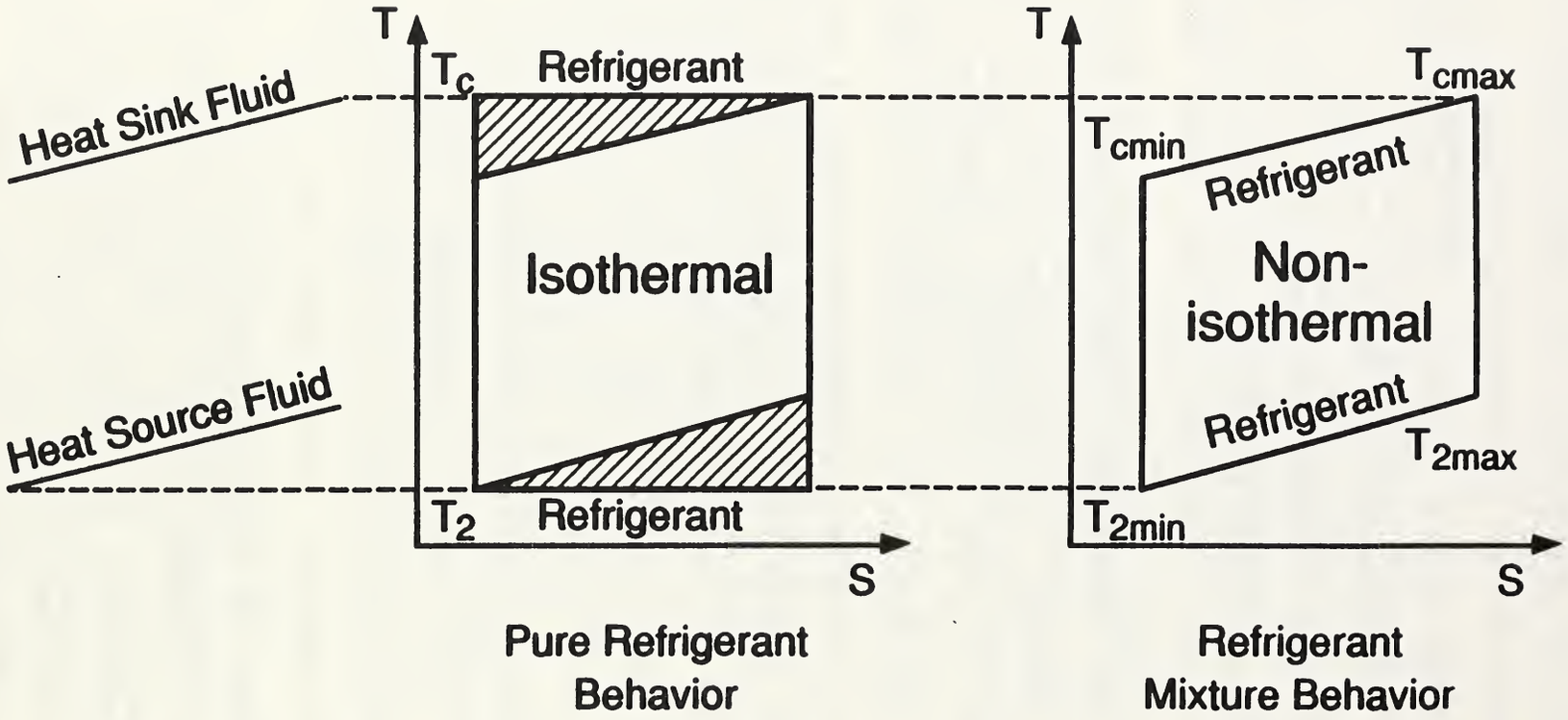

Figure 1.4 Comparison of isothermal and nonisothermal cycles.

Due to the idealities included in the Carnot and the Lorentz cycles, both of them are referred to in Fig. 1.4 as isothermal and nonisothermal, respectively.

LITERATURE SURVEY ON REFRIGERANT MIXTURES PROPERTIES AND APPLICATION

In this chapter an overview of the most important work in the area of nonazeotropic mixtures was presented. Both theoretical and experimental investigations were discussed. A short description of the contributions was presented in the chronological order whenever possible.

Pictet [6] is generally credited with the idea of using a mixture of refrigerants, instead of a single refrigerant, in a vapor compression cycle. He proposed a compression process, in which both sulphur and carbon dioxide were mixed in even molar quantities. Later on he proposed a mixture consisting of 3 percent of carbon dioxide and 97 percent of sulphur dioxide by weight. This mixture was called "liquid Pictet." He presumed that this mixture would possess beneficial thermodynamic properties. In comparison to a system using pure sulphur dioxide, he expected, on the basis of the same load, a smaller compressor displacement volume, a decrease in the pressure ratio and therefore reduced energy requirement. These theoretical estimations did not translate into practical results. Experiments by Blumcke [7] did not show the expected improvements.

It appears that Maiuri [8] was the first to realize, that nonazeotropic mixtures with their gliding temperatures, were well applicable for refrigeration systems. In 1939 he devised and built a system, which consisted of cascades which used a mixture of methane and ethane. However, this system was not

successful.

In 1946, Ruhemann [9] also suggested the application of nonazeotropic mixtures in order to provide the gliding temperature during the phase change. He divided the evaporation and the condensation process into two regions in order to better realize the temperature change. But, again, the practical results were disappointing.

The first detailed thermodynamic analysis of the refrigeration cycle using nonazeotropic mixtures was performed by Carr [10] in 1949. He considered the application of mixtures in an air-conditioning apparatus highly unsuitable. His study was concentrated on the heat exchange process in an evaporator. He conducted experiments with a ternary mixture consisting of the following hydrocarbons: ethane, propane and butane. By the theoretical comparison of the performance of this ternary mixture with that of a pure ammonia operating at the same conditions, he was able to show a 30% to 50% power savings for the mixture.

Haselden [3] made the determination, in 1952, of the theoretical energy savings to be up to 50% for an industrial application employing nonazeotropic mixtures used for cooling brine. In 1958 he undertook an experimental effort with Klimek [11], to validate his theoretical calculations. They conducted their investigations with a propane and n-butane mixture, since at that time, the knowledge of the thermodynamic properties of chlorofluorocarbons was very limited. With a mixture of 30% propane they achieved a seven percent energy savings over pure butane. This poorer than predicted

performance was apparently due to a lower heat transfer coefficient of mixtures. In their work, they focused on the optimization of the heat transfer process and the establishment of the desired temperature glide. In a further paper, Klimek [12] again pointed out the advantage of using nonazeotropic mixtures. However, he also elaborated on reasons for losses in the process.

A study, with favorable results, conducted on the use of nonazeotropic refrigerant mixtures in vapor compression systems was one by Schwind [13]. He suggested the use of nonazeotropic mixtures in refrigeration systems, which have constant compressor displacement, in an effort to achieve capacity modulation. The reason for a capacity modulation is as follows. Refrigerant R22, which is universally used in heat pumps, provides the best overall performance for a residential application. However, a residential application imposes a rather large range of air outdoor temperatures. There are other refrigerants whose performance is better than R22 over specific portions of this range. For example, a more volatile refrigerant at low evaporation temperature may have a higher efficiency and capacity than R22, but also excessive head pressure in the cooling mode. Removal and replacement of R22 at the change of the seasons is not practical, so Schwind suggested replacement of R22 with a binary refrigerant mixture cycle, where distillation is carried out continuously, providing the optimum performance at the particular evaporator temperature. Complexity of system prevented its commercial use.

McHarness and Chapman [14] discuss experimental studies on refrigerant mixtures. The need for experimental work came about for a lack of information

about components of the air conditioning systems. Their work evolved around providing capacity information and operating data for mixtures and comparing them with similar data for pure refrigerants. The test stand used in the study contained the basic components found in any refrigerating unit. The measurements were done at typical operating conditions of refrigerating applications. The refrigerants examined were R12, R13B1, R22, R115, R500. The tests provided detailed information about the behavior of the system. The use of mixture was found to be feasible, practical and beneficial regarding, for example, the capability for varying the capacity of the system. They showed that through the application of the nonazeotropic mixtures a continuous capacity change was possible. It was recognized that the application of mixtures would provide greater flexibility in hardware design. However, the possibility of energy savings through the gliding temperature in the heat exchangers was not noticed. It was recognized that the application of mixtures would necessitate greater flexibility in hardware design.

Burr and Haselden [15] theoretically determined that mixtures used in an air-conditioning system would provide a 20% to 30% reduction in total cost compared to pure R12. They conducted a complete study designated to optimize the energy cost and a capital investment (larger heat exchanger for mixture application). As a mixture they utilized R22/R21.

In 1977, Jakobs et. al. [16] postulated that, because nonazeotropic refrigerant mixtures possess favorable qualities regarding energy economy, capacity control and bridging together wide temperature ranges, they provide considerable

advantages for heat pump applications. A refrigerant mixture boils and condenses over temperature range, which enable the vapor compression cycle to resemble the Lorenz cycle, which, theoretically, offers a 40% energy savings over a cycle which approaches a Carnot cycle. A choice of mixture concentration for a particular application and operating conditions as well as the capacity control problems were discussed. The testing rig, a modified heat pump, was used to demonstrate the practical aspects of the application of refrigerant mixtures. The preliminary experimental results showed significant energy savings and capacity modulation capability for application of mixtures in heat pumps.

In 1979, Rojey et. al. [17] conducted an experimental comparison between the mixture R22/R11 and pure R12 in a heat pump testing rig consisting of a number of internal heat exchangers. The test conditions of water cooling were from 45°C to 15°C and water heating from 25°C to 55°C and did not correspond to typical working conditions of a heat pump. As a result, a 50% improvement in COP for mixture against a pure refrigerant could not be taken at a face value.

Cooper and Borchardt [2] conducted a study in 1979, that considered a compromise between a system suggested by Schwind [13] and a conventional R22 system. They proposed to place a one stage distillation column in a low side accumulator between evaporator and condenser during heating operation for the following reasons. If a nonazeotropic mixture of refrigerants is utilized in such a system, the vapor in the accumulator will be richer in the more volatile component, than the original charge composition. If the more volatile component has a high vapor density, the enrichment of the

circulating mixture in the more volatile component increases the compressor capacity at low outdoor temperatures. Refrigerants first chosen for this study were R22 and R13B1. An increase in efficiency and COP occurred at low evaporator temperatures due to higher vapor density of the more volatile R13B1 when compared to R22. At higher evaporator temperatures, however, the mixture of R22 and R13B1 had a poorer COP than that exhibited by pure R22. This reduction in COP was due to the fact, that R13B1 has a lower COP than R22. This led to the replacement of R22 component with refrigerant R152a and this mixture was nearer in performance to R22 during cooling or high temperature heating operation, than that of the R13B1/R22 mixture.

Investigations by Stokar and Trepp [18] into heat pumps with solution circuit and Radermacher [19] into heat pump cycles with absorber/desorber heat exchangers were typical of many, which occurred during the 1980's. The heat pump with solution circuits offer a relatively easy capacity modulation capability by a large factor by adjusting the composition of the mixture. The approximation of the Lorenz process allowed for a substantially higher COP values and lower pressure ratio.

In 1985, Schultz [20] presented a theoretical background on the different types of binary solutions. He discussed the molecular properties of mixtures and molecular interactions to explain mixture's behavior and departure from Raoult's law. It occurs, when the molecules of one component affect the forces existing between the molecules of the other component. If the molecules of the two components attract one another strongly, the partial pressure of each component and the total pressure will be less, than that

calculated from Raoult's law. Mixtures of components can have various characteristics to produce various results: reduction in the head pressure, change in capacity and the COP, different pressure levels in evaporator and condenser. It is pointed out that, an incremental increase in capacity may be accomplished by adding denser or higher latent heat component, with few or minimal changes in hardware and cost. Nonazeotropic mixtures, i.e., mixtures whose total pressure curve does not pass through an extreme value, provide a potential for capacity improvement, if properly utilized in a heat pump. Implementation of various hardware additions is discussed to enhance the benefits of mixtures. A review of possible reasons for the disagreement between the predicted and the experimentally observed performance was conducted.

Similar in content was a paper by Atwood [21], who discussed the potential benefits of two-fluid mixtures. He underscored the different operating characteristics of mixtures compared to pure refrigerants i.e., liquid and vapor phases are different during phase change and process of evaporation and condensation occurring over the temperature range. The extent to which vapor phase and liquid phase compositions may differ, can be determined from the equation of state routines. It is stipulated that, the above mixture characteristics may be considered liabilities in a conventional cycle, while it may be possible to design system to beneficially exploit these characteristics to accomplish energy savings. Cycle enhancement benefits of mixtures stem from the minimalization of the penalties of heat transfer. The amount of energy saved varies from one application to another and depends on the combined temperature profiles of the heat sink and the heat source. While

COP improvement is a primary incentive for considering cycle enhancement, it is also possible to look at this benefit as an increased temperature lift with no deterioration of COP. The practical feasibility of mixture applications is limited by a number of factors including: the characteristics of the operating cycle, the specialized hardware requirements, the fluid requirements and the servicing aspects. These are discussed in detail including the general requirements of any refrigerant to use on a commercial basis.

Weber [22] conducted a theoretical study of the refrigerant mixture and its influence on a heat pump performance. The study was conducted over the full temperature range of operation in both heating and cooling modes for a system charged with a binary mixture composed of R13B1 and R152a. A computer model, using an equation of state capable of predicting both liquid and vapor properties, was used to simulate heat pump operation with the refrigerant mixture. From this model simulation, results were used to discuss possible benefits resulting from replacing conventional refrigerants with such a mixture. Consideration of equipment design changes to enhance the desired benefits was emphasized. Furthermore, potential benefits of a composition shift were evaluated by assessing seasonal operating cost based on temperature bin analysis. The focus of this study was on the use of non-azeotropic mixtures as a mean of attaining capacity modulation.

Merriam, et.al. [23] explored the potential performance benefits from the use of nonazeotropic refrigerant mixtures in air-to-air heat pumps. Basic concepts for exploiting particular features of nonazeotropic fluids and variety of cycle arrangements were defined. A characterization of seventy

one pure refrigerants provided a basis for selecting thirteen refrigerants, which could be combined into mixtures. Performance evaluations were made for a cycle using pure R22 and mixed refrigerants. Systems had optional components like counterflow heat exchangers, distillation configurations, internal heat exchanger and variable capacity compressors. Two advanced air-to-air heat pump cycle concepts were selected for a detailed analysis. Each cycle contained two accumulators for component separation and employed two different methods for achieving liquid subcooling. The results of this study showed, that no mixture offered any significant benefits. Heating and cooling capacities were tightly correlated with evaporator pressure level. The authors recommended the use of counterflow heat exchangers with minimum added complexity and a development of high efficiency liquid subcooling interchangers.

Mulroy et.al. [1], conducted an experimental study of a relatively unmodified residential heat pump designated for R22 and charged with a binary mixture of R13B1 and R152a. Results were presented for various sizes of fixed expansion devices. This experimental investigation confirmed that flash distillation within the accumulator would improve low temperature heating performance. There was marginal or even worse performance of mixtures compared to R22, except for low temperature heating capacity, which increased by 14% compared to R22. Various system modifications for further performance enhancement were suggested.

Kauffeld et.al. [5], conducted an experimental study of a water-to-water, breadboard heat pump apparatus which could be easily reconfigured to compare

the performance of pure R22 to the mixtures R22/R114 and R13/R12. Three evaporator configurations were extensively studied. In addition, refrigerant from the condenser was routed through the evaporator internal heat exchanger before it was expanded in the expansion device. The purpose of this hardware alteration was to increase the evaporator pressure and to reduce the pressure ratio across the compressor. The tests with the internal heat exchanger were performed for the best channel flow configuration of the evaporator. In all cases the best mixture outperformed R22. The best COP with R22/R114 was 32% higher and with R13/R12 was 16% higher, than the best COP measured with pure R22. An important observation made, was that mixtures exhibit nonlinearity of enthalpy versus temperature in the two phase region, which may have significant impact on both heat exchanger and cycle performance. Large heat exchangers, used in the experimental heat pump, mitigated the impact of the lower heat transfer coefficient of mixture (compared to pure R22) on system performance.

Granryd et. al. [24], developed a theoretical analysis of the thermal performance of a heat exchanger which uses nonazeotropic refrigerant mixtures. Equation of state routines were applied to determine the properties of the mixture flowing through the heat exchanger. The length of the heat exchanger was divided into n-discrete points, at which the properties were determined. The specific heat was found in the intervals between these points and then represented in terms of a linear or a quadratic function. Several examples were given to show that the specific heat of a mixture evaporating in an evaporator is not a constant. A counterflow heat exchanger, linear temperature and heat profiles were assumed in the development of the

Number of Heat Transfer Units equation. The parameters in this equation were effectiveness, air and refrigerant temperature change across a heat exchanger. Due to a complicated nature of this equation, it was evaluated numerically and effectiveness graphs are presented for cases of varying change in the specific heat of a mixture and varying air and refrigerant temperature glide ratio.

OBJECTIVE AND SCOPE OF THIS STUDY

This study was a continuation of the work on the application of the refrigerant mixtures in the air conditioning equipment. The primary objective of this study was to develop the procedure to design an air-to-refrigerant mixture heat exchanger and to optimize it with regard to its size.

Kauffeld [5], has demonstrated that a modified, specially designed heat pump to utilize the benefits of mixtures showed a 32% COP improvement over pure R22. The most significant feature of this heat pump was a counterflow heat exchanger, which was necessary for performance improvement.

The challenge in this project was to design an air-to-refrigerant mixture evaporator (a cross-counterflow heat exchanger). At the same time, the length of the heat exchanger would not exceed the typical one for the residential unit. In addition, the pressure drop of either of the fluids would be kept to a minimum, especially on the refrigerant side. Excessive pressure drop on the refrigerant side would adversely affect the performance of the mixture. Such a heat exchanger would approach a pure counterflow in performance, provided that there is an adequate number of banks. The

objective and the scope of this study were detailed below.

Objective

The objective of this study was accomplished by a combination of both experimental and theoretical means. On the experimental part, a heat exchanger was designed with a special consideration to provide a counterflow in a cycle, which imitates residential air conditioning operating conditions. Such conditions were achieved by mounting this heat exchanger in a testing rig, which was placed in two environmental chambers and tested at a variety of refrigerant mixture compositions and at various operating conditions. Performance measurements of the heat exchanger using both pure refrigerant and nonazeotropic mixture were taken. In order to evaluate the mixture effects clearly, a nonazeotropic R22/R114 mixture was selected as the working fluid because of its wide variation in boiling temperatures, 52°C at 330 kPa and because this mixture was used in a previous experiment [5] as well. A number of tests was conducted to determine if there was a composition, at which the evaporator heat exchanger shows the best performance improvement over pure R22. After proving the usefulness of applying this mixture in such a heat exchanger, the necessary heat transfer parameters required to perform design calculations were determined, i.e., refrigerant temperature profiles, the distribution of the heat load across the heat exchanger, and the overall heat transfer coefficient, as the design parameters for a heat exchanger. The theoretical analysis consisted of two parts. The first, was the analysis of the data and its reduction to obtain the heat transfer coefficient of this heat exchanger at the tested conditions. For this analysis and for the second part, the Carnahan-Starling-deSantis (CSD) equation of state routines

by Morrison et.al.[25] were applied. The CSD equation of state routines allowed to completely evaluate the state of the refrigerant mixture given measurable inputs. These routines were indispensable in the study of refrigerant mixtures.

The second part of the theoretical analysis consisted of derivation of the effectiveness/NTU (ϵ/NTU) relation to determine the effectiveness of this heat exchanger. A modified ϵ/NTU method was the most important aspect of the design procedure of the air-to-mixture heat exchanger. A simplistic, textbook ϵ/NTU method assumes a constant specific heat and a constant overall heat transfer coefficient, no changes in phase in either of the fluids and uniform heat release per a degree drop in temperature. A method based on these idealized assumptions had to be modified through experimentally derived parameters, which must be included in the new model. It was known from the properties of mixtures and a typical air conditioning application, that simplistic assumptions would not be satisfactory in a proper heat exchanger design.

The reasons for a disagreement between the simplistic ϵ/NTU and experimentally derived ϵ/NTU relationship stem from the fact that the nonazeotropic refrigerant mixtures change their temperature and their specific heat during evaporation. A pseudo specific heat concept was defined later. The change of the specific heat in a heat exchanger may be described with the use of a polynomial function dependent on the mixture properties and the composition. The moist air changes its phase when it flows through a heat exchanger. This affects the heat exchanger performance and influences the air temperature

change and the heat load distribution through a heat exchanger. The refrigerant mixture changes its phase and temperature as well, which further complicates the design procedure. Therefore, a realistic performance of such a heat exchanger can not be adequately described with a simplified ϵ/NTU method and all of the above factors must be included in a successful design procedure.

In summary, the objectives of this study were fulfilled as follows:

1. Design of a cross-counterflow heat exchanger.
2. Demonstrate the use of a refrigerant mixture in such a heat exchanger working in the air conditioning application.
3. Obtain the performance characteristics of the heat exchanger.
4. Derive a modified ϵ/NTU method and verify it.
5. Incorporate a modified ϵ/NTU method into a design procedure.

Scope

The contents of this thesis were summarized here in order to provide a coherent picture of the work performed during this study.

In Section 2, the experimental work performed in the laboratory was detailed. A special importance was attached to the description of an innovative cross counterflow heat exchanger, designed for this experiment, and the testing rig, where the heat exchanger was mounted. The experimental apparatus was wired with the necessary probes to determine the performance of the heat exchanger and the system. A method of determining a composition of a refrigerant mixture was provided. The data obtained from the tests was collected,

stored, and reduced to provide a convenient way of evaluating the performance of the heat exchanger and the system. The uncertainty of measurements was determined and could be found in Appendix A for major quantities.

Test results, the discussion and their evaluation was presented in Section 3. All tests were divided into two groups: the constant capacity tests and the variable outdoor load tests. The constant capacity tests were performed at a set air mass flow rate and an air temperature drop across the heat exchanger to provide a convenient way of examining its performance as a function of composition. The variable load tests were conducted at a constant compressor speed and varying outdoor temperature to simulate the operation of an actual residential air conditioning unit. The first group of tests was performed at a number of mixture compositions and with 100% R22, the second, at one mixture composition and with 100% R22. For all these tests, the results and various facets of operation of the heat exchanger were discussed. A number of graphs was shown to illustrate the operation of the heat exchanger.

Since the focus of the design procedure of the air-to-refrigerant mixture heat exchanger was the development of an ϵ/NTU relation, Section 4 contains a discussion and derivation of this method. The ϵ/NTU relation for a constant specific heat refrigerant is presented followed by a development of modified ϵ/NTU relations for a wet coil. The ϵ/NTU method for a wet coil was developed using experimentally derived results. Due to the fact, that the final equations involved numerical integration, a computer model was developed to obtain NTU as a function of several parameters. The same

program could be used for a linear or a quadratic specific heat relationship; calculation stream was directed to different subroutines depending on the relationship.

Section 5 dealt with the verification of the ϵ/NTU relations derived earlier. The experimental ϵ/NTU curves at various compositions were compared with the ϵ/NTU predicted relations. The discussion of the differences between the experimental and the predicted results was presented.

In Section 6, the developed ϵ/NTU relations were incorporated in the design procedure of a heat exchanger. A general outline of the design procedure was provided. The details pertaining to the geometric, material and other parameters, which are typical for coil designs can be found in [26]. Section 7 provided the summary and the conclusions of this study. Several recommendations pertaining to further study of a heat exchanger employing nonazeotropic mixtures were presented.

Section 2

EXPERIMENTS

This chapter describes the experimental facility to evaluate the performance of the air-to-refrigerant mixture heat exchanger and the air conditioning system. First, the experimental apparatus was introduced, described by the way of following air and refrigerant paths. The prototype of a cross-counterflow tube and plate fin heat exchanger was then presented in detail. The methods of various measurements were described, including the experimental procedures. Data collection, reduction schemes and the accuracies of the measurements were discussed. The derivation of the final quantities obtained from the measured data, i.e., the heat exchanger capacity and the heat transfer coefficients was described in detail.

EXPERIMENTAL APPARATUS

All tests were conducted in two adjacent chambers designated for testing of split system air conditioners. The experimental apparatus consisted of several components acquired from different manufacturers to simulate a realistic air conditioning unit, to provide the required operating conditions, a control capability, measuring and recording of various data to allow the analysis of a prototypical, air-to-refrigerant mixture heat exchanger. Since the apparatus was designed for understandability and easy diagnostics, without much concern for size or cost, it included several features that would never be found in a practical device. An overview of the experimental apparatus is shown in Fig. 2.1. The top part of the Fig. 2.1 represents the indoor chamber and contains the indoor section consisting of the indoor coil and

ducting to quantify the air properties. The evaporator was assembled from coil modules (banks) to provide a desired refrigerant flow pattern. The bottom part of the Fig. 2.1 represents the outdoor chamber and contains the outdoor coil (condenser) and a compressor. The condenser used in the experiments was a typical off-line coil routinely applied in the residential systems. For the purpose of circulation of the refrigerant, a variable speed hermetic compressor was utilized in all tests. The apparatus in both chambers was instrumented; the part of the apparatus in the indoor chamber was instrumented more extensively because this study focused on the performance of the indoor coil. A schematic diagram of the experimental apparatus is shown in Fig. 2.2.

A cross counterflow evaporator, whose complete description is presented later in the section, allowed air and refrigerants to flow in the opposite directions. Immediately below, is the description of the testing loop. This description will follow the passage of air and refrigerant in the indoor section.

The evaporator coil was placed in a duct. In order to achieve and maintain a uniform airflow across the evaporator coil, a converging section 1.67 m long, made out of sheet metal was attached to the duct, upstream of the evaporator coil. Except for the converging section, the duct was well insulated. At the end portion of the converging section, the upstream part of the thermopile was placed across the duct. Following the thermopile, an air filter was installed to protect the surface of the coil against dirt particles and subsequent fouling, which would negatively influence the

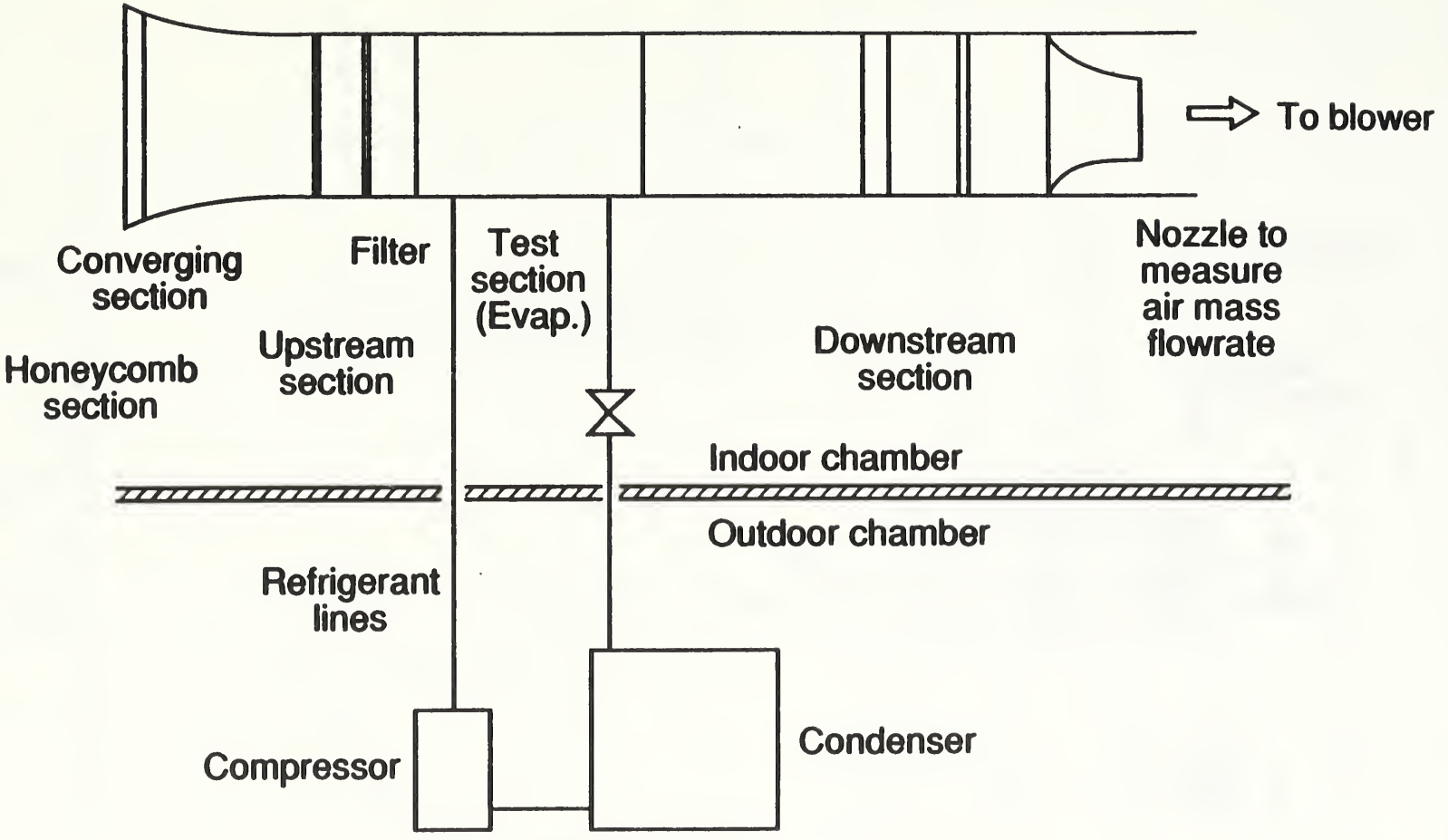

Figure 2.1 Overview of the experimental apparatus.

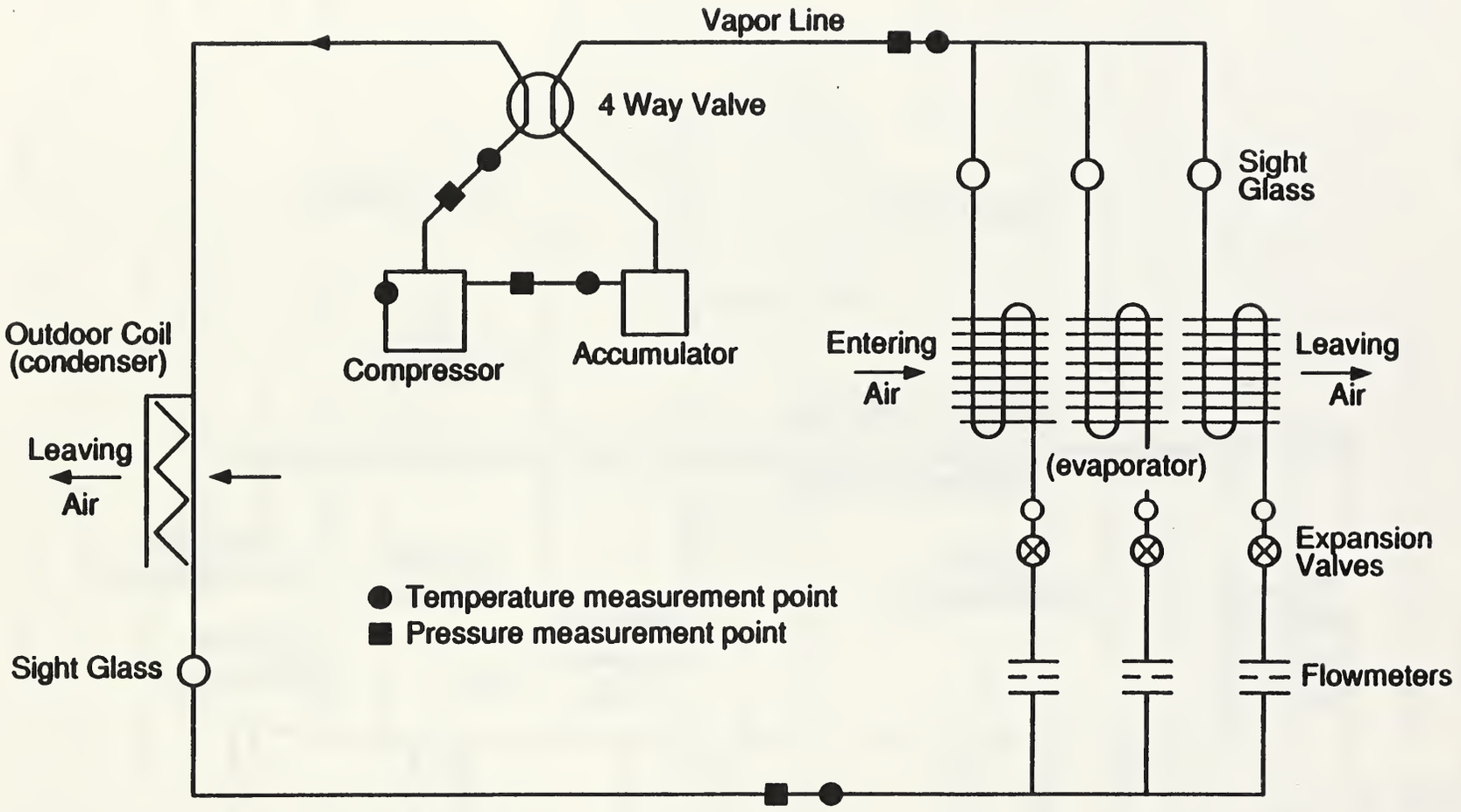

Figure 2.2 Schematic diagram of experimental apparatus.

repeatability of the test results. The cover on the front top portion of the indoor section had several holes drilled to allow the insertion of the airflow measuring instrument. Downstream from the indoor section, two rows of mixers were installed to provide a uniform air temperature across the duct. The second part of the thermopile was placed immediately behind the mixers. An airflow measuring apparatus was connected to the insulated duct attached to the discharge side of the evaporator coil. This apparatus consisted of a receiving chamber and discharge chamber separated by a partition containing a nozzle. An exhaust blower was attached to the duct leaving the discharge chamber, so that the static pressure of the air leaving the evaporator could be adjusted to give the desired airflow rate.

The refrigerant was compressed in the compressor, condensed in the outdoor coil, and was pumped in a liquid state to the indoor chamber. The liquid refrigerant line was modified to incorporate a sightglass, a turbine meter, four valves, a pressure regulated expansion valves and rotameters. A sightglass was used to observe the flow approaching the turbine meter. No flashing condition was mandatory at the turbine meter for accurate determination of the refrigerant flow rate. The valves served to properly direct the flow of refrigerant through the turbine meter and to bypass it during a start-up procedure. The liquid refrigerant first flowed through the sightglass, and then the turbine meter to a point, where the refrigerant line was divided into three circuits. Three rotameters were installed to allow an equal amount of refrigerant flowing in each circuit. Immediately downstream from the rotameters, the three pressure regulated expansion valves were used to expand liquid refrigerant to low pressure, two-phase fluid. More common,

temperature regulated valves were not used because, if applied with mixtures, they would not provide the desired regulating capability. After the refrigerant evaporated in the indoor coil, the three separate circuits were merged into one vapor line. Just before the circuits were merged, a sightglass was placed in each of them, for visual monitoring of the refrigerant. The vapor line followed to the compressor mounted in the outdoor chamber.

At various points of the experimental apparatus thermocouples and pressure gauges were installed and temperatures and pressures were recorded to provide information on the performance of the unit and as a check for consistent operation.

Typical conditions maintained in the environmental chambers were as follows. The chamber containing the indoor unit was maintained at 26.7°C (80°F) dry bulb and 19.5°C (67°F) wet bulb for the wet coil tests. For dry coil tests, the dry bulb temperature remained the same, while the wet bulb temperature was kept at such value, that the air dew point was below the lowest refrigerant temperature in the evaporator.

Prior to any dry coil tests, the air was carried through the coil with no refrigerant running to ensure that the condensate was removed. The outdoor chamber was maintained at either 33.4°C (92°F) or 27.8°C (82°F) for constant capacity tests, since tests were performed at the same mixture composition at two temperature levels. For variable outdoor temperature tests, the temperature ranged between 27.8°C (82°F) and 36.7°C (98°F). Both chambers had sufficiently large volumes and additional fans to help circulate air so

that uniform conditions were maintained.

HEAT EXCHANGER DESCRIPTION

The evaporator heat exchanger consisted of eight banks of finned tubes, all of the same size (see Fig. 2.3). The tubes were made out of copper with a nominal diameter of 9.525 mm (3/8"), and fins were made out of aluminum at the rate of 13 fins per inch. Each bank, or equivalently each row, consisted of 12 tubes. The rows were spaced 3.8 cm (1.5") from each other. The ratio of the outside heat transfer area to the inside heat transfer area was 22.79 : 1. The banks were delivered separately from a manufacturer and they were assembled at the laboratory in such a manner, that refrigerant could flow through the evaporator in three independent circuits. For example, the expanded refrigerant would approach the top tube of the heat exchanger and move downward through four tubes of the first row. At this point, the refrigerant was directed to the next row and this time it would flow upwards through four tubes to the top tube and then to the next row. A similar flow pattern occurred in the middle and in the bottom circuits. A general direction of the refrigerant flow was toward the incoming air, thus a cross counterflow was achieved. The reason for having three refrigerant circuits in the heat exchanger, was to limit the crossflow as much as possible and to give priority to the counterflow. A diagram of the refrigerant and the air flow is shown in Fig. 2.4.

Each bank had its own condensate collecting pan with a sloping bottom such, that any condensate dripping from the bank, immediately flowed into the buret positioned below. Each buret was accompanied by a stop-cock upstream and

downstream from it in the condensate line. By appropriate manipulation of these stop-cocks, the condensate amount was captured and measured during a test.Such evaluation of a heat exchanger has never been done before. Since the banks were not joined together, it was possible to measure condensate at each individual bank, and to evaluate how the refrigerant mixture temperature profile influenced the distribution of the condensate drop. Another reason for separate banks was to eliminate conduction between them.

Each of the three refrigerant circuits had 33 bends, which changed the direction of refrigerant flow by 180°. To monitor the refrigerant temperature in the evaporator, each bend had a thermocouple taped to its surface. Between the banks, immediately upstream from the first bank and immediately downstream after the last bank, were two thermocouples indicating the air temperature. To ensure the accurate reading of air temperatures, each thermocouple was wrapped in short vinyl conduit. Each of the banks, on the surface facing the incoming air, had five thermocouples glued to the fin surfaces. One thermocouple was positioned in the middle of the bank, while the remaining four were located half-distance between a mid-point and a corner of a bank. The thermocouples were glued to the roots of the fins.

This heat exchanger, designed to take advantage of the mixture properties and thoroughly instrumented to provide the performance information, was integrated with the experimental apparatus. In order to evaluate this heat exchanger thermodynamically, not only physical quantities pertaining directly to it were measured, but also those of the rest of the apparatus. They were necessary for a complete evaluation of this heat exchanger i.e., how it would work as

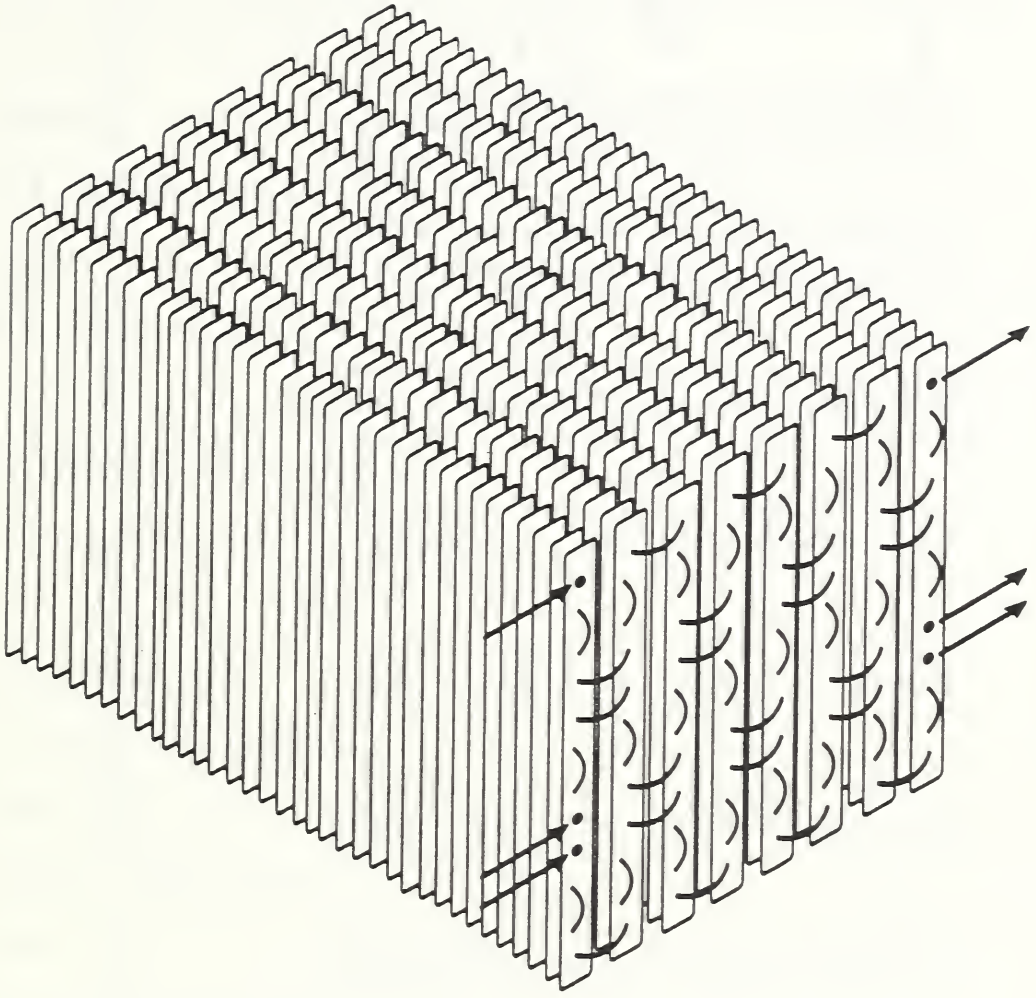

Figure 2.3 Three dimensional view of the evaporator heat exchanger.

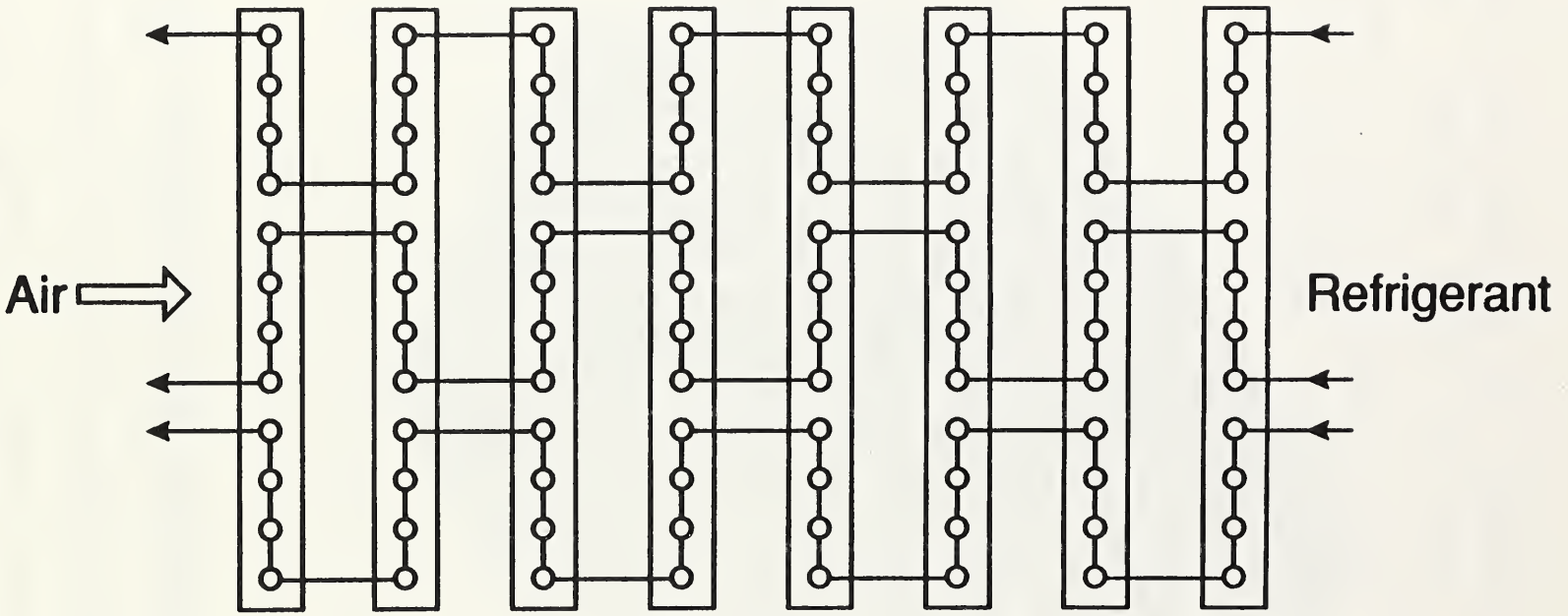

Figure 2.4 Schematic diagram of the evaporator heat exchanger.

a part of an air conditioning system. For instance, power necessary to run the compressor was recorded to determine the coefficient of performance. The next chapter provides details about the measured quantities.

MEASUREMENTS

In this chapter, there is a short description of the measurements which were necessary in evaluation of the heat exchanger and its performance in the context of its function as an evaporator in an air conditioning application. The following measurements were performed: compressor power, air and refrigerant mass flow rate, pressure, temperature, relative humidity of air, and overall composition.

Power Measurement

For an accurate determination of the COP it was essential to have a good measurement of power consumed by the compressor. This was a three phase compressor, whose speed was varied by an inverter. As earlier experiments by Baldwin et.al. [27] have shown, both amperage and voltage phases were strongly affected by the inverter. In addition to this, the power factor of this inverter was as low as 0.7. Due to these problems, an analog watt-hour meter could not be used, since it would provide incorrect readings of the compressor power consumption. As a result, a digital watt-hour meter was installed between the invertor and the compressor thus providing the accurate measurements of power used for a duration of a test.

Mass Flow Rate Measurement

A mass flow rate of refrigerant, $\dot{m}_r$, was needed for determination of the

evaporator capacity as a secondary check. In order to determine a mass flow rate, a turbine meter was used, which was installed in the subcooled liquid line. The signal (frequency, Hz) from the turbine meter was sent to a transducer, which served as a pulse counter. The same transducer also measured the excitation voltage, which, when used in a calibration curve equation, provided the mass flow rate quantity. The two readings from these two counters agreed within 0.35 percent.

Pressure Measurements

To determine pressure drop across the nozzle, manometers were applied in the experimental apparatus; for refrigerant pressure measurements, absolute pressure transducers were used. Manometers accurate to within 1% of the reading, were used to measure the static pressure across the nozzle and pressures obtained by a pitot tube, placed at the nozzle exit. Six calibrated pressure transducers were used for the refrigerant pressure measurements as illustrated in Fig. 2.2. These pressure transducers were calibrated using a dead weight pressure tester twice in a nine month period. They drifted less than ± 2 kPa. When local pressure values were needed along the length of the evaporator, they were linearly interpolated from the known inlet and outlet pressures.

Temperature Measurements

Thermocouples, taped or soldered to the tube surfaces, were used to determine temperatures at various points in the system. The thermocouples were manufactured out of 24 gage copper-constantan wires. All thermocouples used on the evaporator heat exchanger were hardware compensated, the rest were

software compensated. Manufacturers calibration curves were utilized for conversion of voltage measurements into temperatures.

A thirty junction thermopile was used to measure the air temperature difference entering and leaving the evaporator coil. One part of the thermopile was placed in the entering duct 0.15 m from the coil (a filter was installed between this part of the thermopile and the coil face so that the thermopile could not radiate to the coil and thus give erroneous readings), while the other was placed in the insulated discharge duct leading to the receiving chamber of the air flow measuring apparatus. A mixing device was placed 0.3 m in front of the downstream part of the thermopile to obtain uniformly mixed air at the thermopile. The junctions of the thermopile were spaced at centers of equal area across the inlet and discharge ducts.

Relative Humidity Measurement

The relative humidity of the air entering and leaving the evaporator coil was measured using aspirated psychrometers. The psychrometer used to measure the relative humidity of the entering air was placed near the entrance to the converging section. The psychrometer utilized to measure the humidity of air leaving the coil sampled the air at the end of the insulated duct section. The sampled air was then returned back to the duct, so that the total amount of air flowed through the nozzle used to measure the volumetric flow rate. A portable psychrometer was used in the outdoor chamber to determine its humidity. The reason for measuring the outdoor chamber humidity was to ensure that the conditions remained the same for all tests.

Overall Composition Measurement

Overall composition of a mixture, C_o, was determined by taking a subcooled liquid sample from the sampling port in the subcooled liquid line, as shown in Fig. 2.5. The following procedure was applied for each measurement.

1. Evacuate the sample bottle and connect it to the sampling port.
2. Open valve #1 and #2 and evacuate the space in between the valve #1 and shutoff valve.
3. Close valve #1 and #2.
4. Put ice around the sampling line up to the liquid reservoir to avoid flashing.
5. Open valve #1 and shutoff valve consecutively to fill the liquid reservoir.
6. Close valve #1 and shutoff valve and detach the sample bottle from the port.
7. Open valve #2 to have the subcooled liquid expand to the superheated vapor and run hot water over the sample bottle to make certain that no liquid droplets are left.
8. Since the pressure inside the bottle is low (usually below the atmospheric pressure), the bottle is pressurized by dry nitrogen up to 350 kPa and taken to the gas chromatograph for the composition analysis.

The most important step in measuring the overall composition was to make sample bottles large enough to make the expanded vapor to be in the superheated region (100% liquid at state 1 to 100% vapor at state 5 in Fig. 1.2). The addition of a pressure gage to the sample bottle was another way of checking

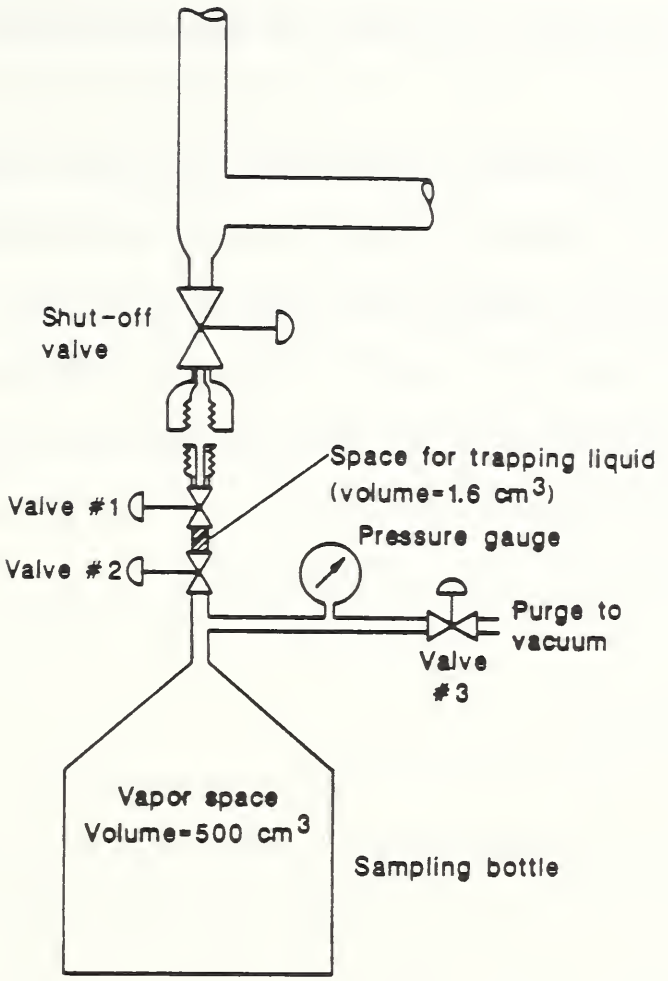

Figure 2.5 Detailed diagram for overall composition measurement.

if the liquid sample had been completely vaporized in the expansion process. If the pressure inside the bottle after the expansion was less than the saturation pressure corresponding to the room temperature, then the vapor was presumed to be in the superheated region. Composition analysis was carried out using a gas chromatograph (HP 5710A). This gas chromatograph employs a thermal conductivity detector which is fairly sensitive to refrigerants. The reproducibility of the measurement was within 0.2 percent for the same

sample. The variation of composition from sample to sample for the same test was less than 0.5 percent in mole composition.

The sample was always taken from the liquid line while the heat pump was running. An important observation was made by Jung [4], who found that the overall measured composition differed from the initially charged composition by 2 to 3 percent in mole fraction. This change was due to the composition shift in the liquid toward the less volatile component. For this reason, a liquid sample was drawn each time for all mixture tests and the measured overall compositions were used in the analysis.

DATA COLLECTION

All tests were run at steady-state conditions. In order to compare the results on the same basis, either the air temperature drop across the evaporator coil and the air mass flow rate, or the compressor speed, were kept at the same level. The air enthalpy method was the primary method of determining the coil capacity. The base line tests were run with pure R22 at the lowest compressor speed possible. The reason was that R114 which was added to R22 to form a non-azeotropic mixture, is a lower capacity refrigerant. In order to maintain the same capacity imposed by the air side, the compressor speed had to be increased to accommodate the increased amount of R114. Another reason for having the pure R22 tests at the lowest compressor speed possible, was that in a previous study [5] it was observed that at high compressor speeds and at high compositions of R114, the compressor efficiency was significantly degraded.

Data collection and control of the system were done by the use of a computer and a data acquisition system. The digital voltmeter integral to the data logger was programmable under computer control. All DC voltages from the thermocouples, pressure transducers, and power bus connections were measured by the voltmeter. The resolution of the voltmeter was 1 μV for the range of 0.1 Volt. The measurement accuracy (percent of the reading, auto-zero on, at 23°C) was 0.003 percent for the range of 0.1 Volt. This data acquisition system also continuously scanned all channels for thermocouples, pressure transducers, DC voltages, and a turbine meter. Several key temperatures and the sum of differences between the successive scans were observed while the system was coming to the steady-state. The following steps were taken for each test.

1. The machinery and the control system for the environmental chambers were started two hours before the system was started.
2. The blower, the condenser fan and the compressor were started. The compressor speed was maintained at the increased level to faster circulate the refrigerant.
3. The humidity level in the chamber containing evaporator was increased temporarily to faster wet the coil.
4. The compressor speed was gradually decreased. A required amount of subcooling and superheat was established and verified by the use of the program employing the equation of state routines.
5. The system was allowed to come to equilibrium while fine adjustments were being made on the mass flow rate and the outlet air temperature.
6. Nine scans at five minute intervals were taken and stored at steady state

condition.

7. In the beginning of the first scan the stop-cocks below burets were closed and the stop-cocks above the burets were closed after the last scan. The amount of condensate collected was evaluated manually.
8. For mixture tests, a subcooled liquid sample was drawn for measuring the overall composition immediately after steady state data was taken.

It usually took 4 to 5 hours for the system to reach a steady-state. After the tests were completed, it was found out that the mass flow rate of air assumed values within 5 percent of a mean, even though the settings were unchanged for the whole series of tests. While different reasons were attributed for the mass flow rate oscillations, it appears that the dry evaporator coil tests provided an explanation for this phenomenon. For dry coil tests, the air mass flow rate increased by 12% from the average air mass flow rate for the wet coil. A possible explanation is that for the wet coil tests, water droplets attached to the fins offered resistance to the to the airflow. For various mixture compositions, a different refrigerant temperature profile existed in the evaporator. This forced a changing amount of condensate to accumulate on various parts of the evaporator surface. Since the net amount of condensate on the coil surface changed, so did the air passage obstruction. For dry coil tests, there was no condensate to increase the pressure drop across the evaporator, so the air mass flow rate was the highest.

DATA REDUCTION

All of the data, except for the mass of the condensate was raw data, which had

to be converted to the engineering units. This was accomplished with the help of a data reduction program. Then, the quantities in engineering units were evaluated, regarding their uncertainty and were utilized to calculate the required and the final quantities. Following below are some of the details of the data reduction process.

The final quantities, which were derived from the tests where the capacity, the COP of the experimental apparatus, the inside and the outside heat transfer coefficients for a bank and for the total heat exchanger and the average temperature difference in the evaporator. To obtain these quantities, several intermediate values had to be determined and their uncertainties evaluated.

Heat Exchanger Capacity

The air enthalpy method was used as the primary method to evaluate the evaporator capacity. This quantity consists of the sensible and the latent load:

$$Q_t = Q_s + Q_l \tag{2.1}$$

The sensible load was determined from the equation (2.2):

$$Q_s = M_a \cdot c_p \cdot \Delta T_a \tag{2.2}$$

where M_a is the air mass flow rate, c_p is the specific heat of air (considered constant), and ΔT_a is air temperature change across the heat exchanger. The

latent load was found from the amount of the condensate collected and the latent heat of condensation:

$$Q_l = \dot{m}_w \cdot h_{fg} \tag{2.3}$$

The sensible, the latent, and the total heat loads were calculated for the heat exchanger and for each bank, to obtain a heat load profile for a particular mixture composition. The air temperatures used in calculation of the sensible load were not the actual temperatures between the evaporator banks, but were fitted using a fourth degree polynomial. A typical standard deviation of a polynomial fit for air temperatures was 0.51°C.

The secondary method used to determine the evaporator capacity was the refrigerant enthalpy method as shown by equation (2.4).

$$Q_t = \dot{m}_r \cdot (h_o - h_i) \tag{2.4}$$

where h_o is the enthalpy of refrigerant leaving the evaporator, h_i is the enthalpy of refrigerant entering the evaporator, and $\dot{m}_r$ is refrigerant mass flow rate in the evaporator. The enthalpy of a mixture entering the evaporator is the same as the enthalpy of a subcooled mixture leaving condenser, because expansion in the choking valve is approximately adiabatic. For pure components, the thermodynamic equilibrium temperature and the pressure were used to obtain the refrigerant enthalpy. For mixtures, however, the thermodynamic equilibrium temperature, is a function of quality as well as pressure. As Gibbs phase rule states, two intensive properties are necessary,

to define the thermodynamic equilibrium state for a given binary mixture of a certain composition.

The CSD equation of state routines were used to calculate the subcooled liquid enthalpy and the enthalpy of the refrigerant leaving the evaporator. Given pressure, temperature, and overall composition, these routines provided all thermodynamic properties such as enthalpy, equilibrium temperature, quality, and liquid and vapor phase compositions.

For pure components, the accuracy of the enthalpy calculation depended largely on the accuracies of the local pressure measurements (typically 3-4 kPa corresponding to 0.3°-0.4°C in saturation temperature of studied fluids), refrigerant temperature measurements (0.2°C) and the CSD equation state (0.2°C). For mixtures, besides the uncertainties in the local pressure and temperature measurements, the errors in the enthalpy evaluation were due to the uncertainties involved in the overall composition measurement (typically 0.5 percent corresponding to 0.3°C in saturation temperature for R22/R114) and due to the inaccuracy of the CSD equation of state (0.4°C).

The refrigerant mass flow rate and the refrigerant enthalpy drop were utilized to calculate the capacity of the evaporator coil. The test was considered valid, when the difference in the capacity calculation between the two methods was less then 6 percent.

The COP of the experimental apparatus was found from the ratio of a total evaporator capacity, Q_t, and the power input to the compressor, P:

$$COP = Q_t/P \tag{2.5}$$

Heat Transfer Coefficients Calculations

Both inside and outside heat transfer coefficients were calculated from the experimental data using the following respective equations:

$$h_i = Q/A_i\ \Delta T_{fr} \tag{2.6}$$

$$h_o = Q/A_o\ \Delta T_{af} \tag{2.7}$$

where Q is the total heat transferred, A_i and A_o are the inside and outside heat transfer area respectively, ΔT_{fr} is the temperature difference between fin root and refrigerant, and ΔT_{af} is the temperature difference between air and fin root. For the purpose of calculating the temperature profiles, polynomial fits of the temperatures were found. The polynomial fits of the refrigerant and fin root temperatures had standard deviations of 0.21°C and 0.32°C, respectively. For pure refrigerant, a linear fit of temperature was used, while for mixtures and for fin temperatures second degree polynomials were used. These temperature fits, together with the air temperature fit, were utilized for the determination of the inside and outside heat transfer coefficients and the average temperature in the evaporator. The same equation was used for a bank and for the total heat exchanger. The overall heat transfer coefficient was calculated using the following expression:

$$\frac{1}{U_o} = \frac{1}{\eta_o h_o} + \frac{a}{(A_w/A_o)k} + \frac{1}{(A_i/A_o)h_i} \tag{2.8}$$

where, η_o is the outside heat transfer area effectiveness, h_o is the outside heat transfer coefficient, a is the tube thickness, k thermal conductivity of the tube wall, A_w is the arithmetic average of A_o and A_i, A_o and A_i are the outside and inside heat transfer areas, respectively, h_i is the inside heat transfer coefficient. The conductance term was dropped because the thermal resistance of tube wall was negligible compared to other terms.

The uncertainty of the overall heat transfer coefficient for one bank at typical test conditions was calculated to be 6 to 7 percent. The uncertainty analysis of the data is presented in Appendix A.

Section 3

EXPERIMENTAL RESULTS

In this chapter, a general description of the experimental results was provided. These results were divided into two groups: the constant capacity tests and the variable outdoor load tests. For constant capacity tests, a constant mass flow rate of air moved across the heat exchanger with the same air temperature drop. The following results were discussed; the gliding temperature profiles of air and mixture, the condensate profiles, the heat profiles for the range of compositions, the heat transfer coefficients, the mixture specific heat and the overall heat transfer coefficient. The above mentioned profiles were obtained by recording the respective quantities, as they changed across the heat exchanger and by deriving polynomial functions to represent them. Some aspects of the total system performance were mentioned. The variable outdoor load tests were performed to simulate an operation of a realistic air conditioning system whose compressor speed remains constant, while the outdoor temperature changes. The tests were run at three different outdoor temperatures for 100% R22 and for 57% R22/R114 mixture. Similarly, various aspects of operation of the heat exchanger were discussed. Table 3.1 shows typical conditions at which most of these tests were run.

CONSTANT CAPACITY TESTS

A series of tests was performed for mixtures of R22/R114 at several overall compositions and at two different outdoor chamber temperatures i.e., 33.4°C (92°F) and 27.8°C (82°F). The tests were run at a constant capacity rate on

the air side, meaning that the inlet and the exit air temperatures as well as the air mass flow rate were held constant. The compressor speed was adjusted for various compositions to obtain desired air outlet temperature. The tests were started with

Table 3.1 Range of Test Conditions.

Item	Quantity
Total refrigerant mass flow rate (kg/h)	68.1 to 86.3
Mixture composition (% mass of R22)	100 to 46
Air mass flow rate (kg/h)	668.1 to 707
Air face velocity (m/s)	1.15 to 1.22
Air temperature drop across coil (°C)	13.6 to 15.8
Indoor chamber conditions:	
dry bulb °C (°F)	26.7±.2 (80±.3)
wet bulb °C (°F)	19.5±.2 (67±.3)

100% R22 and were continued to about 46% R22 by mass. With increased amount of R114, the efficiency deteriorated significantly. Even though the tests were run at two outdoor temperature levels, only the 33.4°C (92°F) tests were discussed here in detail. One test at 63% R22 was run above a dew point of the air so that no condensate was collected (a dry coil test).

Figs. 3.1 to 3.3 illustrate temperature glide of refrigerant mixtures and air for three different compositions of R22/R114. For a 100% R22 test, its temperature falls off along the evaporator due to a pressure drop. At 76% R22 by mass, the mixture glide is 5.5°C and for 46% R22, the glide is 12.2°C. In these figures, the air and the refrigerant flow in the opposite directions. The temperature of pure refrigerant decreases as a result of a drop in its saturation pressure. A general shape of a mixture temperature profile may be estimated by using Fig. 1.3. For example, for an overall composition of 76% R22, the vapor composition would be higher than 76% and the liquid composition would be less than 76%. This is due to the fact that the refrigerant R22 is more volatile than R114, it evaporates faster and

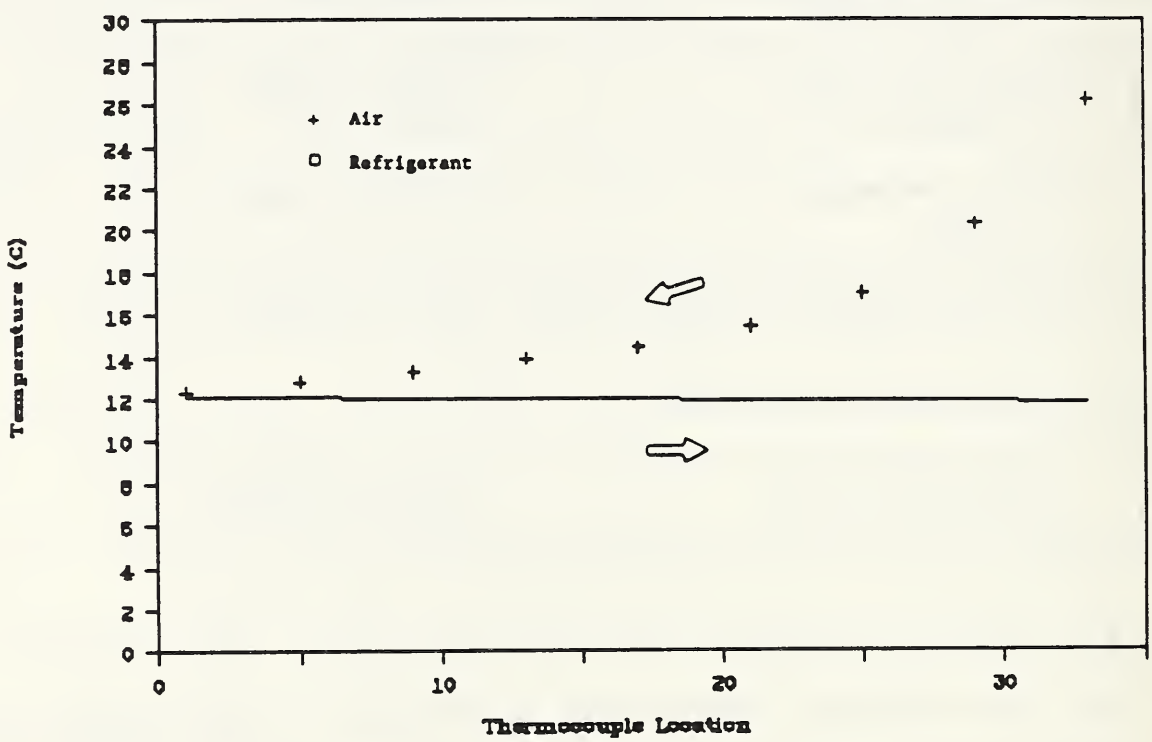

Figure 3.1 Air and refrigerant profiles through the heat exchanger (100% R22).

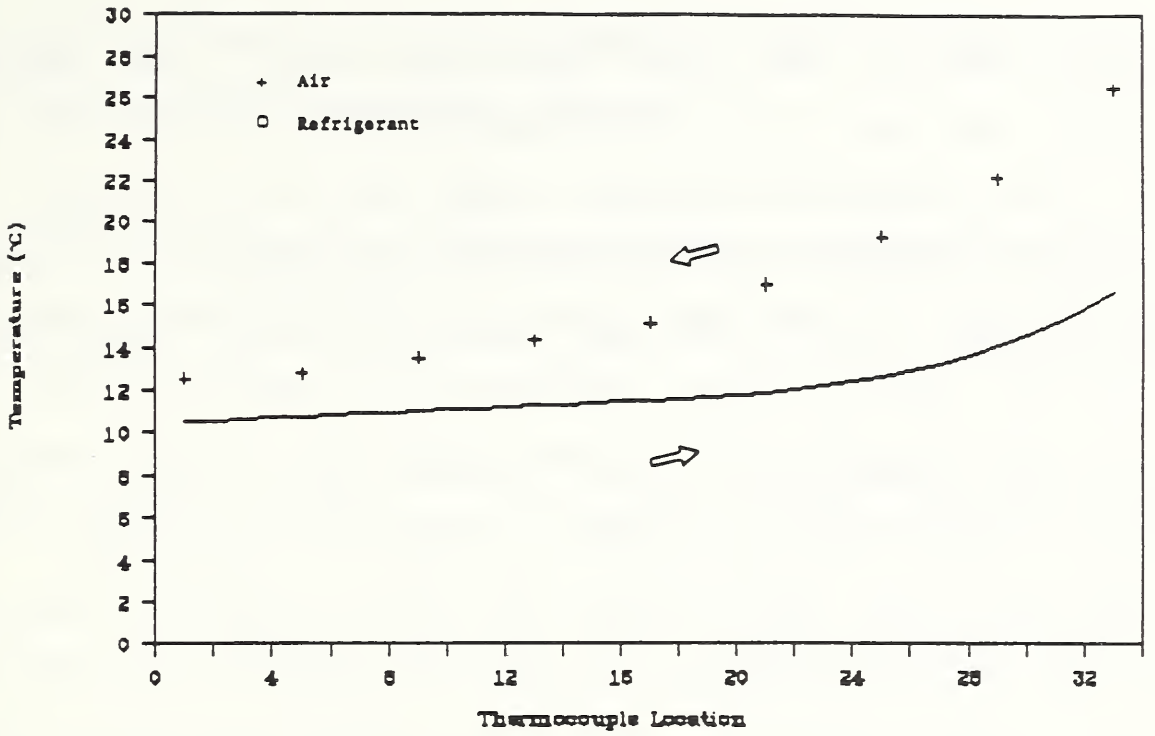

Figure 3.2 Air and refrigerant profiles through the heat exchanger (76% R22).

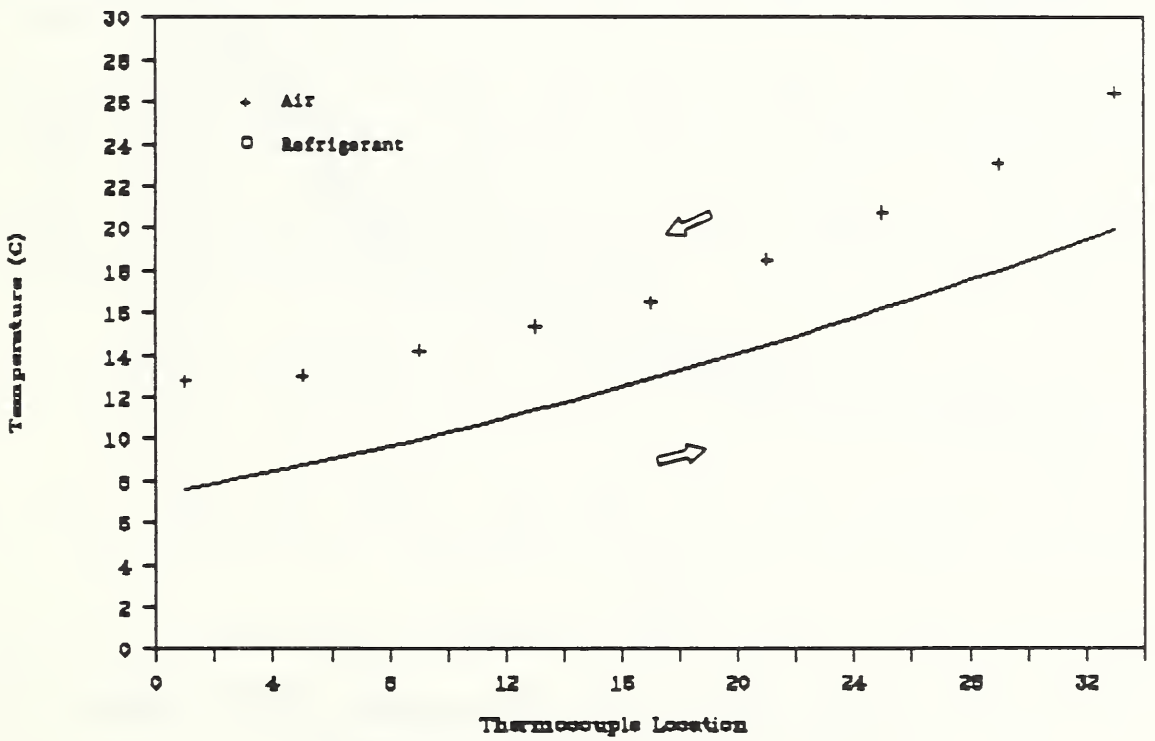

Figure 3.3 Air and refrigerant profiles through the heat exchanger (46% R22).

initially there is very little temperature glide in the evaporator. Therefore, the vapor is rich in refrigerant R22, while liquid is rich in R114. As the evaporation progresses, almost all R22 is evaporated, while R114 begins to evaporate in greater quantities. The slope of the temperature glide increases. Finally, only vapor exists at the overall composition.

For an overall composition of 46% R22, initially vapor is more than 80% R22. However, in this region the bubble line slope is steeper than at higher compositions of R22, while the dew line slope increases at a decreasing rate. As a result, more R114 is evaporated earlier in the evaporation process. The temperature glide for a composition of 46% R22 is steeper as shown in Fig. 3.3.

For a 100% R22 test, the air temperature across the heat exchanger falls very quickly for the first three rows, while for the remaining ones, the air temperature profile is almost horizontal. This is due the refrigerant temperature being almost constant and the air temperature closely approaching its value, thus reducing the rate of heat exchange near the exit (see Fig. 3.1). For 46% R22 in the mixture, the air temperature change across the heat exchanger deviates less from a linear temperature drop than the air temperature profile does for 100% R22. These two cases, and several intermediate compositions are shown in Fig. 3.4. It is clear that, the air temperature change across the heat exchanger is not linear. As a matter of fact, it is not linear for dry coil tests either, which suggests that the cause of nonlinearity is a non constant heat flux. A varying quantity of heat flux causes the temperature profile to deviate from a linear one. The

additional nonlinearity in the air temperature profile is due to the latent heat, once dew point temperature is reached.

As previously mentioned, the coil was extensively instrumented and each coil bank had its own condensate pan to collect moisture. A condensate profile for the heat exchanger was determined. Fig. 3.5 shows the amount of condensate collected from each coil bank. For 100% R22 test, the condensate profile resembles a shifted dome. As warm air crosses the first two banks, only a small amount is cooled below its dew point to produce condensate. From the third bank downstream, the air is cooled sufficiently to produce greater amounts of condensate. The amount of moisture collected drops off

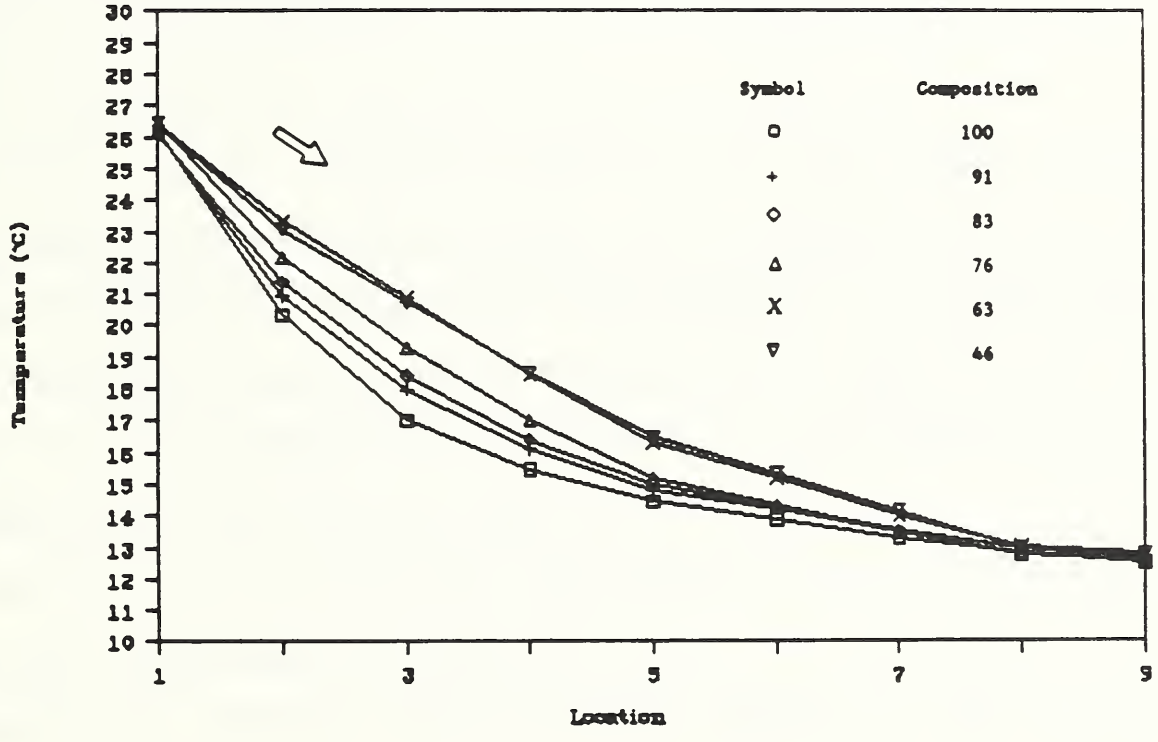

Figure 3.4 Air temperature profile versus heat exchanger bank for various compositions of R22/R114.

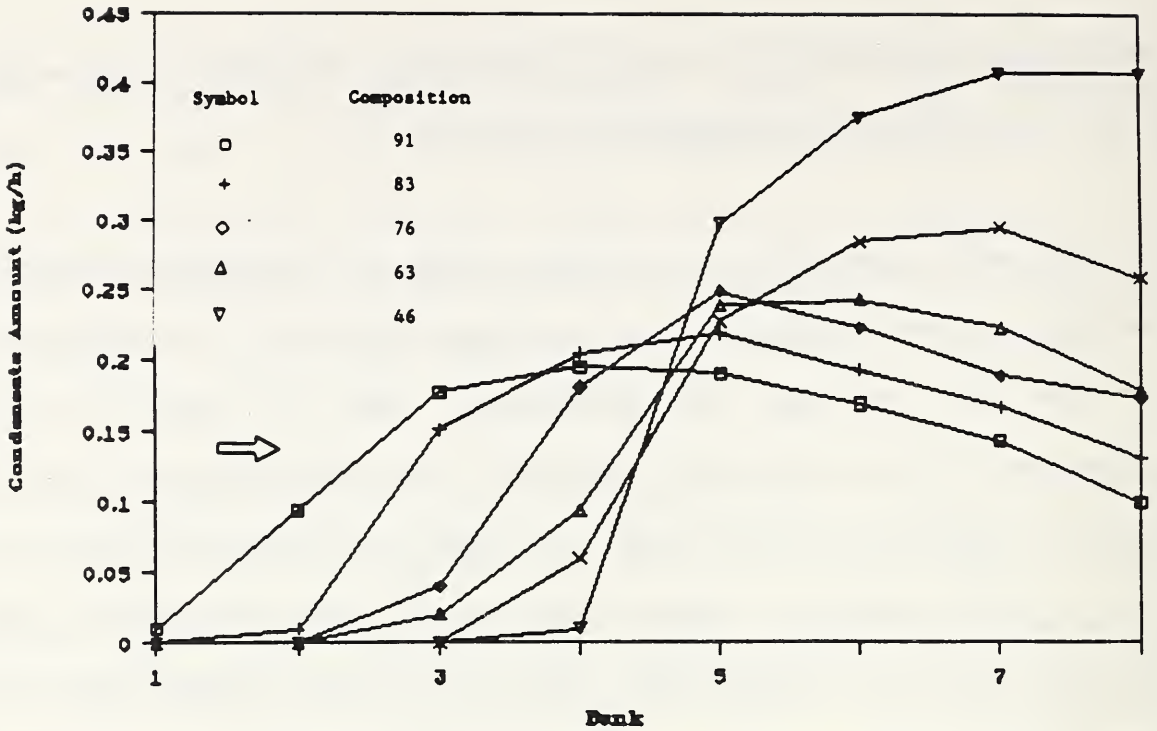

Figure 3.5 Condensate collected versus bank for various compositions R22/R114.

slightly towards the end of the heat exchanger. As the composition is changed, the distribution of the condensate moves from the front of the coil to the back of it. The reason for such condensate distribution is that, for mixtures containing lower concentrations of R22, the temperature of the mixture is above the dew point of the air in the front portion of the heat exchanger. At the same time, the mixture temperature at the refrigerant inlet to the evaporator decreases to match the air load (outlet air temperature remains constant). The temperature difference between air and mixture increases and with mixture temperature below dew point, more moisture is collected. Therefore, at the cold end of the evaporator where air leaves, a larger amount of water is condensed, while at the evaporator air inlet, lower amounts of water are condensed.

Fig. 3.6 shows the heat transferred to each bank, Q_b, for various compositions of R22/R114 mixture. For a 100% R22 test, the largest amount of heat is transferred at the first coil bank and the lowest, at the last bank. The amount of heat transferred follows a parabola with a steep drop of heat transferred in the front rows of the coil and an almost constant heat amount in the second half of the coil. For decreased amount of R22 in the mixture, heat transferred to the front banks of the coil drops off. In these cases, the distribution of the heat transferred is more equalized across the coil, due to constant temperature difference between air and refrigerant. For the two lowest R22 compositions in the mixture, i.e., 46% and 63%, there is an inflection point of the heat profile in the fourth bank. While the amount of sensible heat decreases, more latent heat is transferred because of low moisture temperatures in a larger part of the heat exchanger.

Fig. 3.7 shows the amount of the sensible and the latent heat as a function of mixture composition. For all tests, except for the one with the lowest composition of R22 (46%), the latent heat constitutes 26% to 28% of the sensible heat. For 46% R22 test, the latent heat is 35.5% of the sensible heat, even though the condensate distribution is the most uneven in this case. However, the inlet refrigerant temperature is also the coldest and it produces the largest amount of condensate to occur. The above proportion of the latent and the sensible heat was dictated by the surface temperature of the coil, the ΔT between air and refrigerant, and by the percentage of the heat exchanger area which is below air dew point temperature i.e., it was dictated by the chosen operating conditions. The lower surface temperature

would generally increase the latent component, while the smaller ΔT would tend to reduce the sensible phase component. These trends are best seen when a 100% R22 test is compared with a 46% R22 test.

For a 100% R22 test, the temperature difference between air and refrigerant in the front portion of the coil is the highest. This results in a high sensible and a low latent heat for this part of the coil. For a 46% R22 test, the temperature difference in the front part of the coil is smaller and almost constant through the coil. The sensible heat is lower because of lower ΔT, while the latent heat increases because of the lower surface temperature.

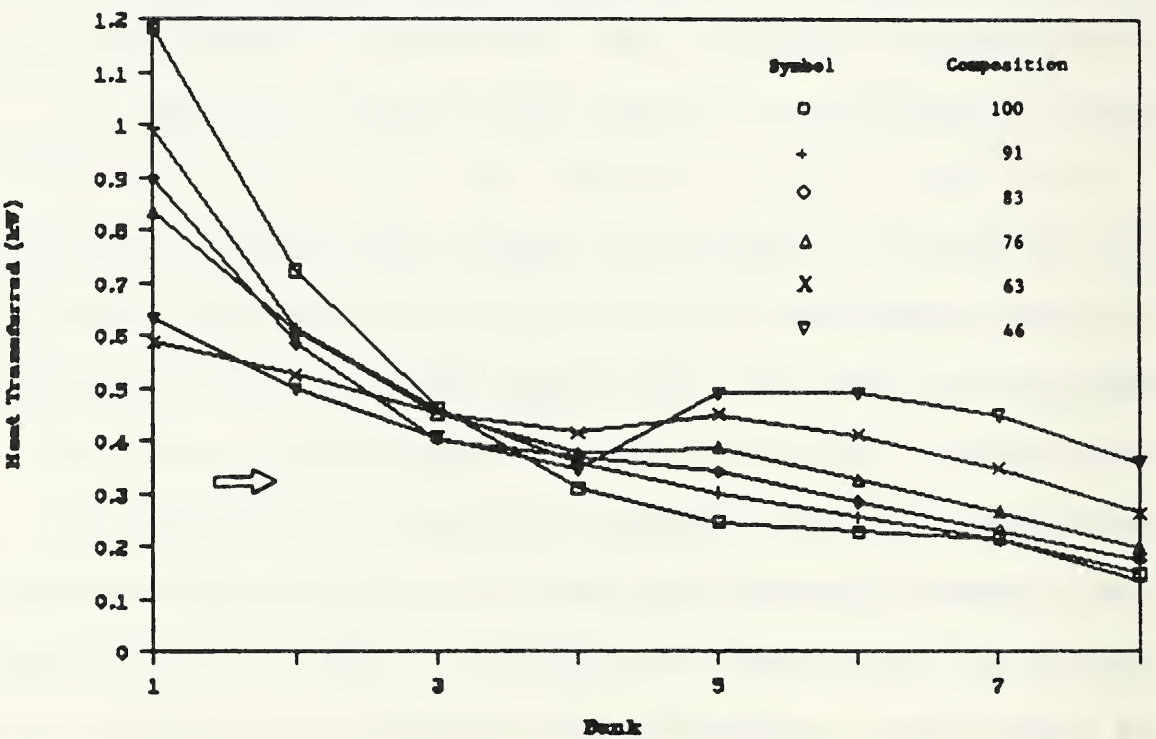

Figure 3.6 Heat profiles versus bank for various compositions of R22/R114.

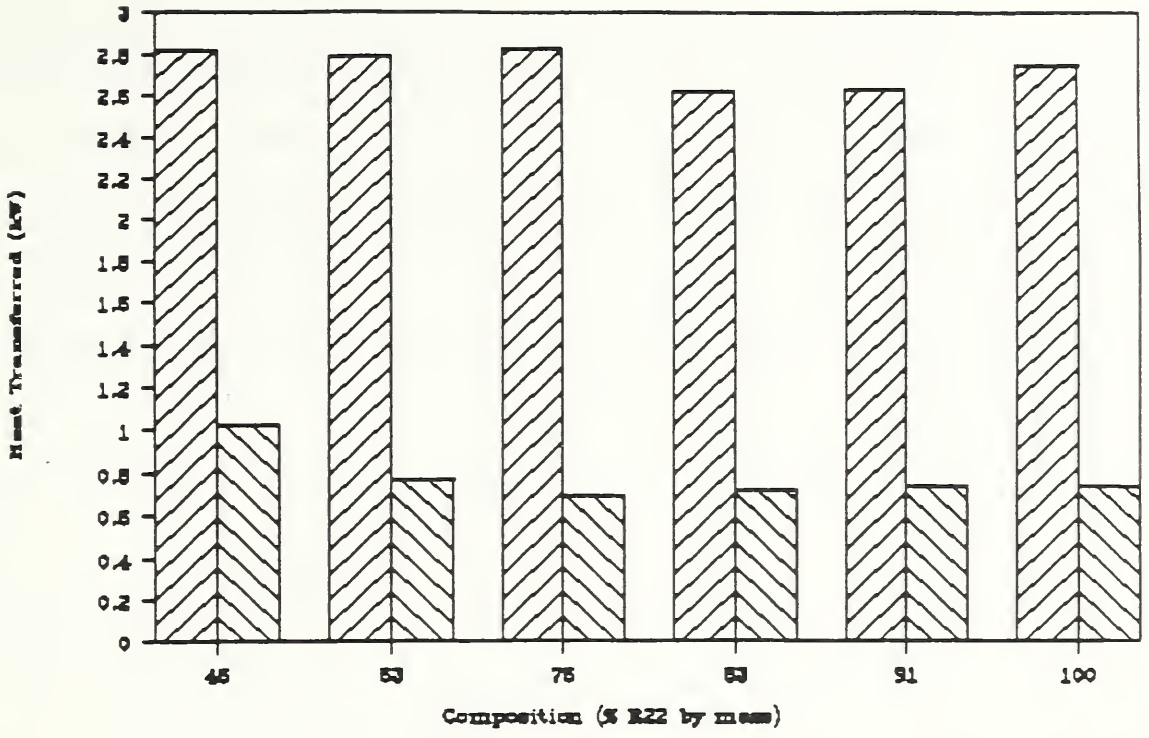

Figure 3.7 Latent and sensible heat for various compositions of R22/R114.

As was mentioned earlier, the mixture specific heat varies with the quality through the evaporator. An example of this variation is shown in Fig. 3.8 for a 46% composition of R22. In this case, the specific heat of the mixture, calculated from the ratios of the refrigerant enthalpy change over the temperature change for a number of divisions in the evaporator, changes by a factor of two.

The overall heat transfer coefficient for each test and for each bank was determined from the experimental data. The results are shown in Fig. 3.9 for several mixture compositions.

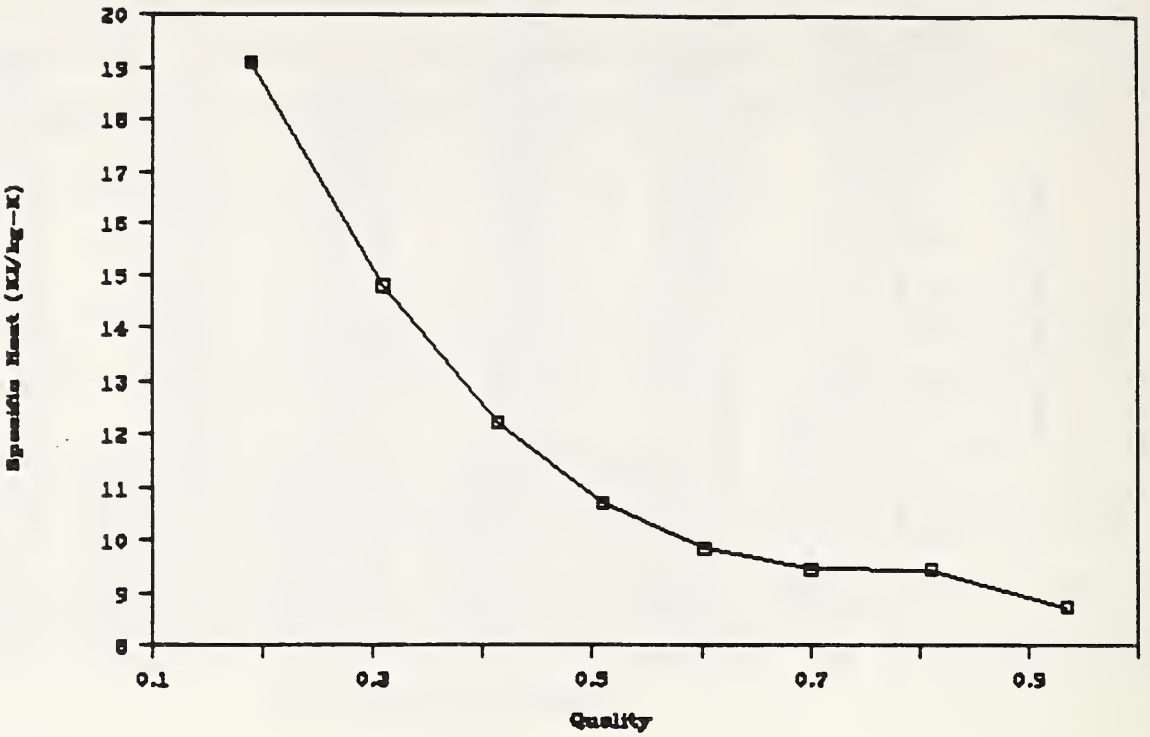

Figure 3.8 Specific heat change versus quality of 46% R22/R114 mixture in evaporator.

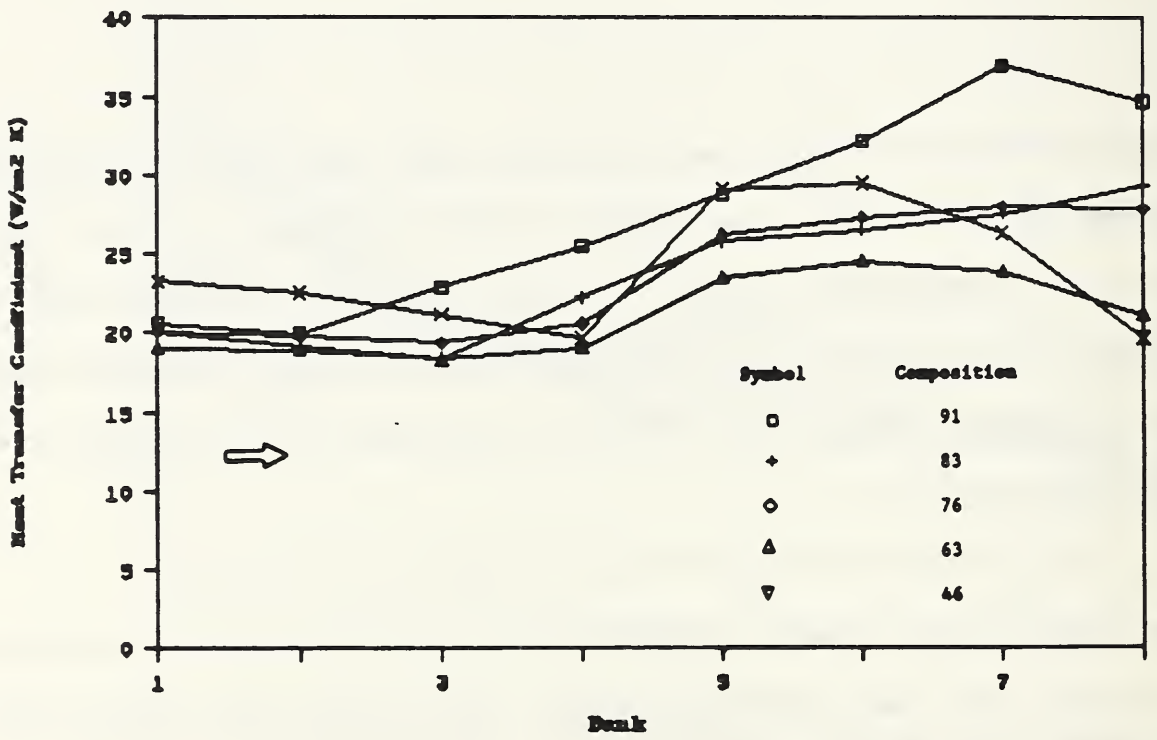

Figure 3.9 Overall heat transfer coefficient versus bank for various compositions of R22/R114.

This is not exactly true, because the heat transfer coefficient varies along the heat exchanger, however it does not vary as much as the experimental data suggest. The largest deviation was observed for a test, in which mixture composition was 91% R22 and it was caused by the uncertainty of air and refrigerant temperature measurements. The experimental results show that, the heat transfer coefficient increases almost by a factor of two, where air leaves and refrigerant enters the heat exchanger. In this part of the evaporator, the temperature difference between fin root and air, which is used to determine the heat transfer coefficient, is of the order of magnitude of the measurement uncertainty (0.2°C). This results in a poor knowledge of the local heat transfer coefficient. The standard deviation was found for the highest and the lowest heat transfer coefficient variations and it was 2.33 and 1.49 for mean values of 27.7 and 21.0 (W/m^2K), respectively. Therefore, for the worst case, the value of the heat transfer coefficient is known within 25% for 99.7% confidence.

Comments about the System Performance

The analysis of the evaporator heat exchanger must be also performed in the context of the complete system performance, in order to obtain a thorough understanding of the heat exchanger duty. Several aspects of the system performance were discussed below: the COP, the pressure ratio in the system, individual evaporator and condenser pressures, and the compressor power requirements as a function of composition.

Fig. 3.10 shows the COP for the system as a function of composition. The highest COP was recorded for a composition of 91% R22. At this composition

the COP was 14% higher, than the COP of pure refrigerant R22.

Fig. 3.11 describes the change in compressor power requirements as a function of composition. The power requirement is the lowest for a composition of 91% R22. It is higher (19.5%) both for 100% R22 and for mixture compositions lower than 91% R22. Since R114 has higher vapor specific volume than R22, the compressor power requirement increases, as more R114 is added to the system, to maintain the same evaporator capacity. As the power requirement increases, so does the mixture pressure drop through the evaporator. Fig. 3.12 shows the pressure drop in the evaporator as a function of refrigerant mixture composition.

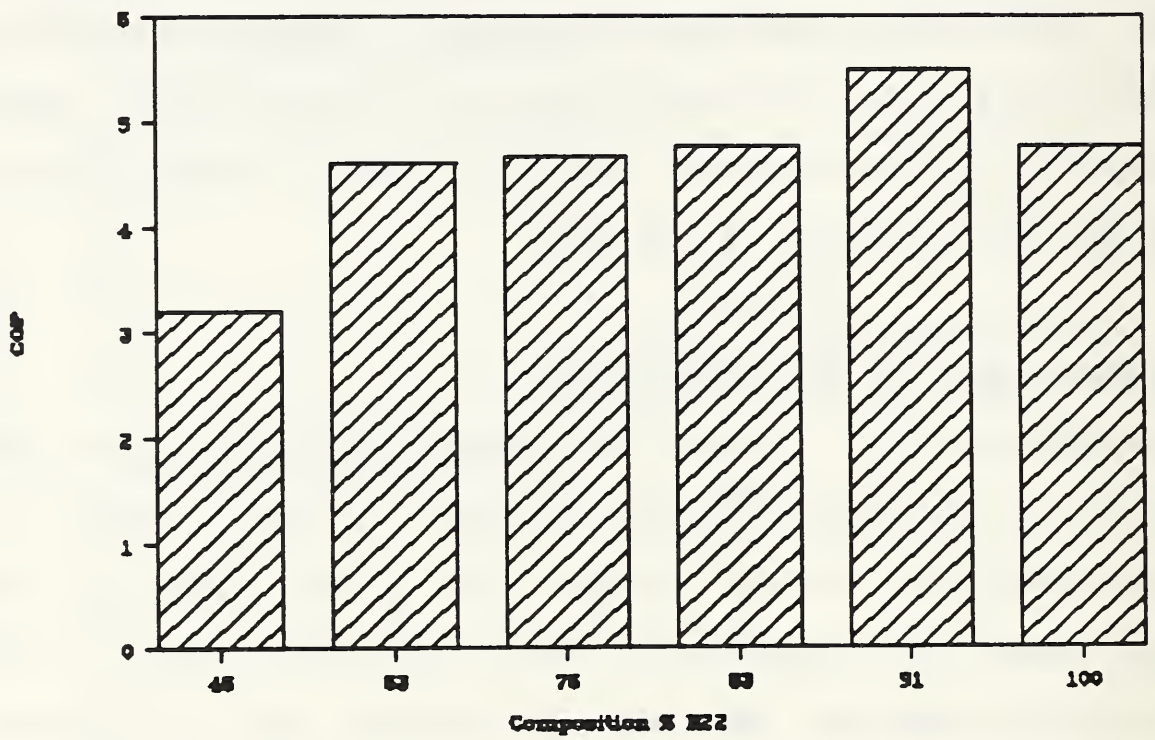

Figure 3.10 COP as a function of mixture composition.

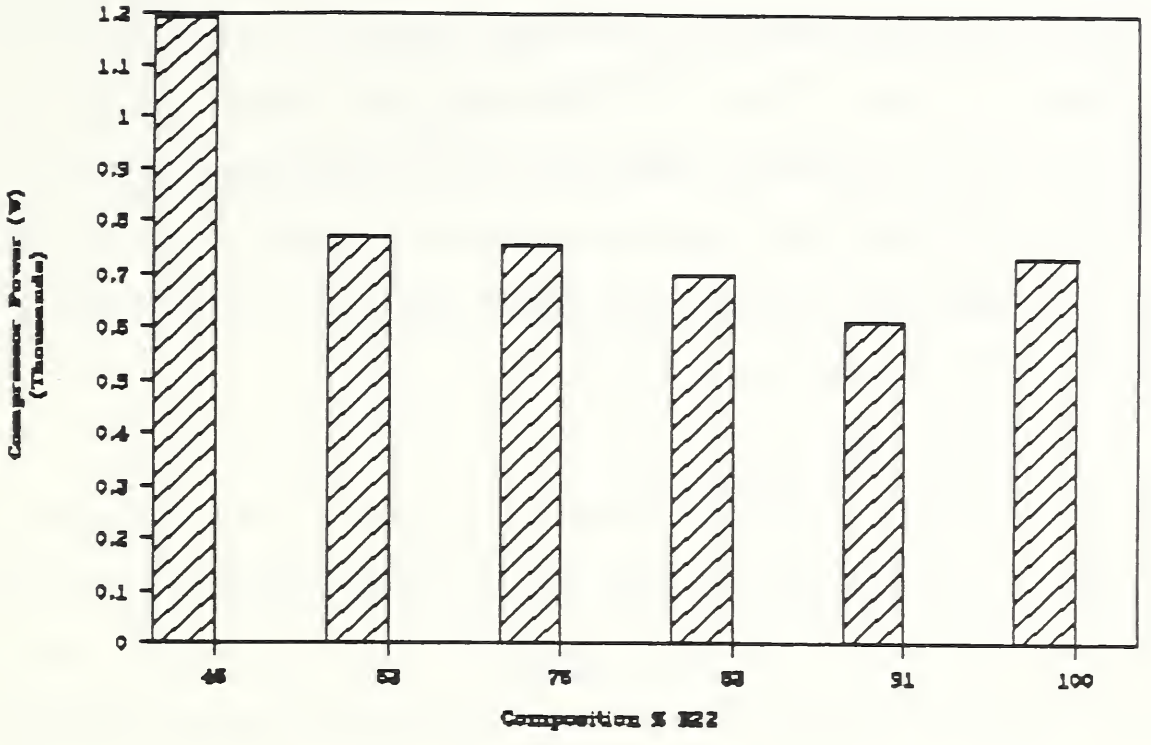

Figure 3.11 Compressor power requirement versus composition.

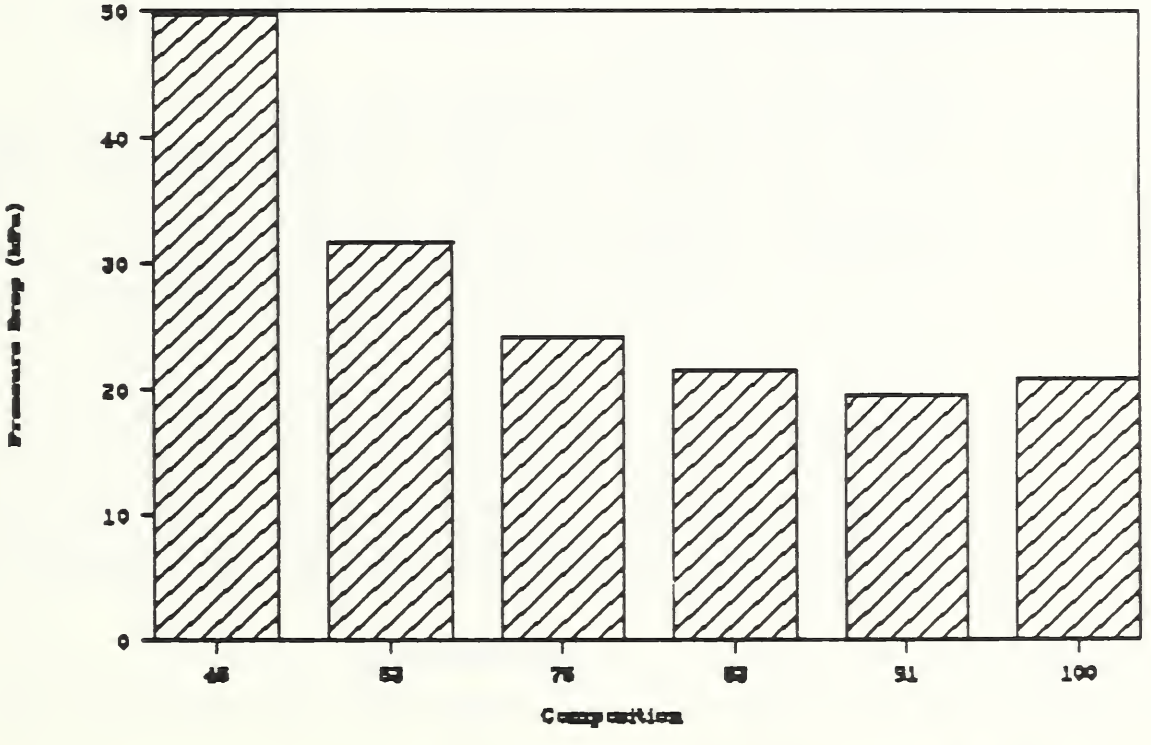

Figure 3.12 Pressure drop in the evaporator heat exchanger.

Pressure ratio across the compressor is also a function of composition. The addition of R114 causes the absolute pressure in both evaporator and condenser to drop. Fig. 3.13 shows that the lowest pressure ratio was observed for the mixture composition of 91% R22, because the condenser pressure decreased more than the evaporator pressure. The pressure ratio was 4.4% higher for the pure refrigerant test and it also increased for the tests with lower compositions of R22.

Fig. 3.14 shows the absolute values of pressure in the evaporator and the condenser. As more R114 is added to the system, the pressure both in the evaporator and in the condenser decreases. Initially, however, the pressure in the condenser decreased faster, than the pressure in the evaporator. For

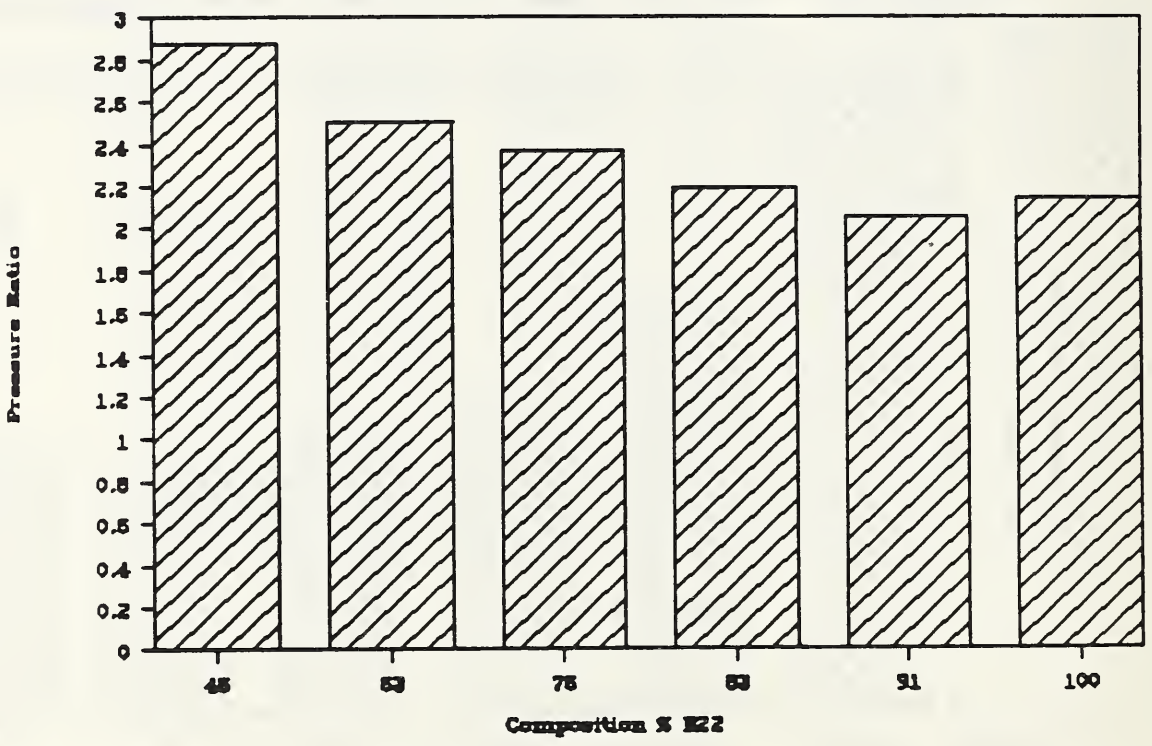

Figure 3.13 Pressure ratio across the compressor versus composition.

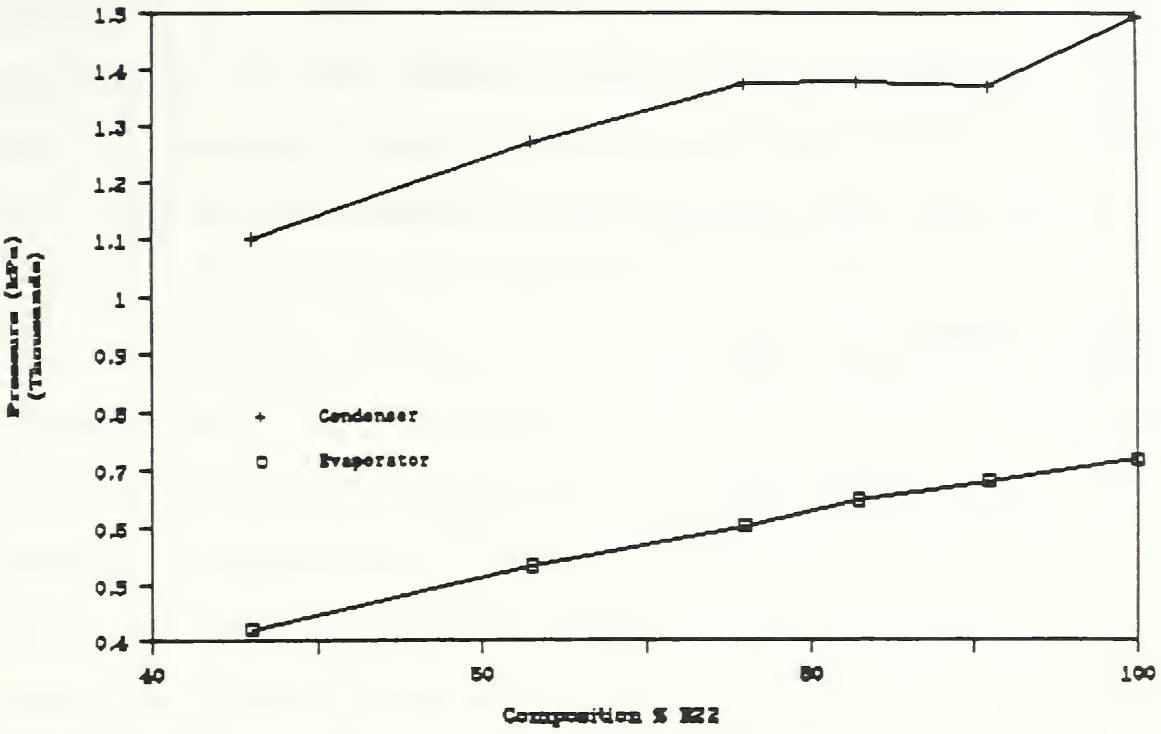

Figure 3.14 Evaporator and condenser pressure versus composition.

high compositions of R22, the pressure in the condenser fell by 9.1% and stayed constant until the composition of R22 reached about 75%. At the same time, for high compositions of R22, the pressure drop in the evaporator was 5.6% and it fell almost uniformly with the mixture composition change. This explains the reason for the highest COP at 91% R22.

For this specific heat exchanger, a small amount of R114 in the mixture, provided the best overall performance of this experimental apparatus. Further addition of the refrigerant R114 to the mixture decreased the performance. The reasons for this behavior are that, the refrigerant R114 is a less volatile one, with higher boiling pressure, lower capacity and lower density compared to R22. Since R114 has lower capacity, then to

provide the same gain on the air side, the compressor has to use more power. However, a compressor is a constant capacity machine and the addition of more R114, which is less dense than R22, causes it to pump less refrigerant and therefore the experimental apparatus provides lower refrigerating capacity.

VARIABLE OUTDOOR LOAD TESTS

The variable outdoor load tests were performed at the following three outdoor chamber temperatures: 27.8°C (82 F), 32.2°C (90 F) and 36.7°C (98 F). While the outdoor chamber temperature was changed for each test, the compressor speed was kept constant. Just as an actual air conditioning system would automatically adjust the superheat amount in response to a heavier load, the expansion valve opening was adjusted manually for different outdoor temperatures to maintain the saturated vapor leaving the evaporator. Similarly to the constant capacity tests, the performance of the heat exchanger under these conditions was analyzed. Two sets of tests were conducted; one at a composition of 57% R22 and the other at 100% R22.

In Fig. 3.15 the COP achieved at each test is shown. As the outdoor temperature increases, the COP decreases. The reason for this behavior is that, in response to the increasing outdoor temperature, the refrigerant temperature level in the evaporator increases as well. The evaporator, having the working fluid at a higher temperature, produces lower capacity. At the same time, the compressor has to pump refrigerant to a higher temperature level to affect the heat exchange in the condenser. Therefore, the COP drops.

The condensate profile (Fig. 3.16) is similar to that in constant capacity tests (Fig. 3.5). For cases, when the composition of the mixture was low in R22, hardly any condensate was collected in the first few rows, while the most was gathered in the last four rows. This was also the case for the variable load tests. Since the composition of the mixture was 57%, the majority of condensate was collected in the end part of the heat exchanger. As the outdoor temperature was increased, the amount of condensate collected decreased. The reason for this behavior was that, the refrigerant temperature went up together with the outdoor temperature. The higher refrigerant temperature level meant that less condensate could be collected.

The heat profiles shown in Fig. 3.17 resemble those at constant capacity for lower compositions of R22. The heat transfer is more evenly distributed for all banks. It is characteristic to see an inflection point in the heat profile at a point, where air temperature has dropped to the local dew point and the condensate begins to form. In the front part of the heat exchanger, the most of the sensible heat transfer occurs, while in the latter part it is the latent heat which dominates. As the outdoor temperature increases, the heat profile, while maintaining its shape, drops off. The drop-off is smaller in the front part and larger in the end part of the heat exchanger.

Fig. 3.18 shows the amount of the latent and the sensible heat for varying outdoor temperature. For the lowest outdoor temperature,i.e. 27.8°C (82°F), the latent heat is 33.5% of the sensible heat. For 36.7°C (98°F), the latent heat is 27.7% of the sensible heat. This is consistent with results in Fig. 3.17, which shows the heat profiles. For higher outdoor temperature,

a drop in the sensible heat is lower than the drop in the latent heat. As a result of this, the latent heat as a percentage of the sensible heat, decreases with the increase in the outdoor temperature.

Fig. 3.19 presents the air temperature profile for the heat exchanger. The air temperature profile for the three different outdoor temperatures is almost the same. The temperature drop for all three cases is approximately 13°C, and the slope of the temperature change is uniform.

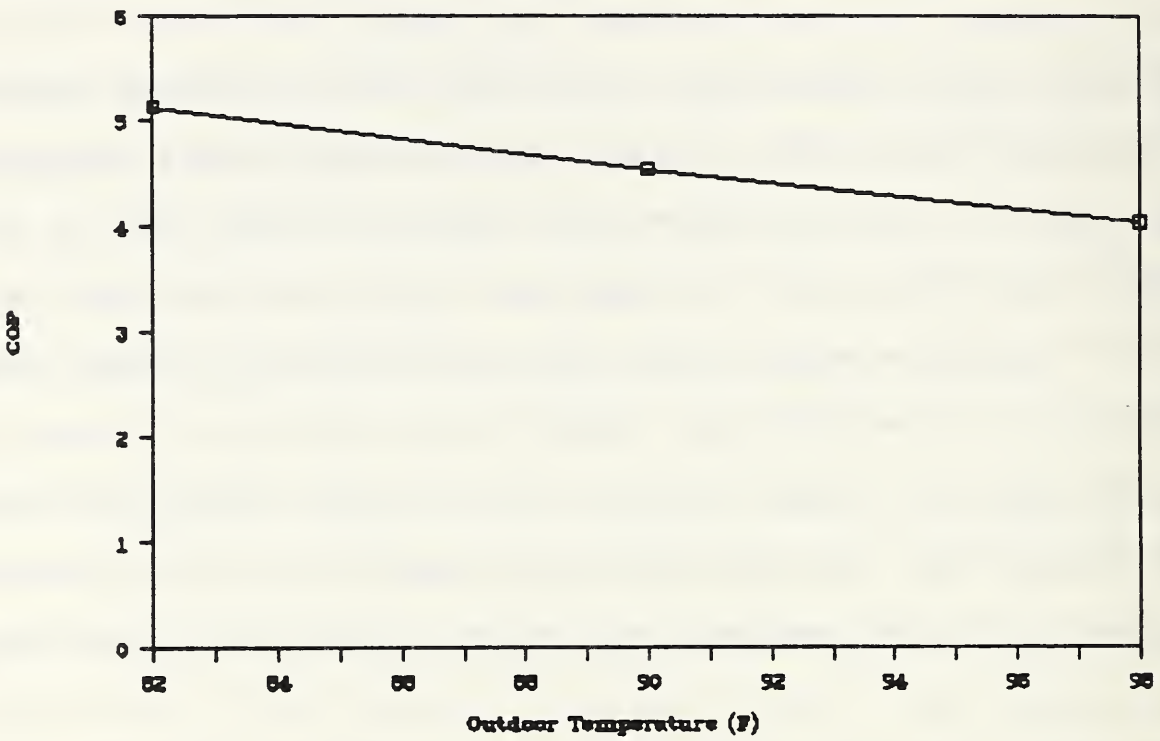

Figure 3.15 System COP for different outdoor temperatures for 57% R22/R114.

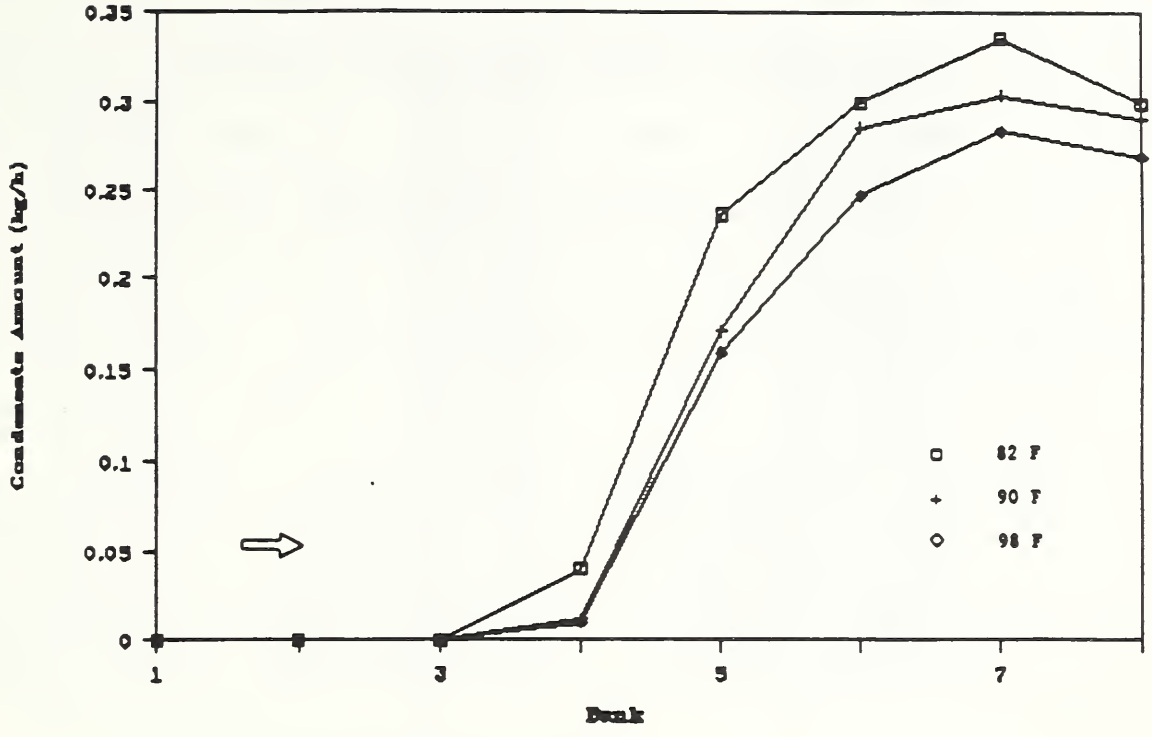

Figure 3.16 Condensate profiles for various outdoor temperatures for 57% R22/R114.

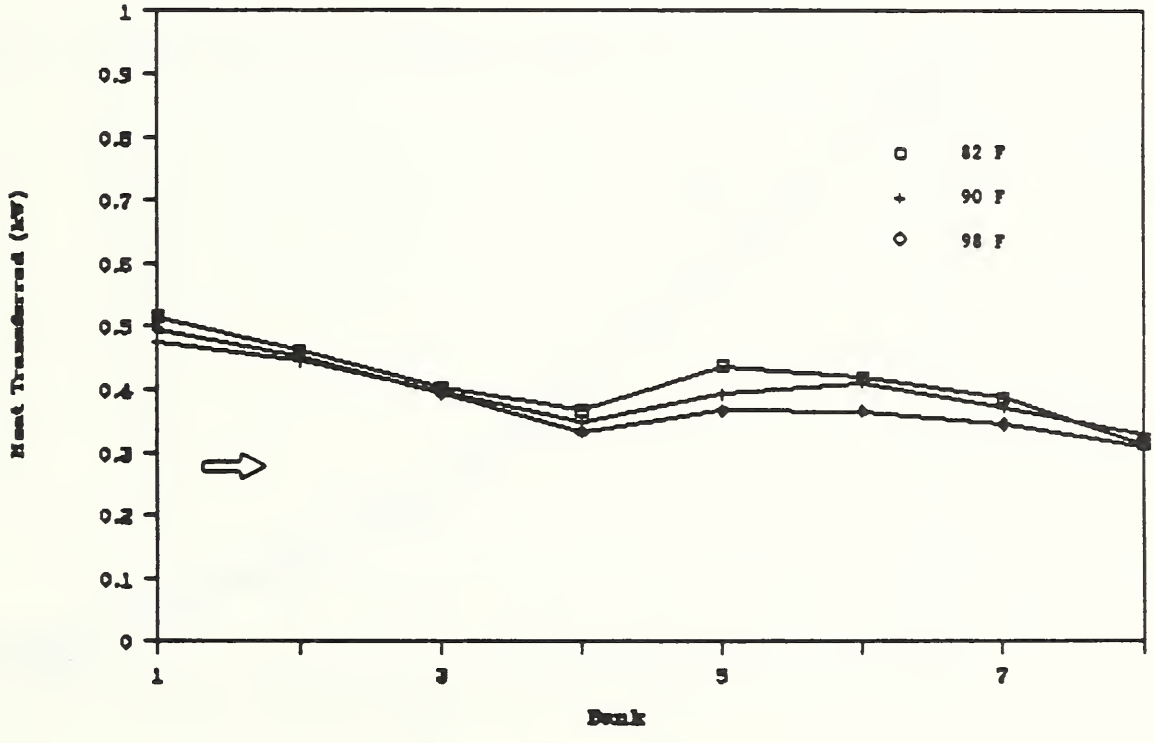

Figure 3.17 Heat profile for various outdoor temperatures for 57% R22/R114.

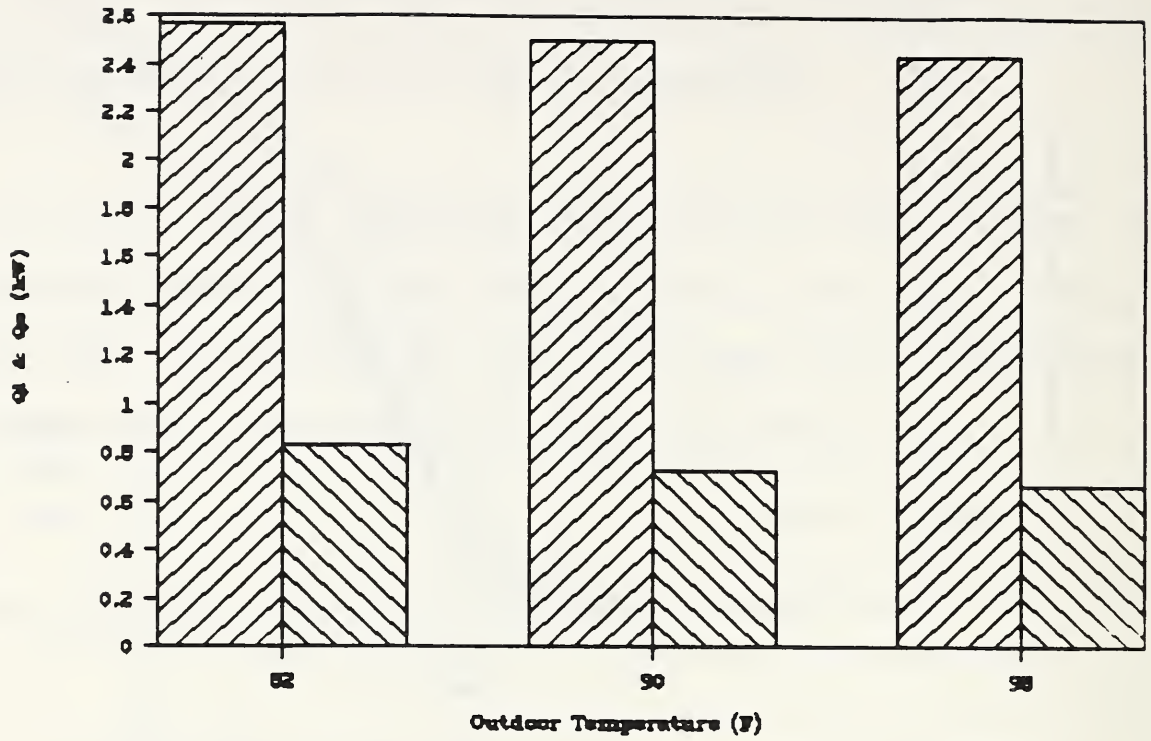

Figure 3.18 Latent and sensible heat for various outdoor temperature for 57% R22/R114.

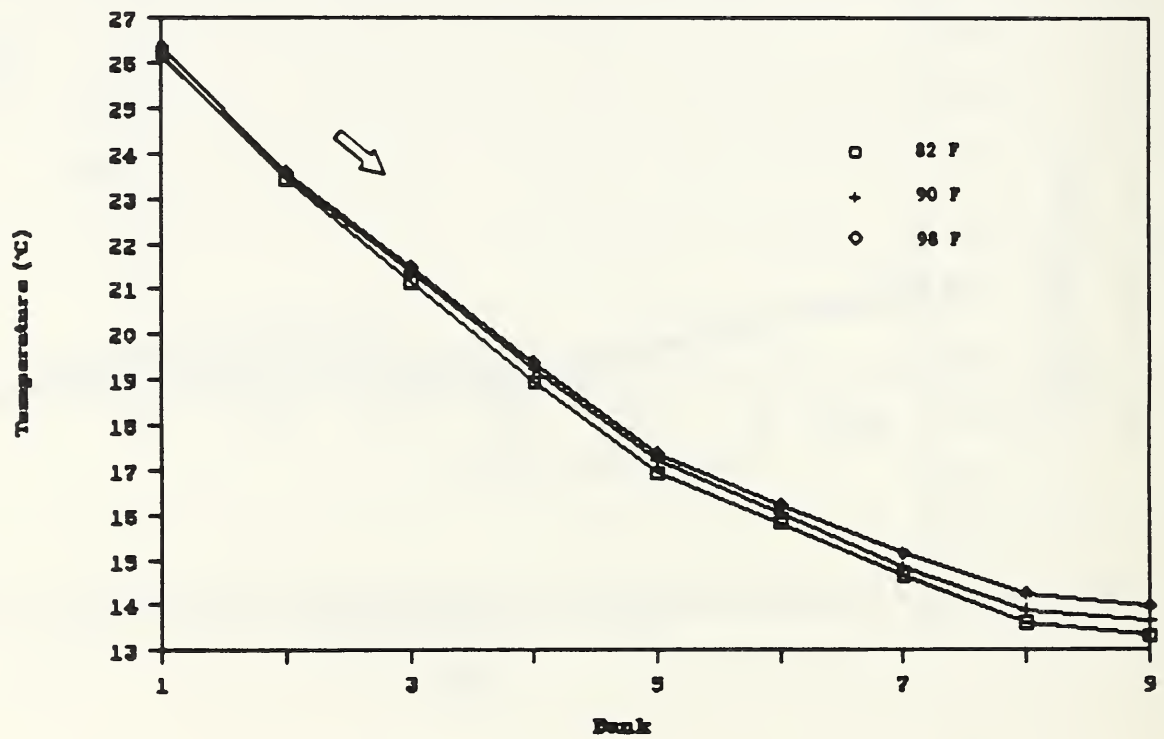

Figure 3.19 Air temperature profiles for various outdoor temperatures for 57% R22/R114.

For a better understanding of the effect of the outdoor temperature on the performance of the mixture, tests were run with 100% R22 at the same outdoor temperatures and compared. Fig. 3.20 shows the change in COP with the change of the outdoor temperature. As outdoor temperature increases, the COP drops. For all outdoor tests, the COP of 100% R22 tests was higher than that of the mixture. This is consistent with the results of the constant capacity tests, for which a mixture of 57% R22 would have lower COP than 100% R22 test. At the lowest outdoor temperature, i.e. 27.8°C (82°F), the mixture's COP decreases the most, compared to 100% R22 test. For the two higher outdoor temperatures, COP of mixture tests is only slightly lower than COP of pure R22 tests. The condensate profile, shown in Fig. 3.21, is

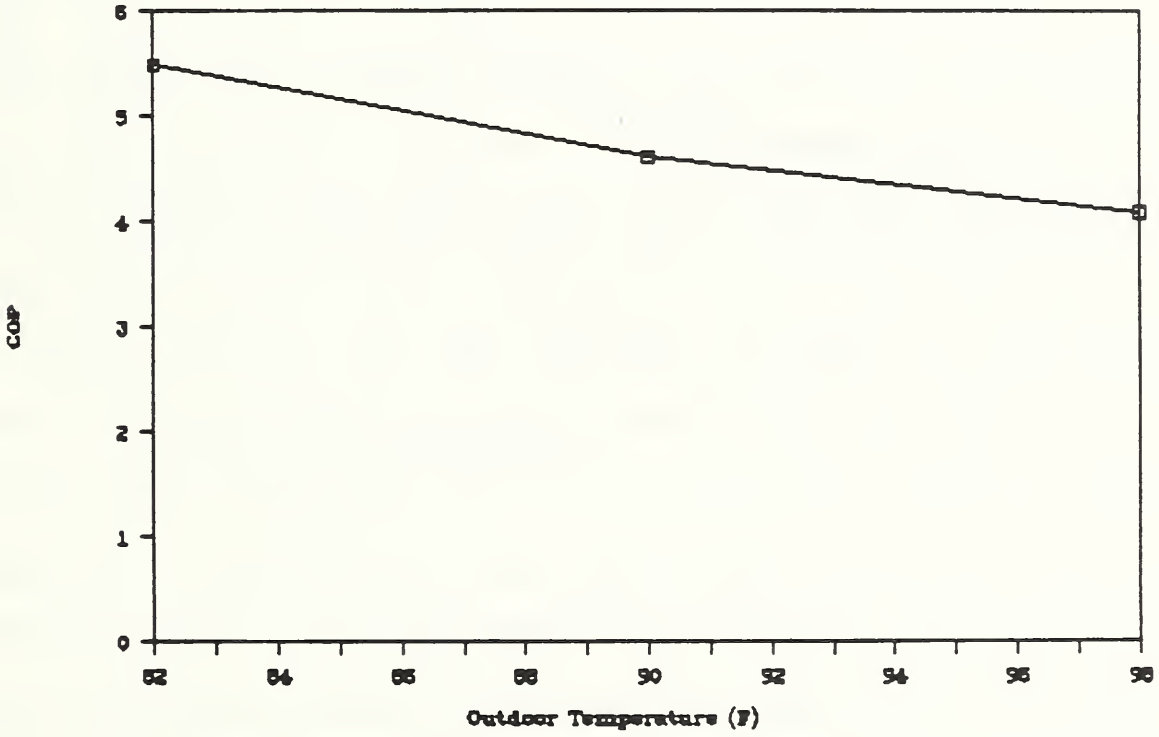

Figure 3.20 COP for various outdoor temperatures for 100% R22.

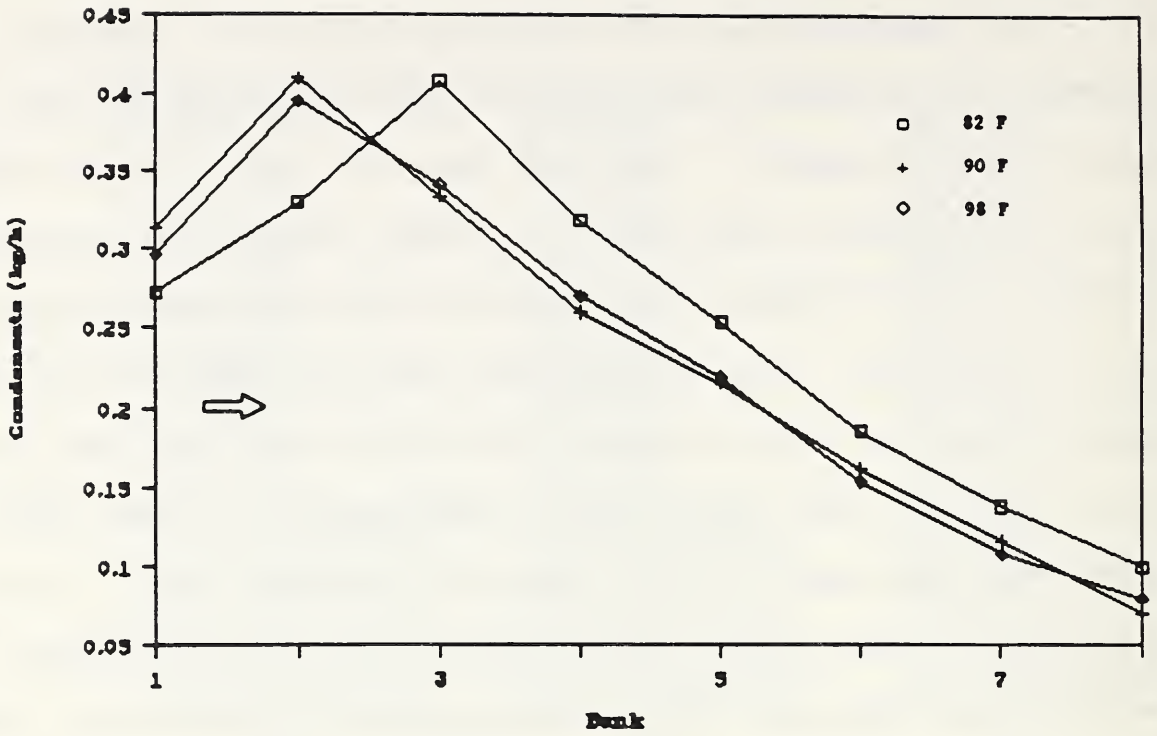

Figure 3.21 Condensate profiles for various outdoor temperatures for 100% R22.

significantly different from a similar profile for the mixture test. In this case, the greatest amount of condensate is obtained in the second and the third bank counting from the front of the heat exchanger. From there, the condensate amount drops off sharply to the last bank. Such condensate distribution is caused by the fact that, the compressor speed remains constant, while only R22, which has higher capacity than mixture, circulates in the apparatus. As a result of this, the same amount of air crossing the heat exchanger is cooled much faster, in the front part of the heat exchanger. Since R22 has a constant evaporating temperature throughout the heat exchanger, which is below the dew point for these tests, much more condensate is collected in the front banks, than for a mixture test.

This condensate distribution is supported by heat and air temperature

profiles in the heat exchanger for 100% R22 tests. The heat and air temperature profiles are shown in Figs. 3.22 and 3.23, respectively. The slope of both profiles is steep in the front part of the heat exchanger. Both level off after the third bank. The air temperature drop for pure R22 is 16°C, compared with 13°C for mixture test, which again shows that pure R22 possesses higher cooling capacity then mixture.

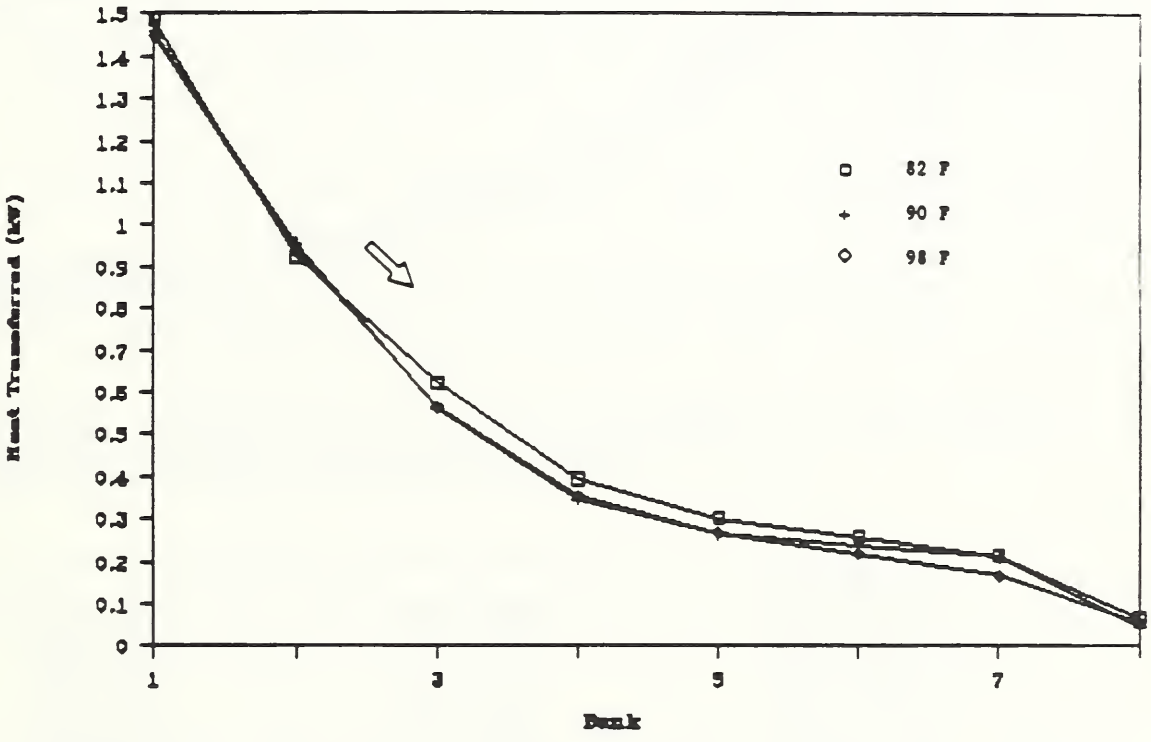

Figure 3.22 Heat profiles across the heat exchanger for various outdoor temperatures for 100% R22.

The ratio of the latent load to the sensible load for pure R22 tests is different than that, observed for the mixture tests. The latent load is 46% to 47% of the sensible load at all three outdoor temperatures. The reason for a high latent load is that a refrigerant temperature is below the dew point across the heat exchanger. As the outdoor temperature increases, sensible and latent loads decrease by the same percentage. Fig. 3.24

presents the latent and the sensible heat for a 100% R22 test.

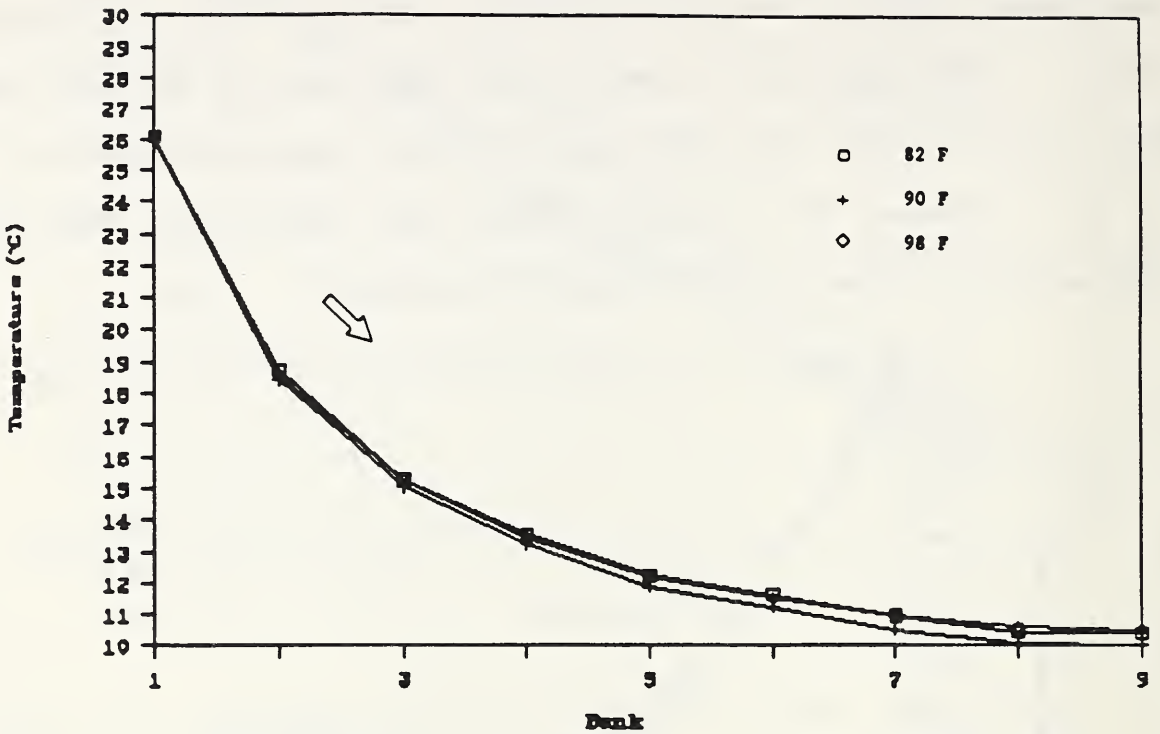

Figure 3.23 Air temperature profiles across the heat exchanger for various outdoor temperatures for 100% R22.

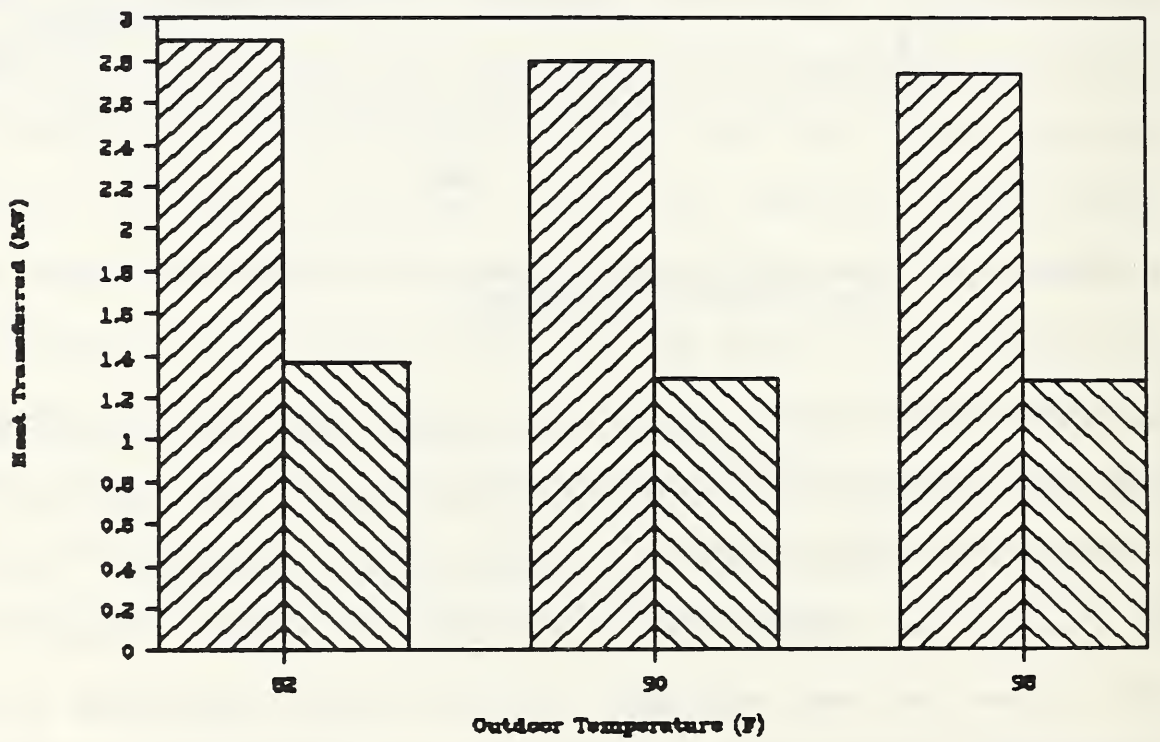

Figure 3.24 Latent and sensible heat for various outdoor temperature for 100% R22.

Section 4

DEVELOPMENT OF EFFECTIVENESS/NTU RELATIONS

In this chapter, two methods of an increasing level of sophistication of deriving effectiveness/NTU relations were presented. These relations are known for a case, where both fluids have constant specific heats (or they are assumed constant) and there is no change of phase in either of the fluids. The implicit assumption made in the derivation of these relations is that, the specific heat and the heat transfer coefficients are constant. This is not true for a heat exchanger which uses a refrigerant mixture with a variable specific heat during evaporation and for a typical air conditioning application, where moist air flows through the heat exchanger. Therefore, these physical phenomena must be included in the design procedure of any heat exchanger using a refrigerant mixture.

Immediately below is a discussion regarding the use of ϵ/NTU relation with assumed constant specific heat. This is followed by the derivation of the ϵ/NTU relation for a wet coil. The ϵ/NTU relation is then incorporated (Section 6) in the design procedure of a heat exchanger using nonazeotropic refrigerant mixture.

EFFECTIVENESS/NTU RELATION FOR A CONSTANT SPECIFIC HEAT REFRIGERANT

The effectiveness/NTU relation for a counterflow heat exchanger using a constant specific heat fluid may be represented by the following equation which is derived in [26]:

$$\epsilon = \frac{1 - \exp(-NTU \cdot (1 - C_{min}/C_{max}))}{1 - (C_{min}/C_{max}) \cdot \exp(-NTU \cdot (1 - C_{min}/C_{max}))} \qquad (4.1)$$

where C_{min} and C_{max} are the minimum and maximum capacity rates, respectively. In this case, air is the minimum capacity rate fluid and the refrigerant, a maximum capacity rate fluid.

The following assumptions were made in the development of this relation:

— constant refrigerant and air specific heats,
— no change in phase in either of the fluids,
— constant heat transfer coefficient,
— constant mass flow rate of air and refrigerant.

To account for various mixture compositions, the value of the refrigerant capacity rate is recalculated. In this way, a family of curves may be obtained for the whole range of compositions of a particular mixture.

EFFECTIVENESS/NTU RELATION FOR A WET COIL

The following observations were made in the development of the effectiveness/NTU relation for a wet coil:

— a variable mixture specific heat,
— a constant air specific heat,
— experimentally derived air temperature profile,
— experimentally derived heat profile (includes a phase change of the moist air).

The subsequent equation for ϵ/NTU relationship could be solved in terms of either quality or the nondimensinalized length of the heat exchanger along the air path. In the first case, polynomials representing the specific heat, heat profile and air temperature profile were developed in terms of quality. In the second case, these polynomials were presented in terms of the nondimensionalized length. Since the only difference in the two approaches was in the complexity of the computer model, only the first one was shown here.

The heat profile across the heat exchanger was defined as a function of the refrigerant quality. The amount of heat transferred to each bank was determined experimentally. The average refrigerant quality in each bank was found by applying the refrigerant temperature profiles obtained from the tests in the CSD equation of state routines. Even though the heat profile is a linear function of quality (this line would have a different slope depending on the composition), it is nonlinear in terms of the nondimensionalized length. Therefore, in order to have a generalized function, the heat profile through the heat exchanger was represented by the following polynomial function:

$$Q(z) = Q_0 + Q_1 \cdot z + Q_2 \cdot z^2 + Q_3 \cdot z^3 + Q_4 \cdot z^4 \qquad (4.2)$$

Similarly, as was explained in detail in the previous chapter, the air temperature profile through the heat exchanger is parabolic. The degree of curvature depends on the composition of the refrigerant mixture. The temperature profile in terms of quality is represented by the following

polynomial function:

$$T_a(z) = T_{a0} + T_{a1} \cdot (-z+1) + T_{a2} \cdot (-z+1)^2 \qquad (4.3)$$

For mixtures, a change in enthalpy is accompanied by a change in temperature, and the following thermodynamic definition of specific heat at constant pressure is utilized in the calculations:

$$c_p = (\partial h/\partial T)_p \qquad (4.4)$$

This is an apparent specific heat for mixtures, which can be used for evaluation of thermal performance in the two phase region.

To generalize the development of the procedure, the calculations were performed in terms of dimensionless enthalpy, which, at any point in the heat exchanger, is denoted as z and is defined as $(h-h_i)/(h_o-h_i)$, where the subscript "i" refers to the inlet and the subscript "o" refers to the outlet. For an evaporator, variable z also represents the quality.

The specific heat of the refrigerant may assume any functional variation with z. It may be represented by the following equations at any value z:

$$c_{p,z} = c_{p,i} + (c_{p,o}-c_{p,i}) \cdot z \qquad (4.5)$$

$$c_{p,z} = c_{p,i} + (c_{p,o}-c_{p,i}) \cdot z^2 \qquad (4.6)$$

where $c_{p,i}$ is the specific heat at inlet conditions, $c_{p,o}$ the specific

heat at outlet conditions. If the pressure-enthalpy diagram is known for the mixture under consideration, the properties $c_{p,i}$ and $c_{p,o}$ can be easily determined. These values were generated with the algorithms from [25] that implement the CSD equation of state.

Figure 4.1 shows the schematic of air and refrigerant temperature profiles in an evaporator with respect to variable z. A differentially small amount of heat dQ, equal to Q(z)dz, will be transferred to refrigerant, with a corresponding change in temperature dT_b. The heat balance on a differentially small segment for the refrigerant side of the heat exchanger can be written as follows:

$$Q(z)dz = \dot{m}_r \cdot c_{p,z} \cdot dT_r \tag{4.7}$$

Rearranging and integrating, the following relationship is obtained:

$$\int_0^1 \frac{Q(z)\ dz}{c_{p,z}} = \dot{m}_r \cdot \Delta T_r \tag{4.8}$$

Utilizing the relationship for the mean specific heat of the refrigerant and multiplying both sides of equation (4.8) by $1/Q_t$, the following expression is obtained:

$$\frac{1}{\bar{c}_{p,z}} = \frac{1}{Q_t} \int_0^1 \frac{Q(z)\ dz}{c_{p,z}} \tag{4.9}$$

In the above expressions, Q_t, the total amount of heat transferred in the heat exchanger, should be substituted into the equations.

The relationship for a refrigerant temperature at an arbitrary value of z is

derived by first integrating equation (4.7):

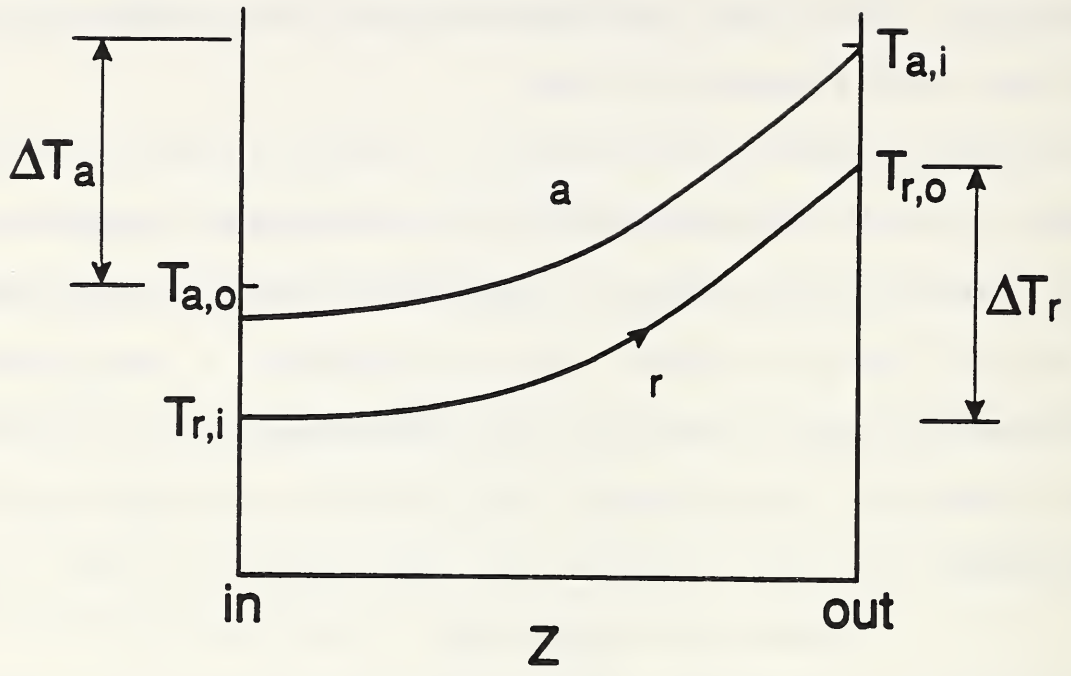

Figure 4.1 Schematic of the process occurring in the heat exchanger.

$$\int_0^z \frac{Q(z)}{c_{p,z}} dz = \dot{m}_r \cdot (T_{r,z} - T_{r,i}) \tag{4.10}$$

Multiplying by $1/Q_t$, utilizing the relationship (4.8) and rearranging, the following result is obtained:

$$\frac{1}{\bar{c}_{p,z}} = \frac{1}{Q_t} \frac{\Delta T_r}{T_{r,z}-T_{r,i}} \int_0^z \frac{Q(z)}{c_{p,z}} \tag{4.11}$$

Setting equation (4.9) and the above equal, the following relationship for the refrigerant temperature at any point in the heat exchanger is obtained:

$$\frac{T_{r,z} - T_{r,i}}{\Delta T_r} = \frac{\int_0^z \frac{Q(z)}{c_{p,z}}\, dz}{\int_0^1 \frac{Q(z)}{c_{p,z}}\, dz} \tag{4.12}$$

The refrigerant temperature at any distance z may be obtained by integrating the above expression. A term generally used in heat exchanger design is the temperature effectiveness, denoted by ϵ. Using the symbols shown in Fig. 4.1, the temperature effectiveness on the air side, denoted by ϵ_a, is defined as follows:

$$\epsilon_a = \frac{T_{a,i}-T_{a,o}}{T_{a,i}-T_{r,i}} = \frac{\Delta T_a}{T_{a,i}-T_{r,i}} \tag{4.13}$$

The differential heat balance for the heat transferred from air to refrigerant can be written as:

$$dQ = U \cdot (T_{a,z} - T_{r,z}) \cdot dA \tag{4.14}$$

Here infinitesimal amount of heat from air to refrigerant can be represented as follows:

$$dQ = Q(z) \cdot dz \tag{4.15}$$

where Q(z) is a polynomial fit of the heat transferred profile through the heat exchanger. Substituting this differential heat flow into equation

(4.14) and rearranging, results in the following:

$$dA = \frac{Q(z)}{U} \frac{dz}{T_{a,z}-T_{r,z}} \tag{4.16}$$

Multiplying both sides by $U\Delta T_a/Q_t$, where Q_t is the total amount of heat transferred, and rearranging, the following expression for NTU is obtained:

$$NTU = \frac{1}{Q_t} \int_0^1 \frac{\Delta T_a \cdot Q(z)}{T_{a,z}-T_{r,z}} dz \tag{4.17}$$

Utilizing the experimentally derived expressions for $Q(z)$, $T_{a,z}$ and the refrigerant temperature $T_{r,z}$ from equation (4.12), the final expression for NTU for a wet coil is as follows:

$$NTU = \frac{1}{Q_t} \int_0^1 \left(\frac{1}{\epsilon_a Q(z)} + \frac{T_{a1}(-z+1)+T_{a2}(-z+1)^2}{\Delta T_a \quad Q(z)} - \frac{\Delta T_r}{\Delta T_a Q(z)} \frac{\int_0^z \frac{Q(z)dz'}{c_{p,z'}}}{\int_0^1 \frac{Q(z)dz'}{c_{p,z'}}} \right)^{-1} dz \tag{4.18}$$

Physical Significance of Effectiveness/NTU Relationship

To understand the physical significance of equation (4.18), it was rewritten by applying the definition of effectiveness and by writing out the temperature components as well as moving ΔT_a outside of an integral since it was a

constant. Equation (4.19) reflects these changes:

$$NTU = \frac{\Delta T_a}{Q_t} \int_0^1 \left[\frac{T_{ai}-T_{ri}}{Q(z)} + \frac{T_{a1}(-z+1)+T_{a2}(-z+1)^2}{Q(z)} - \frac{\Delta T_r}{Q(z)} \frac{\int_0^z \frac{Q(z)dz'}{c_{p,z'}}}{\int_0^1 \frac{Q(z)dz'}{c_{p,z'}}} \right]^{-1} dz \tag{4.19}$$

The summation of terms under the integral must be equal U•A as the following analysis showss. The U•A term is a function of the temperature difference and a heat transfer at a specific location. Total sum of the ratio of the heat transferred over the appropriate temperature difference should be equal to U•A. The U•A term depends on the temperature level at which the heat transfer takes place and the slope of air and refrigerant temperature profiles.

The temperature level could be defined by specifying inlet air and refrigerant temperatures. The temperature difference between these two quantities, occurring at a localized value of the heat transfer, would be one component to influence U•A. This corresponds to the first term under the integral.

The second important factor influencing the U•A value, is the shape of air and refrigerant profiles at a localized value of heat transfer. The slope of air and refrigerant profiles could be defined by specifying how much a profile deviates from an inlet value. This is the way the second and the third terms are structured. The value of numerator of the second term determines by how much air temperature is different from its inlet value at

any location in the heat exchanger. The third term, which is a part of equation (4.12), is a change of the refrigerant temperature from its inlet value at a location z in the heat exchanger. Both the second and the third term are divided by the amount of heat transferred at this location. By subtracting the third term from the second, a temperature difference was obtained, which was the other driving force of the heat exchange between air and refrigerant.

The term U·A could be also explained in a simpler manner. A part of the first and the second term under the integral is an equation representing air temperature profile. Similarly, a part of the first and the third term is refrigerant temperature profile. The temperature difference between these two profiles occurring at a given Q(z) and summed over the whole heat exchanger yield U·A. Due to summation of these nonlinear terms in this manner, a correct ϵ/NTU relationship could be developed for each mixture composition. Equation (4.20) reflects these modifications.

$$NTU = \frac{\Delta T_a}{Q_t} \int_0^1 \left[\frac{T_{ai}+T_{a1}(-z+1)+T_{a2}(-z+1)^2}{Q(z)} - \frac{T_{ri} + \Delta T_r \cdot \int_0^z \frac{Q(z)dz'}{c_{p,z'}}}{Q(z) \quad \int_0^1 \frac{Q(z)dz'}{c_{p,z'}}} \right]^{-1} dz \qquad (4.20)$$

As a result of this analysis, the term U·A is fully defined for this type

of a heat exchanger by specifying air and refrigerant temperature quantities and their profiles, which affect the value of NTU.

Description of the Computer Model

A computer program was used to generate NTU as a function of effectiveness for a wet coil using equations derived above. All quantities were derived in terms of quality.

This program has the following inputs:

— overall mixture composition,
— liquid line temperature and pressure,
— evaporator inlet temperature and pressure,
— evaporator outlet pressure,
— refrigerant temperature polynomial coefficients,
— heat profile polynomial coefficients,
— air temperature polynomial coefficients.

The program has the following outputs:

— quality, temperature, enthalpy through the evaporator,
— specific heat of the mixture,
— NTU as a function of effectiveness.

The program uses the mixture temperature profile as a function of the thermocouple locations through the heat exchanger to provide the refrigerant enthalpy values along the refrigerant path. The ratio of the enthalpy

difference over the temperature difference is used to determine the specific heat of the evaporating refrigerant.

Depending on the mixture type and the composition, either a linear or a quadratic fit of the specific heat is generated in terms of the quality Similarly, polynomials representing the heat profile of the heat exchanger and the air temperature profile are used in terms of quality. The heat profile polynomial was developed from the experimental data by the use of the quantities of heat transferred at each bank.

The integrals containing the ratio of the heat profile over a specific heat profiles are calculated as follows. Since the degree of the numerator is higher than that of the denominator, the heat profile polynomial is first divided by the specific heat polynomial so that the degree of the numerator is lower than denominator. Two integrals are thus obtained, which then are integrated using the integral formulas included in the program. The main integral is integrated numerically.

The equation (4.19) is to be used to find NTU as a function of effectiveness for a wet coil. One of the inputs to this equation are the heat profile polynomial coefficients, which were obtained from the experimental data. The limitation in using these heat profiles is that, they are different for every mixture composition. A large number of tests would have to be made, to cover the whole range of mixture compositions as well as any conceivable mixture. To circumvent this problem, a program by Domanski [28] was modified and used to predict the heat exchanger heat profile. This program

simulates operation of a residential heat pump and it uses tube-by-tube approach in determining evaporator capacity. Refrigerant and air properties are calculated through the heat exchanger until the convergence criterion is met. Only the evaporator part of this program was used in the study.

Several modifications were made in the tube-by-tube program to ensure its correctness in predicting the amount of heat transferred to each bank. Initially, even though capacity predicted and recorded were within 5%, the program predicted results which did not conform to the experimental results for each bank. The modifications included using the new transport properties for R22/R114 mixture, a more sophisticated inside heat transfer coefficient [4], as well as a better manipulation of the data within the program. Since this evaporator model has never been used to predict capacity of a heat exchanger which had more than four rows, a simple relaxation technique was applied in determination of air temperatures and humidity ratio. After these modifications were incorporated into the program, the predicted and the experimental results were found to be in a good agreement. An example of verification of the experimental data is shown in Fig. 4.2 for mixture containing 83% R22. Similarly, a good agreement was found for other mixture compositions. The output of this program,i.e. the heat transferred to each bank was used as an input to the program which calculated NTU.

Problem Reduction from Three Dimensional to Two Dimensional

There were several reasons for reducing this problem from a three dimensional to a two dimensional one. The main reason was that the additional amount of calculations necessary to include crossflow would not produce added benefit

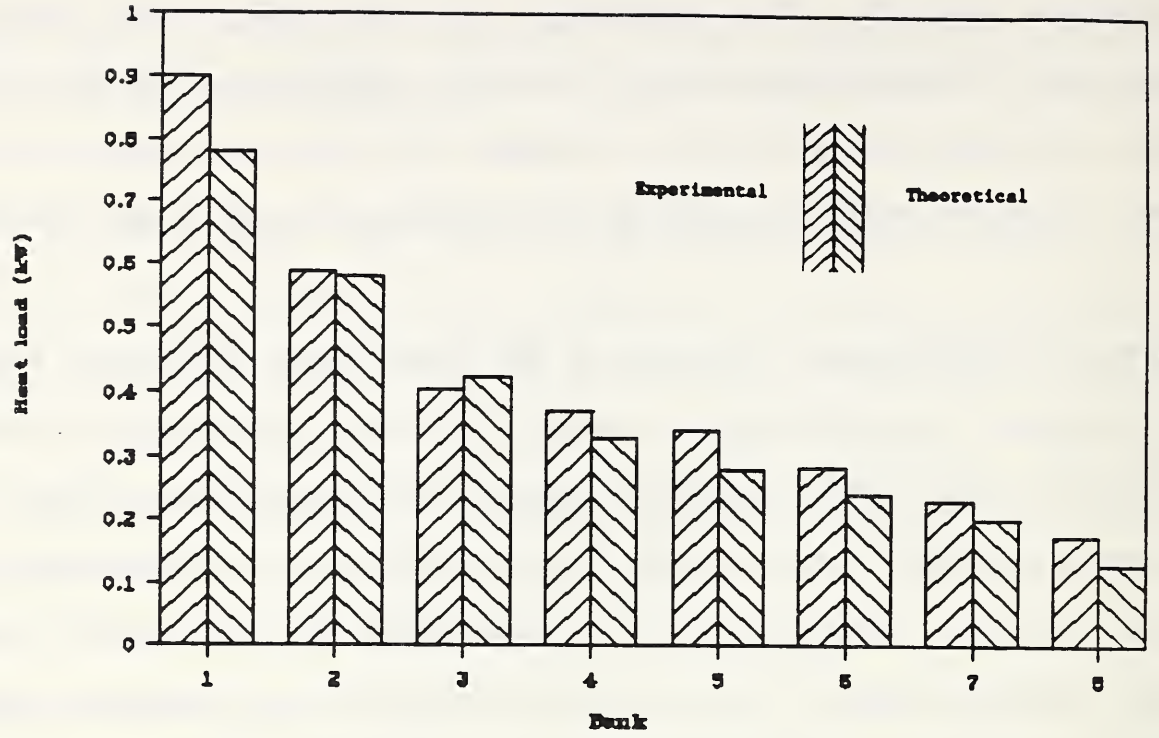

Figure 4.2 Experimental and theoretical heat transferred in each bank for 83% R22 by mass.

of a better design procedure. As a comparison between experimental and simulated results showed, the simplified two dimensional approach yielded satisfactory results.

There were other reasons as well. First, an ϵ/NTU method to determine a correlation for crossflow produces an unwieldy expression with many terms (this is the case for four passes in one row). Any physical significance is lost. In addition, a combination of crossflow and counterflow would undoubtedly result in an expression hard to use in practice.

The application of the LMTD method poses a different problem. LMTD is

usually calculated for either a counterflow or a parallel flow. Here, the LMTD for a counterflow would be calculated and a correction factor F would be applied to account for a crossflow. The problem is that for lower values of the correction factor, the correction curves have a very steep gradient. It means that a relatively small change in temperature conditions will cause a large change in F and consequently of the mean temperature difference. If calculations were made for each bank separately, the error associated with the correction factor would be compounded and overall LMTD could be vastly under- or overpredicted.

Apart from this, there were other overriding reasons for not using a standard ϵ/NTU or LMTD approach. In the ϵ/NTU development an operating line is established with a constant slope since it is assumed that the specific heat of both fluids is constant. LMTD method, while taking into account the flow pattern in the exchanger, disregards the phase change of a fluid, a constant specific heat is assumed as well as uniform heat release per degree drop in temperature. These conditions are violated in a heat exchanger working as an evaporator in the air conditioning application.

The problem could be solved using a finite difference method. It would involve solving numerically a sequence of eight differential equations. However, for a user such method would constitute a "black box," where data would be inputted and results outputted without understanding of the computational process. On the contrary, reduction of this problem to a two dimensional one, emphasis of the counterflow over the crossflow, showing the physical significance of the operational ϵ/NTU equation significantly

facilitates the solution of this problem. Due to the above reasons, a three dimensional problem was simplified to a two dimensional problem without significant alteration of the physical reference frame.

Section 5

VERIFICATION OF EFFECTIVENESS/NTU RELATIONS

In this Section, the theoretical predictions were compared with the experimental results. Among many experimental runs, the following were compared with the computer model predictions:

—— at composition of 76% R22 by mass both a dry and a wet coil test.

—— at composition of 46%, 63%, 76%, 83%, 91% R22 by mass, wet coil tests.

The experimental ϵ/NTU curves were derived in the following way. The overall heat transfer coefficient, the mass flow rate of air across the heat exchanger and the area of each bank were known. NTU was calculated separately for bank 1, for bank 1+2, for bank 1+2+3, etc. Similarly, effectiveness was determined for the above groups of banks using the known air and refrigerant temperatures. The theoretical ϵ/NTU curves were found as a function of ϵ and several experimentally derived parameters. The comparisons were made in the same order as the ϵ/NTU relation developments were made.

Verification of ϵ/NTU Relation Based on the Assumption of a Constant Specific Heat Refrigerant

This is the simplest model, for which one of the assumptions was that, the mixture has a constant specific heat. As seen in Fig. 3.8, the specific heat for a refrigerant mixture is not constant, but rather it can change by a factor of 2 to 5, as a mixture evaporates in the heat exchanger. Due to

this fact, a simple model can not adequately predict the performance of a mixture heat exchanger. In addition, the model does not contain any other quantities which may be used to describe operation of a heat exchanger. As an example, Fig. 5.1 shows that there is a poor agreement between the theory and the experimental run for a mixture composition of 46% R22.

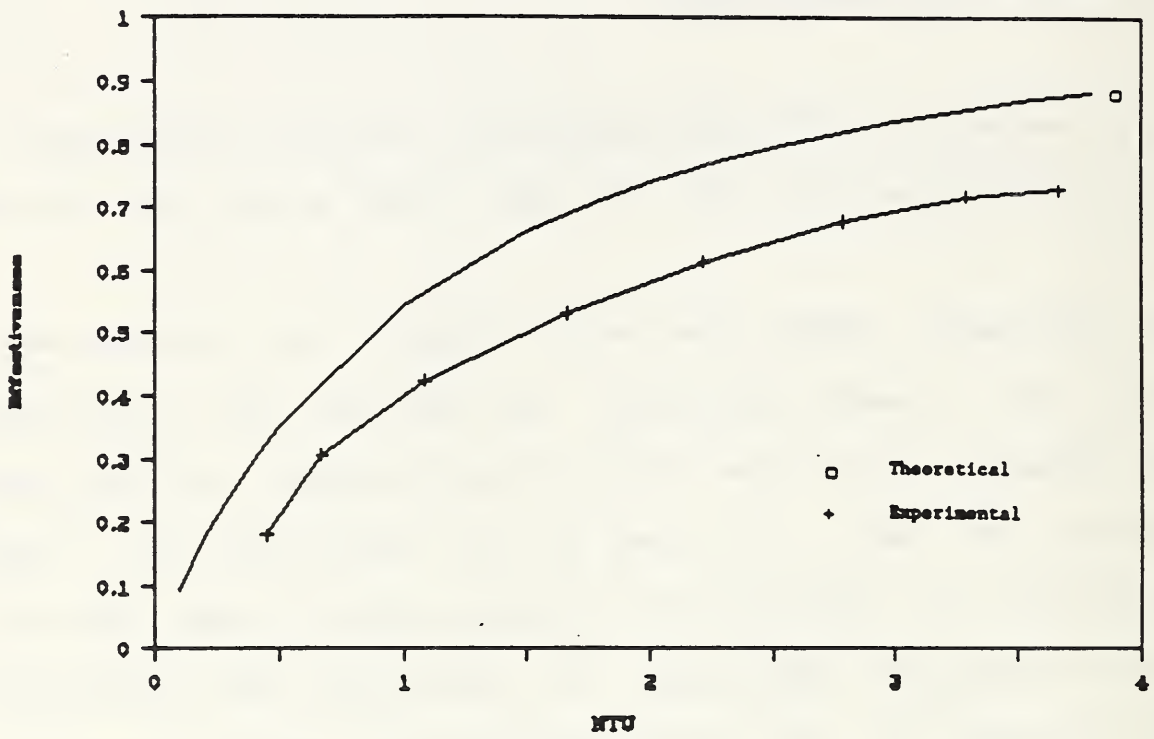

Figure 5.1 Theoretical ϵ/NTU curve for a constant specific heat refrigerant and the experimental result for 46% R22.

However, it is instructive to compare this model to a test result with a 100% R22. For a single component refrigerant, the specific heat is undefined and the ratio of the capacity ratios equals zero for practical calculations. In this case, equation (4.1) reduces to the following:

$$\epsilon = 1 - \exp(-NTU) \qquad (5.1)$$

This equation is valid for all types of flow patterns and it emphasizes that flow arrangement is unimportant where one capacity rate is very much greater than the other one. The theoretical curve developed with the use of equation (5.1) was compared with the experimental results for a 100% R22 test as shown in Fig. 5.2. There is a good correlation between this simple formula and the test results.

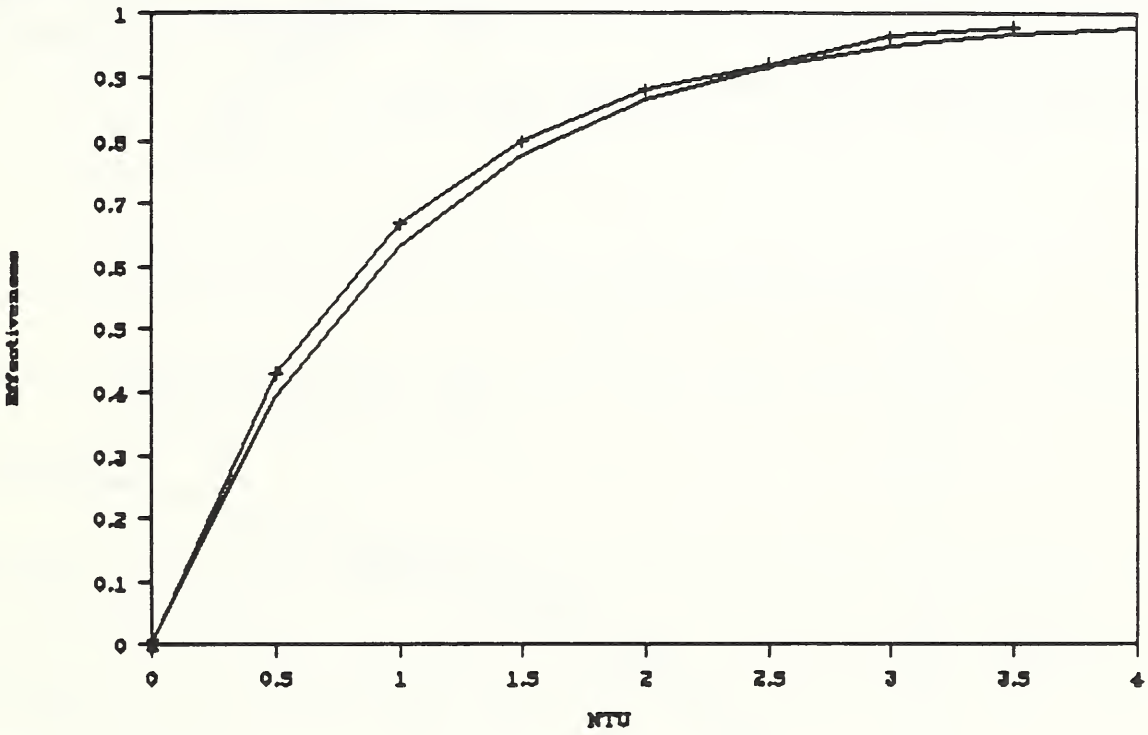

Figure 5.2 Theoretical and experimental relationship between effectiveness and NTU for 100% R22.

Verification of ϵ/NTU Relation for a Wet Coil

This model accounts for a variable specific heat of the mixture and it uses a heat and an air temperature profile appropriate for a given composition. Due to the fact that, the mathematical formulae reflects a realistic interaction between the refrigerant mixture and the air, there is a very

good agreement between the experimentally derived ϵ/NTU relation and the theoretical predictions. Fig. 5.3 shows both the experimental and the theoretical results for refrigerant composition of 46% R22. A mixture pressure drop is included in the derivation of the theoretical ϵ/NTU relation. Similarly, good agreement between the theory and the experiment was obtained for other compositions. Fig. 5.4 shows ϵ/NTU relations for compositions of 46%, 63% and 76% of R22. There is a consistently good agreement between the model and the experiment.

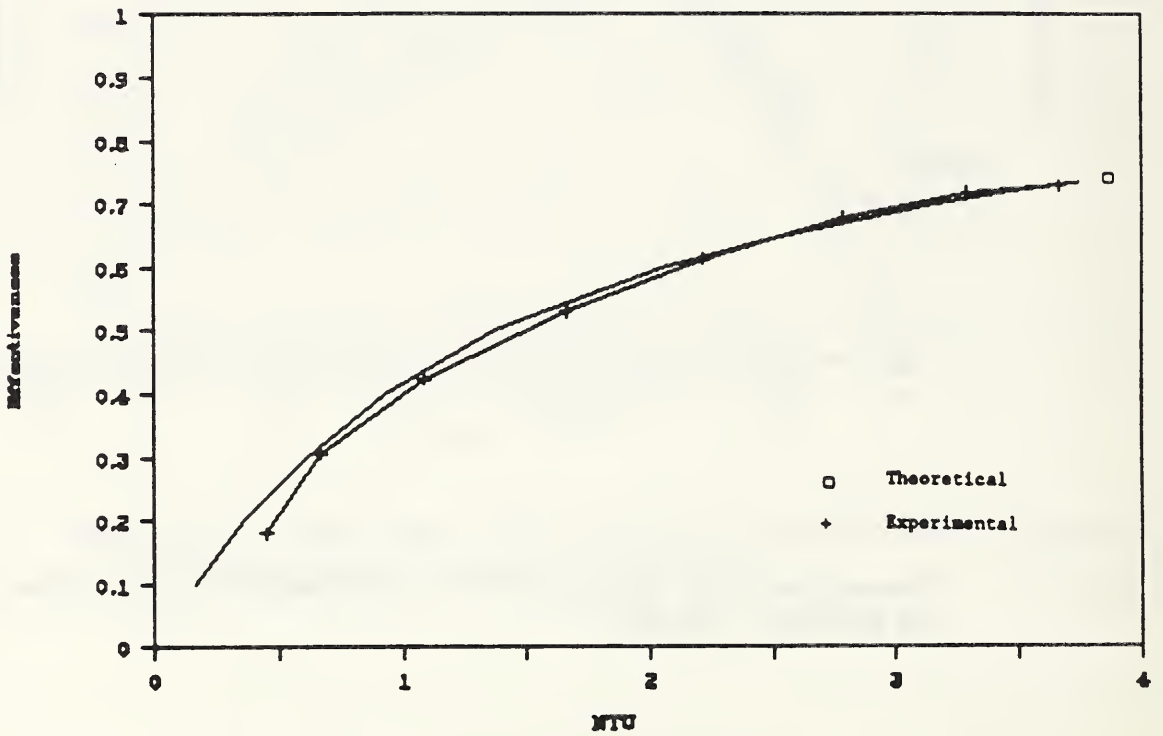

Figure 5.3 Comparison between theory and experiment for a wet coil at 46% R22 by mass.

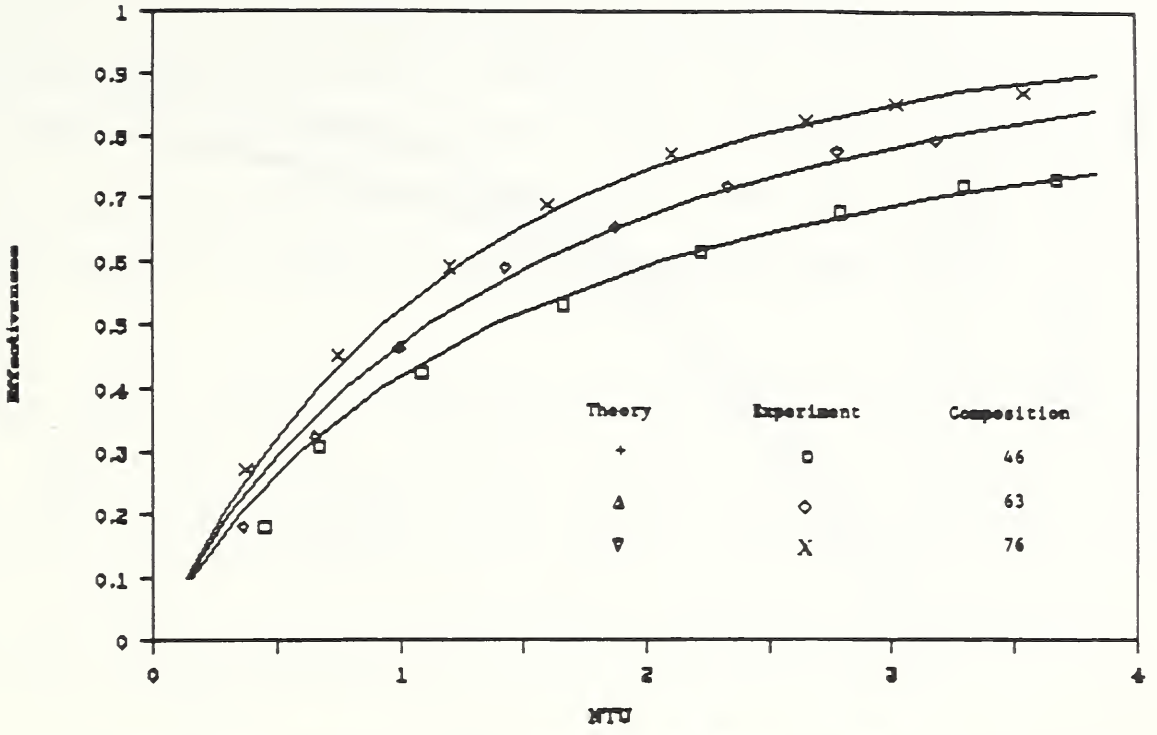

Figure 5.4 Comparison bewteen theory and experiment for a wet coil at 46%, 63%, and 76% R22 by mass.

To find out how well the model simulates heat exchanger operation in dry air, two tests were first run, both at 76% R22. One was run with dry air flowing through the heat exchanger (dew point of air was below the coldest refrigerant temperature), and the second one with moist air at standard test conditions. The experimental ϵ/NTU curves were developed for each test in a manner described earlier. The theoretical ϵ/NTU curves were calculated with the obtained experimental data. Except for the region of low effectiveness, there is a good agreement between the two sets of results (see Fig. 5.5).

Similarly, a good agreement was obtained for compositions of 83% and 91% of R22 (see Fig. 5.6). A comparison of Figs. 5.4 and 5.6 shows that for higher

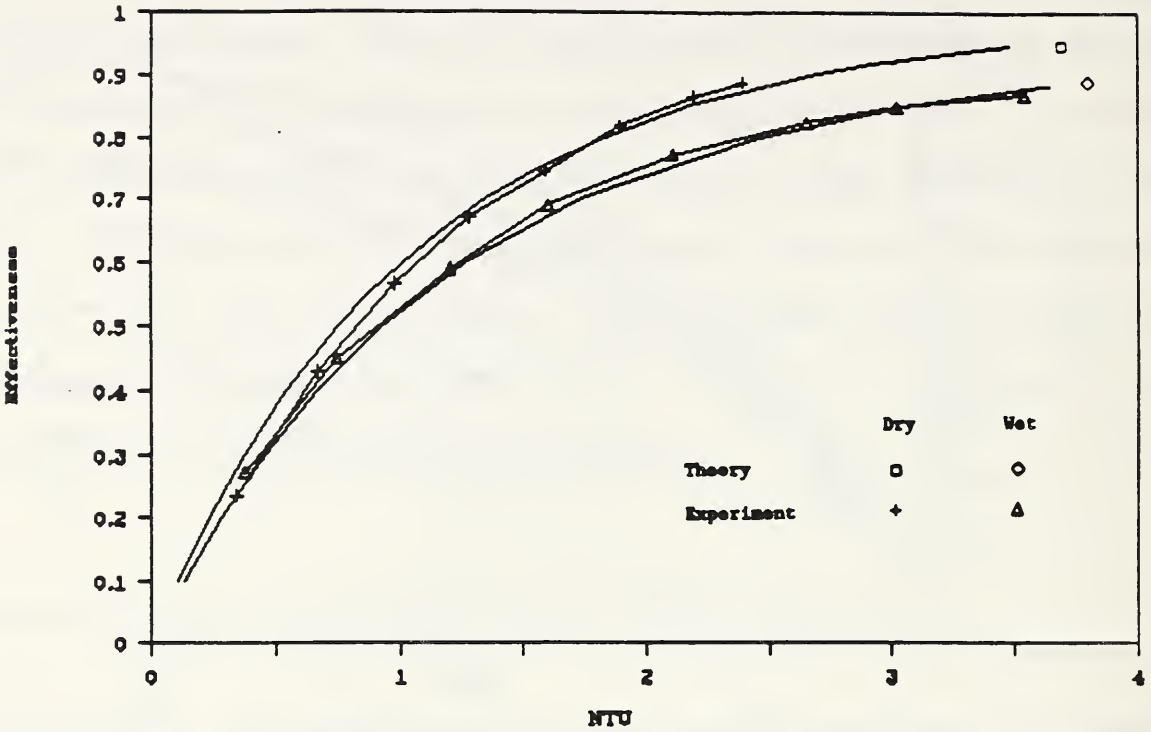

Figure 5.5 Theoretical and experimental ϵ/NTU curves for dry and wet coil at 76% R22.

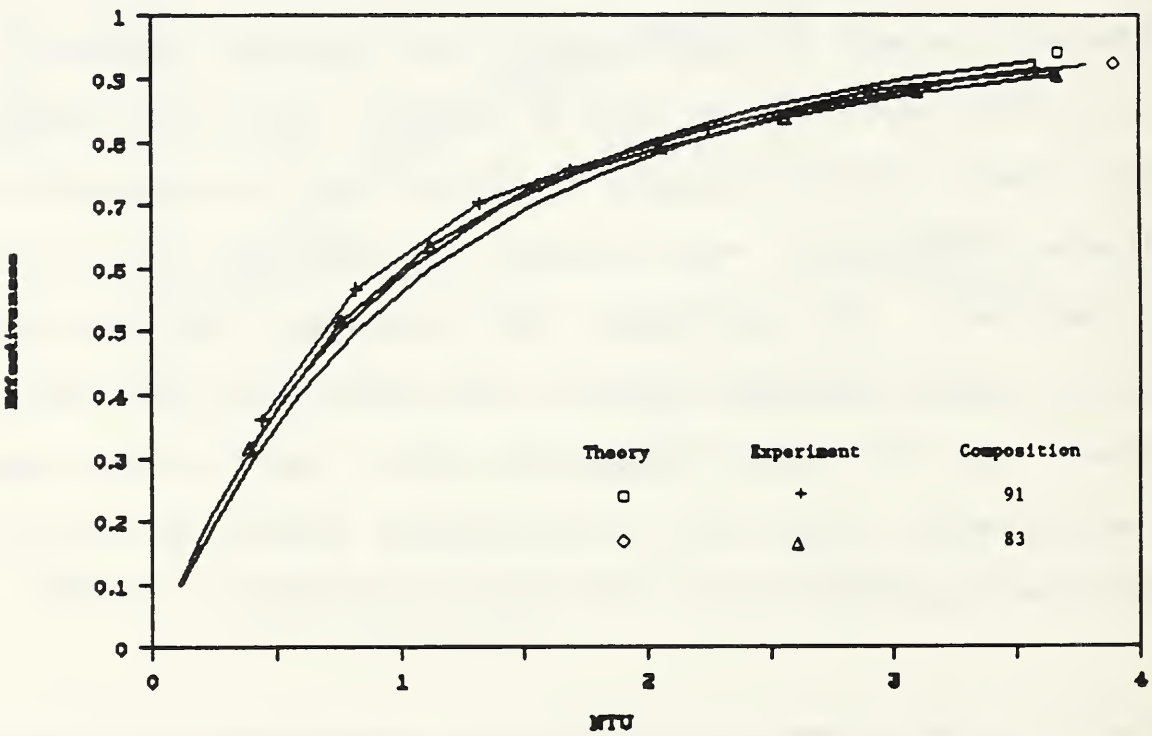

Figure 5.6 Comparison between theory and experiment for a wet coil at 83% and 91% R22.

compositions of R22, ϵ/NTU curves are closer together than for the lower R22 compositions. This means that for compositions from 75% to 100% R22, fewer ϵ/NTU curves are needed for an accurate design information. These results also show that the lower the composition of R22, the larger the heat exchanger has to be, in order to operate at the same effectiveness.

Figs. 5.7 and 5.8 present a composite of experimental and predicted ϵ/NTU curves, respectively. The ϵ/NTU curves become steeper as the amount of R22 in a mixture prevails. As a result, the highest heat exchanger effectiveness would be achieved for a pure R22 refrigerant. However, when designing a

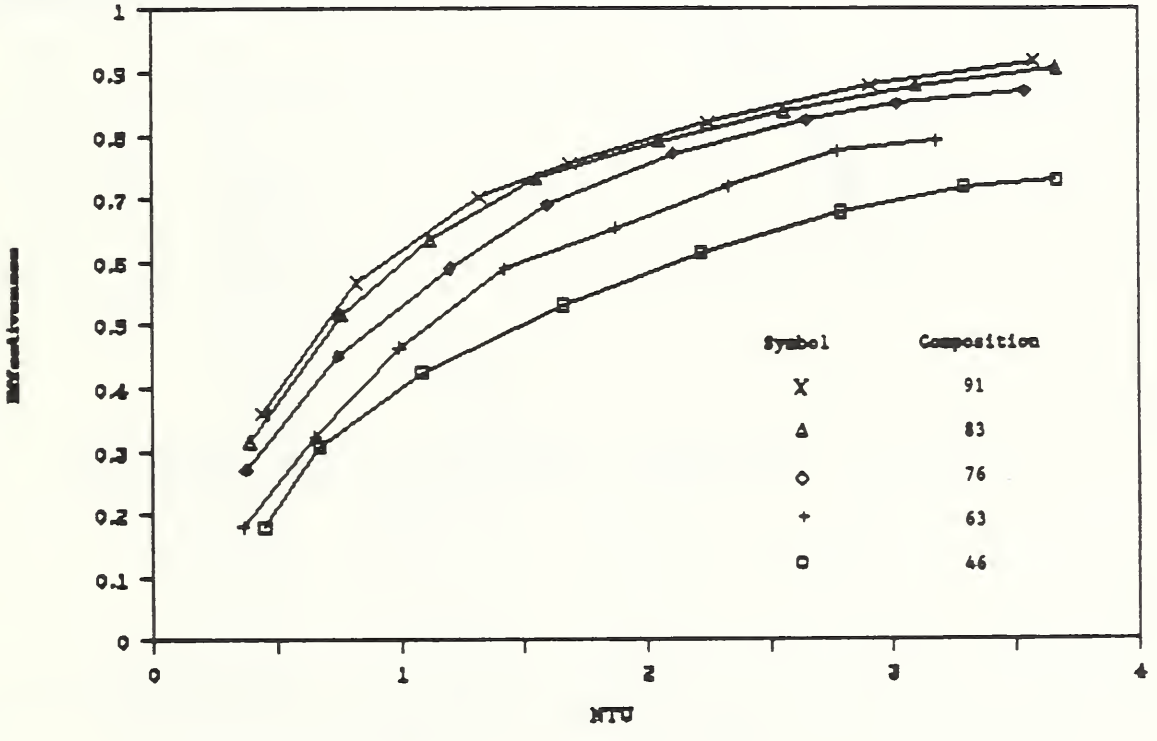

Figure 5.7 Experimental ϵ/NTU graphs for wet coil tests.

heat exchanger as a part of the air conditioning system, the system performance and a mixture effect must be taken into consideration. Figs. 3.9 through 3.13 show, that the system would best perform at 91% R22 mixture. Therefore, when designing such a heat exchanger for a maximum operational effectiveness, one can not rely only on ϵ/NTU curves.

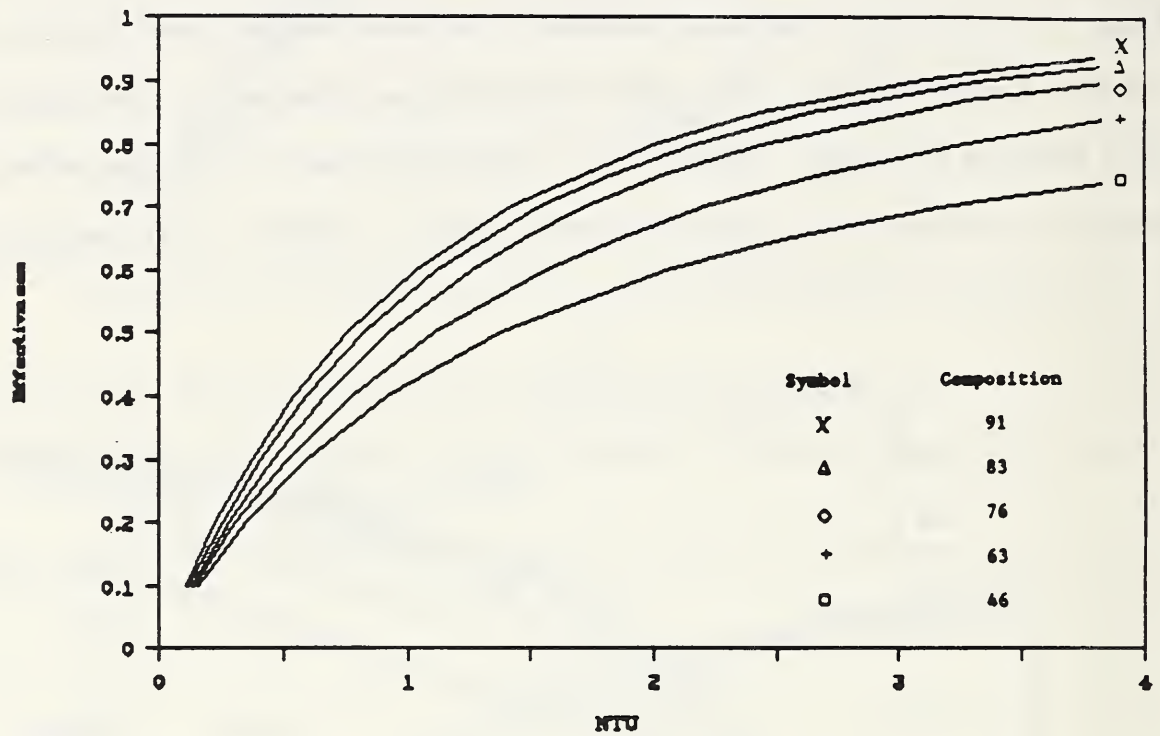

Figure 5.8 Theoretical ϵ/NTU graphs for wet coil tests.

Another implication of the use of mixtures in a heat exchanger is its size for providing the same effectiveness for different compositions. For higher compositions of R22, the size of the heat exchanger needed to operate at a certain effectiveness is smaller. Since the fluid temperatures would pinch at one point in a heat exchanger, a part of it would not be in use. For

lower compositions of R22, and for the same size of a heat exchanger, the effectiveness would be lower. To achieve a higher effectiveness for mixtures, a bigger heat exchanger should be used. This relationship can be seen in Fig. 5.9 where NTU is presented as a function of composition at temperature effectiveness of 0.7. Bars on the left represent NTU calculated at constant specific heat, bars on the right at variable specific heat. At a composition of 91% R22 in the mixture, a heat exchanger required to provide the same effectiveness would have NTU 18% greater than for 100% R22. At 46% R22 in a mixture, NTU would have to be 200% greater to result in the same effectiveness. Similarly, when LMTD method was used to verify the area of the heat exchanger for 46% R22 mixture, the area was underestimated by 20% due to the reasons explained earlier.

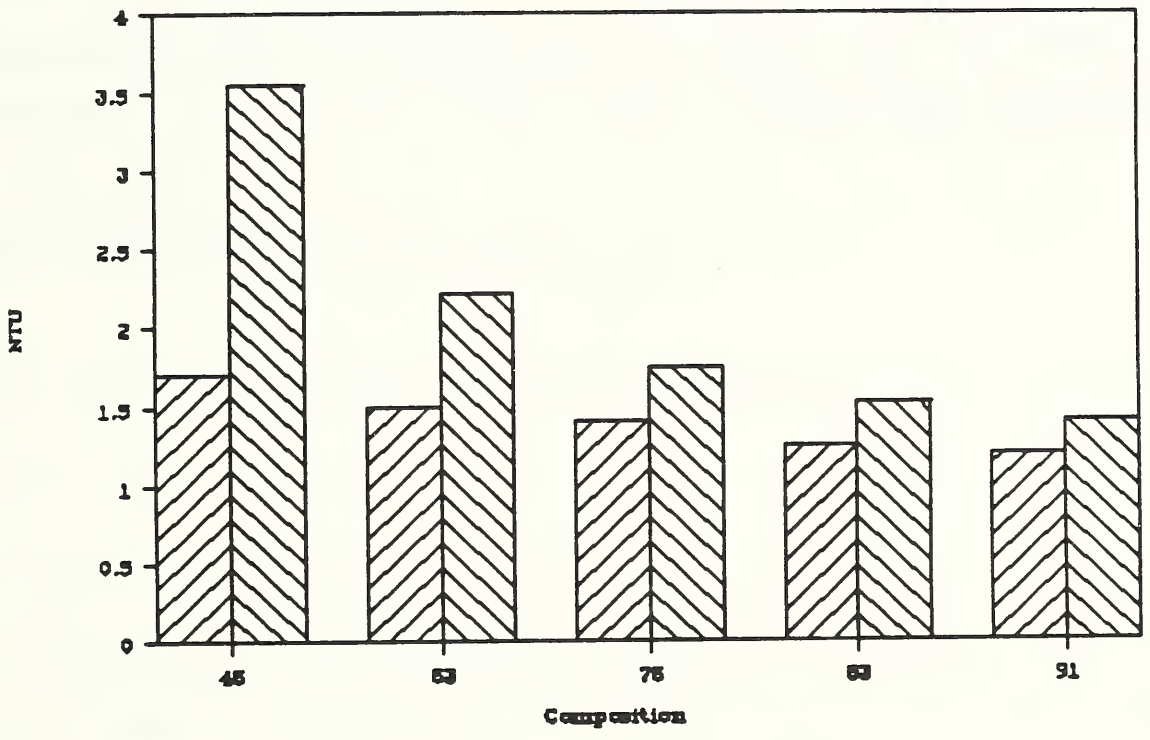

Figure 5.9 NTU as a function of mixture composition at effectiveness of 0.7, for constant and variable specific heat.

In design of heat exchangers, after the value of NTU is obtained from ϵ/NTU relation, a designer can take two approaches. One is to keep the ratio U/C_a constant and to change the area of the heat exchanger to meet the temperature drop requirement across the heat exchanger. The other, is to maintain the area constant, while changing the ratio U/C_a by adjusting the flow rate and type of heat exchanging fluids. In the study of this heat exchanger, the first option was used. It was assumed that the overall heat transfer coefficient (obtained experimentally) and the specific heat of the air were constant. It was shown in Section 3 that the experimentally derived heat transfer coefficient was known to be a constant within 25.2% for 99.7% confidence for the worst case of heat transfer. The specific heat of moist air decreased by 0.7 percent for typical test conditions and it was also assumed to be a constant. Therefore, the ratio of U/C_a approached a constant, while heat transfer area was changed for the derivation of both experimental and theoretical ϵ/NTU curves.

Section 6

DESIGN PROCEDURE FOR NONAZEOTROPIC MIXTURE HEAT EXCHANGER

To some degree, the procedure described below is similar to the design of a heat exchanger which uses a pure refrigerant. The most important is the development of the effectiveness/NTU curves which can be used for a mixture having a variable specific heat.

The design procedure is limited to the extent that it uses the experimentally derived parameters, which are applicable for this particular type of the heat exchanger configuration. Since the experiments were conducted with a particular heat exchanger, the term design will be used in a restricted sense. This means that not only the performance characteristics are completely established, but also the general type of the heat exchanger, the flow arrangement and the heat transfer surface configurations for the two fluid sides have been selected. The problem then, is to determine the dimensions of the overall heat exchanger.

The first step is to assemble the geometric characteristics of the heat transfer surfaces:

— the ratio of the free-flow area to the frontal area,
— the ratio of total transfer area on one side of the exchanger to total volume of the exchanger,
— the ratio of the fin area to the total area,
— the ratio of the wall area to the total area,

— fin thickness.

A very convenient variable to use as an iteration variable is the mass velocity G of the fluids exchanging heat. Since G is the mass flow rate divided by the cross-sectional area (related to the front area) and if it is fixed, then the frontal area is fixed as well. The complete dimensions of the heat exchanger are then established when the volume V is determined.

With initial estimates of the mass velocity on both sides, the following variables can be evaluated. The inside heat transfer coefficient is determined based on a correlation in [4]. As input data, the pressure, temperature, composition, tube diameter, heat flux are utilized to determine a localized value of the inside heat transfer coefficient. An average value of the heat transfer coefficient is assumed based on the average refrigerant quality in the heat exchanger.

The inside heat transfer coefficient is calculated from the following equation :

$$h_i = \frac{N}{C_{un}} \cdot h_{un} + C_{me} \cdot F_p \cdot h_{lo} \qquad (6.1)$$

where h_i = two-phase inside heat transfer coefficient
N = a factor due to nucleate boiling
C_{un} = Unal's correlation
C_{me} = a correction factor to include a mass transfer resistance effect in the convective evaporation region
F = heat transfer enhancement factor
h_{lo} = liquid heat transfer coefficient

In order to evaluate the forced convection heat transfer outside a flat finned tube, the total exterior surface area, A_o, the fin area, A_f, the air side heat transfer coefficient, h_o, and the fin efficiency have to be known. From the number of air side heat transfer correlations available in the literature, the one proposed by Briggs and Young [29] is most applicable here. This correlation was developed after extensive tests on 18 tube banks of different fin geometry. A regression analysis of the test data for the Reynolds number range from 1000 to 20000 yielded the following equation:

$$Nu = \frac{h_o \cdot D_0}{k_a} = 0.134 \cdot Re^{0.168} \cdot Pr^{0.333} \cdot (z/y)^{0.2} \cdot (z/t)^{0.1134} \qquad (6.2)$$

where D_o = outside tube diameter
h_o = air side mean convective heat transfer coefficient for dry air
k_a = air thermal conductivity
Pr = Prandtl number
Re = Reynolds number
t = fin thickness
y = fin height
z = distance between adjacent fins

The fin temperature effectiveness is calculated using the following equation:

$$\eta_f = \frac{\tanh (m \cdot l)}{(m \cdot l)} \qquad (6.3)$$

and the total surface temperature effectiveness from:

$$\eta_o = 1 - \frac{A_f}{A} \cdot (1 - \eta_f) \tag{6.4}$$

All the necessary components have been calculated in order to determine the overall heat transfer coefficient:

$$\frac{1}{U_o} = \frac{1}{\eta_o h_o} + \frac{a}{(A_w/A_o)\cdot k} + \frac{1}{(A_i/A_o)\cdot h_i} \tag{6.5}$$

The concept of the Number of Transfer Units can now be applied. Its basic definition is as follows:

$$NTU = \frac{U \cdot A}{C_{min}} \tag{6.6}$$

Effectiveness/NTU curves developed for a heat exchanger operating with a moist air are used to determine the outside heat transfer area. Since the terminal refrigerant and air temperatures are known, thus giving the value of effectiveness, a value of NTU can be found from the diagram for the appropriate refrigerant composition. The overall heat transfer coefficient and the capacity rate in the above equation are known as well, and the outside heat transfer area can be easily determined. The parameter α, which links the total heat transfer area and the total volume of the heat exchanger is used to calculate the volume of the heat exchanger. Thus the dimensions of the heat exchanger are determined.

The remaining step is the calculation of the pressure drop in both fluids

through the heat exchanger. The pressure drop inside the tubes for refrigerant mixture is calculated from the correlations applicable to mixtures. The often used is a correlation proposed by Pierre [30]. This correlation is based on experiments with refrigerants R12 and R22, and has the following form:

$$\Delta P = \left(f \frac{L}{D} + \frac{\Delta x}{x_m}\right) \cdot G^2 \cdot v_m \qquad (6.7)$$

where D = inner tube diameter
L = tube length
f = friction factor
x_m = mean quality
Δx = quality change
$v_m = v_L + x_m(v_v - v_L)$, mean specific volume

The correlation proposed by Pierre is in the conventional format for the single pressure drop formula. The first term of equation (6.7) is for frictional pressure drop while the second is for pressure drop due to change of momentum.

The air pressure drop is found from the following formula in Kays et.al.[26]:

$$\frac{\Delta P}{P_1} = \frac{G_2}{2g_c} \frac{v_1}{P_1} \left[(K_c + 1 - \sigma^2) + \left(\frac{v_2}{v_1} - 1\right) + f\frac{A}{A_c}\frac{v_m}{v_1} - (1 - \sigma^2 - K_e)\frac{v_2}{v_1} \right] \qquad (6.8)$$

The parameters K_c and K_e are the entrance and the exit pressure drop coefficients. The pressure drops calculated above are then compared with those specified for the design, the new estimates of the mass fluxes are

made and the procedure repeated until the pressure drops are within the established tolerance.

Section 7

SUMMARY AND RECOMMENDATIONS

The performance analysis and the preliminary design procedure for a heat exchanger, which uses nonazeotropic refrigerant mixture operating in an air conditioning experimental apparatus has been presented. This course of action was pursued, because of lack of knowledge about such heat exchanger performance and unavailability of a design procedure. The contributions provided in this work are the design of the heat exchanger, which was thoroughly analyzed to provide the understanding of its principles of operation with a nonazeotropic mixture, and the classical ϵ/NTU method which was modified and extended to include a typical air conditioning application. In the summary which follows, the major conclusions are presented together with recommendations for future work.

Summary

Special considerations in the design of the heat exchanger allowed a most exhaustive analysis to evaluate its performance. Refrigerant and air temperatures were measured and monitored for both streams, as were the fin roots temperatures. Separate moisture collecting pans for each bank helped quantify the moisture removal process and define the latent and the sensible heat profiles across the heat exchanger. The inside and the outside experimental heat transfer coefficients were obtained for each bank and for the heat exchanger.

The highest COP of the tested air-conditioner system was recorded at a

mixture composition of 91% R22 and it was 14% higher than the COP for 100% R22. Lower condenser pressure, smaller compressor friction losses, only slightly decreased cooling capacity by the addition of small quantity of R114, contributed to the best overall performance. The best performance did not occur when air and mixture glides were best matched, because of other losses which outweighed the benefits of the matched temperature glides.

The composition of the mixture strongly affected the moisture removal and the heat profiles across the heat exchanger. The lower the percentage of R22 in a mixture, the more uneven the distribution of the condensate, with the moisture accumulating at the back rows of the heat exchanger. The latent component of the total heat transferred increased for low compositions of R22 despite the fact that, the condensate profile was the most uneven in these cases.

The ability of the heat exchanger to transfer heat was also dependent on the mixture composition, which influenced the mixture temperature glide. For a low composition of R22 in the mixture (46%), its glide followed the air temperature glide, thus smoothing the heat profile across the heat exchanger. Due to the fact that, the heat transfer area and the temperature difference between air and refrigerant were constant in such a case, the heat transfer coefficient was also approached a constant value, even though the ratio of sensible and latent across the heat exchanger varied by several orders of magnitude. For the cases when air and mixture glides were not matched, the amount of heat flux across the heat exchanger varied.

Due to lower liquid thermal conductivity in mixed refrigerants as compared to pure refrigerants, the heat transfer coefficient in mixtures was significantly lower, than it would have been from weighted quantities of pure refrigerants as described by Kedzierski et. al. [31]. Even though the primary barrier to heat transfer is on the air side, for the overall heat transfer coefficient is strogly influenced by the inside heat transfer coefficient.

The value of heat transfer at an arbitrary location of the heat exchanger must be known to produce ϵ/NTU relations for a wet coil. It can be obtained by running an experiment with a given mixture composition or, alternatively, it can be determined by running a modified "tube-by-tube" model. This model is capable of estimating the value of heat transferred in any portion of the heat exchanger. Values of the heat transferred in banks are used as an input to the program which calculates NTU as a function of effectiveness.

The ϵ/NTU relationship must include appropriate physical quantities to constitute a reliable tool in a design procedure of a heat exchanger involving the use of nonazeotropic refrigerants. For a wet coil, an actual air temperature and a heat profile as a function of quality must be included into the development of ϵ/NTU relations. These relations were verified theoretically and found in good agreement for both a dry and a wet coil.

Recommendations for Future Study

This study was built upon the previous knowledge of the refrigerant mixture properties and their application in different apparatus. The research undertaken in this project extended the feasibility of applying refrigerant

mixtures in air-to-refrigerant heat exchangers in air-conditioning applications. As a result of this research project, the design procedure and the potential benefits for the use of nonazeotropic refrigerant mixtures in an air conditioning application have been demonstrated. However, the test results have shown that more research is needed into this particular application of mixtures to improve the performance of such a system.

As mentioned before, mixtures exhibit lower heat transfer coefficient and thus require a bigger heat exchanger. The analysis of the air and refrigerant glides for pure component and for mixture has shown that the heat exchanger used in this study was too small (approximately 50%) for full utilization of the mixture potential. A larger heat exchanger would bring both fluid temperature glides closer together and increase the effectiveness of the heat transfer.

The design of the tested heat exchanger was arrived at based on standard heat exchanger design practices, but it was configured by applying knowledge from studies of mixtures. The other components used in the apparatus were typical hardware elements from various manufacturers. The behavior and the performance of a mixture depends to some extent on the design of all parts of the apparatus. It is believed that the apparatus can be optimized to provide a better performance by designing for a specific mixture and composition. In addition to optimization, a simple modification of the apparatus, for example, by adding a suction line heat exchanger to reduce the pressure ratio, may prove beneficial for the studied mixture.

On a larger scale, work must continue to identify refrigerants which may be used together in a mixture. These refrigerants should be nontoxic, have beneficial refrigerating characteristics, negligible environmental impact and a low cost. A continued research effort into mixtures is needed for the purpose of a better understanding their applications and the potential of increased energy conservation.

REFERENCES

1. Mulroy, W., Didion, D.A., The Performance of Conventional Residential Sized Heat Pump Operating with a Nonazeotropic Binary Refrigerant Mixtures, NBSIR 86-3422, NBS, Gaithersburg, MD, 1986.

2. Cooper, W.D., Borchardt, H.J., The Use of Refrigerant Mixtures in Air-to-Air Heat Pumps, 15th Int. Cong. of Refrig., Venice 1979, Com. E 1.

3. Haselden, G.G., Refrigeration Cycles Providing Cooling Over a Temperature Range, Proc. Inst. of Refrigeration, 49, London, 136-141, 1952/53.

4. Jung, D.S., Horizontal Flow Boiling Heat Transfer Using Refrigerant Mixtures, EPRI ER-6364, Gaithersburg, 1989.

5. Kauffeld, M., Mulroy, W.,McLinden, M.,Didion, D.A., An Experimental Evaluation of Two Nonazeotropic Refrigerant Mixtures in a Water to Water, Breadboard Heat Pump, NBSIR, To be published, NBS, Gaithersburg, MD, 1988.

6. Pictet, R., British Patent 12, 514, 1888.

7. Blumcke, A., Uber die Bestimmung der Spezifischen Gewichte und Dampfspannung Einiger Gemische von Schwefliger Saure und Kohlensaure, Wied. Ann. 34, 10-21, 1888.

8. Maiuri, G., Nouvelles Machines a Absorption Pour Tres Basses Temperatures, British Patent 461,981 , 1929 and British Patent 494,693 , 1938.

9. Ruhemann, M., Industrial Refrigeration - New Problems and Methods, Chemical Products, Sept., 91-97, 1946.

10. Carr, F., Power Savings in Process Refrigeration, Ind. and Eng. Chem. 41, 776-780, 1949.

11. Haselden, G.G., Klimek, L., An Experimental Study of the Use of Mixed Refrigerants for Non-isothermal Refrigeration, Journal of Refrigeration, 2, 87-89, 1958.

12. Klimek L., The Refrigeration Process with Refrigerant Mixtures and Practical Application, Allg. Warmetechnik, 9, 219-224, 1968.

13. Schwind, H., Application of Binary Refrigerant Mixtures and Their Presentation in the Enthalpy-Pressure Diagram. Kaltetechnik, No. 14, 98-105, 1962.

14. McHarness, R.C., Chapman, D.D., Refrigerating Capacity and Performance Data for Various Refrigerants, Azeotropes and Mixtures, ASHRAE Journal

4, 49-58, 1962.

15. Burr, P.S., Haselden, G.G., A Non-isothermal Mixed Refrigerant Cycle or Air-conditioning Duties, The Institute of Refrigeration, London, Nov., 1974.

16. Jakobs, R., Kruse, H., The Use of Nonazeotropic Refrigerant Mixtures in Heat Pumps for Energy Saving, The International Journal of Refrigeration 2, 1979, 1, 29-33.

17. Roley, A., Meyer, C., Choffe, B., Jacq, J., Asselineau, L., Heat Pump Operating with a Fluid Mixture, New Ways to Save Energy, Commission of the European Communities International Seminar, Brussels, 1979.

18. Stokar, M., Trepp, Ch., Compression Heat Pump with Solution Circuit, Part 1: Design and Experimental Results, Rev. Int. Froid., vol. 10, 1987.

19. Radermacher,R., Vapor Compression Heat Pump Cycle with Desorber/Absorber Heat Exchange, 17th Int. Congress of Refrig., 1987.

20. Schultz,U.W, The Characteristics of Fluid Mixtures and Their Utilization in Vapor Compression Refrigeration Systems, ASHRAE Trans., Vol.2, 1985.

21. Atwood, T.,The ABCs of NARRBs (Nonazeotropic Refrigerant Blends), ASHRAE Trans., No.1, 1985 .

22. Weber, B., Effect of Composition Shift of a Binary Nonazeotropic Refrigerant Mixture on Heat Pump Performance, MS Thesis, Catholic University of America, Washington, DC, 1985.

23. Merriam, R.L., Mathias, S., Evaluation of Advanced Vapor Compression Cycles for Use with Nonazeotropic Refrigerant Mixtures, Draft Report, Oak Ridge National Laboratory, Oak Ridge, TN 37831, 1988.

24. Granryd, E., Conklin, J.C., Thermal Performance Analysis For Heat Exchangers Using Nonazeotropic Refrigerant Mixtures, ASME Winter Annual Meeting, Dallas, Texas, Nov. 25, 1990.

25. Morrison, G., McLinden, M., Application of a Hard Sphere Equation of State to Refrigerants and Refrigerant Mixtures, NBS Technical Note 1226, NBS, Gaithersburg, MD, 1986.

26. Kays, W.M., London, A.L., Compact Heat Exchangers, 3rd edition, McGraw -Hill, New York, 1984.

27. Baldwin, A.J., Planer, N.G., Nordell, D.E. and Mohan, N., Evaluation of Electrical Interference to the Induction Watthour Meter, Electric Research Power Institute, EL-2315, Palo Alto, CA, 1982.

28. Domanski, P.A., Modeling of a Heat Pump Charged with a Nonazeotropic Refrigerant Mixture, NBS Technical Note No. 1218, Gaithersburg, 1986.

29. Briggs, D.E., Young, E.H., Convection Heat Transfer and Pressure Drop of Air Flowing Across Triangular Pitch Banks of Finned Tubes, 5th AICHE/ ASME National Heat Transfer Conference, Houston, Texas, 1962.

30. Pierre, B., Flow Resistance with Boiling Refrigerants, ASHRAE Journal, September, 1964.

31. Kedzierski,M.A., Didion, D.A., Visualization of Nucleate Flow Boiling for an R22/R114 Mixture and its Components, Experimental Heat Transfer, vol. 3, p 447-463, 1990.

32. Barry, B.A., Errors in Practical Measurement in Science, Engineering and Technology, 1st edition, Wiley & Sons, New York, 1978.

Appendix A

UNCERTAINTY ANALYSIS

B.1 Introduction

This Appendix presents the analysis of the errors associated with heat transfer coefficient measurements. Errors in thermodynamic fluid properties are not considered.

B.2 Theory

Barry [32] presents a procedure for the calculation of the precision of a calculation that depends on several measurements which are subjected to individual precision. The calculated quantity (N) is a function of j independent variables, i.e.,

$$N = f(u_1, u_2, u_3, \ldots u_j) \qquad (B.2.1)$$

The u's are the measurements that are used to make the calculation of N. Each u are in error by $\pm\Delta u_1, \pm\Delta u_2, \pm\Delta u_3, \ldots, \pm\Delta u_j$. The u's are taken as three standard deviations of the statistically evaluated u's. The absolute error E_a of N is given by:

$$E_a = \Delta u_1 \, \partial f/\partial u_1 + \Delta u_2 \, \partial f/\partial u_2 + \Delta u_3 \, \partial f/\partial u_3 + \ldots. \Delta u_j \, \partial f/\partial u_j + \ldots. \qquad (B.2.2)$$

Equation (B.2.2) is the maximum possible error in the calculation of N. The root-sum square error is:

$$E_r = \{ (\Delta u_1 \, \partial f/\partial u_1)^2 + (\Delta u_2 \, \partial f/\partial u_2)^2 + \ldots + (\Delta u_j \, \partial f/\partial u_j)^2 \}^{1/2}$$

(B.2.3)

Equation (B.2.3) represents a ±3 standard deviation limit on N. Therefore 99.7% of the values of N can be expected to fall within these limits. The uncertainty percentage of the calculation of N is:

%error = (1-(N-Er)/N)*100 (B.2.4)

B.3 Precision of the Total Sensible Heat Calculation

In this sub-chapter the precisions of all measurements used to determine the air sensible heat loss were presented. The precisions of the following quantities were calculated: the specific volume of the moist air, the volumetric airflow, the air mass flow rate, the temperature difference and the sensible heat. Since the humidity ratio was a complicated function of pressure, temperature and the specific humidity, the precision of its measurement was estimated by repeatedly holding two values constant and changing the third one. Following below are the calculations of the respective accuracies.

Precision of the Specific Volume of the Moist Air Calculation

The specific volume of the moist air (v) is calculated as follows.

$$v = (R \cdot T)/p \cdot (1.+1.6078W) \quad (B.3.1)$$

where R is a gas constant, T temperature, p pressure and W humidity ratio. The following are typical values for component measurements above. These values are then used in a sample calculation of the uncertainty of the v calculation.

R = 287 kJ/kg*K

$T = 300 \pm .12$ K

$p = 101{,}325 \pm 10$ Pa

$W = 0.011346 \pm 0.001$

The partial derivatives necessary to calculate the uncertainty of v are:

$$\partial v/\partial T=(R/p)\ (1+1.6078\ W) =$$

$$=(\ 287\ J/kg\ K/101325\ N/m^2)\ (1+1.6078*.011346) = 0.865\ m^3/kgK$$

$$\partial v/\partial W=(R\ T)/p\ 1.6078 =$$

$$= 287\ J/kg\ K\ 300\ K/101325\ N/m^2\ 1.6078 = 1.37\ m^3/kg$$

$$\partial v/\partial p=-(R\ T)/p^2\ (1+1.6078\ .011346) =$$

$$=-287\ J/kg\ K\ 300\ K/101325\ N/m^2*101325\ N/m^2\ (1+1.6078\ .011346)=$$

$$= 0.865\ m^5/kg\ N$$

Substitution of the above into equation (B.2.3) results in $E_r = \pm.00042$. Therefore, the calculation of the specific volume of the moist air is precise within ±0.05% for 99.7% confidence.

Precision of the Volumetric Airflow Rate Calculation

The volumetric flow rate calculation is determined from the following relationship:

$$V = \{(2\cdot\Delta p\cdot v)/(1-(A_2/A_1)^2\} A_2 \qquad (B.3.2)$$

where A_1 is the area of the duct upstream of the nozzle, A_2 is the area of the nozzle, v is the specific volume, Δp is the pressure drop across the nozzle. The typical values used in the calculations are:

$\Delta p = 28.9 \pm .0004\ N/m^2$

$v = 0.865 \pm 0.00042\ m^3/kg$

$A_1 = 0.543\ m^2$

$A_2 = 0.0248\ m^2$

The partial derivatives necessary to calculate the uncertainty of V are:

$$\partial V/\Delta p = 0.5/(\Delta p)^{1/2}\ (2\ v/(1-(A_2/A_1))^{1/2}\ A_2 =$$

$$= 0.5/28.9^{1/2} N/m^2 \{\ 2\ 0.865 m^3/kg/(1-(.0248/.543)^2\}^{1/2}\ 0.0248 m^2 =$$

$$= 0.00327$$

$$\partial V/\partial v = 0.5/(v)^{1/2}\ (2\ \Delta p/(1-(A_2/A_1))^{1/2}\ A_2 =$$

$$= 0.5/.865^{1/2} m^3/kg \{(2\ 28.9 N/m^2/(1-(.0248/.543)^2\}^{1/2}\ 0.0248 m^2 =$$

$$= 0.1015$$

Substitution of the above partial derivatives into equation (B.2.3) results in an error of ±0.00004 in volumetric flow rate measurement. Therefore, from equation (B.2.4), the volumetric flow rate calculation is accurate within ±.023% for 99.7% certainty.

Precision the Mass Flow Rate of Air Calculation

The mass flow rate of air is determined from the following equation:

$$M_a = V/v\ (1+W) \qquad (B.3.4)$$

where V is the volumetric flow rate, v the specific volume of the moist air, W the humidity ratio. The typical values used in the calculations are:

$V = 0.163 \pm 0.00004\ m^3/s$

$v = 0.865 \pm 0.00042\ m^3/kg$

$W = 0.011346 \pm 0.001$

The partial derivatives necessary to determine the air mass flow rate are as follows:

$$\partial M_a/\partial V = 1/v \cdot (1+W) =$$

$$= 1/0.865 \cdot (1+.011346) = 1.143\ kg/m^3$$

$$\partial M_a/\partial v = V/v^2 \cdot (1+W) =$$

$$= .177/.865^2 \cdot (1+.011346) = .1863\ kg^2/sm^3$$

$$\partial Ma/\partial W = V/v \cdot (1+W)^2 =$$

$$= .177/.865 \cdot (1+.011346)^2 = 0.2\ kg/s$$

Substitution of the above into equation (B.2.3) yields .00022. Therefore, from equation (B.2.4), the mass flow rate calculation is precise within 0.001% for 99.7% confidence.

Precision of Temperature Difference Calculation

The air temperature difference across the evaporator coil is:

$$\Delta T = T_i - T_o \qquad (B.3.5)$$

The entering air temperature was typically 300 ±0.12K, a typical value for the air temperature leaving the coil was 286 ±.12K.The partial derivatives necessary to calculate the precision of the ΔT calculation are $\partial \Delta T/\partial T_i = 1$

and $\partial\Delta T/\partial T_o = -1$. Evaluation of the Equation (B.2.4) yields the precision of the temperature calculation as ±0.51% for 99.7% confidence.

Precision of the Total Sensible Heat Rate Calculation

The total sensible heat transfer rate was calculated as follows.

$$Q_s = M_a \cdot c_p \cdot \Delta T \qquad (B.3.6)$$

where M_a is the mass flow rate of air, c_p a specific heat of air and ΔT a temperature change of the air across the heat exchanger. The following typical values were used.

$M_a = .202 \pm .00022$ kg/s

$c_p = 1004$ J/kg K

$\Delta T = 14.22 \pm 0.51$K

The partial derivatives necessary to calculate the precision of the Q_s calculation are:

$\partial Q_s/\partial M_a = c_p \cdot \Delta T = 1004 \cdot 14.22 = 14277$ J/kg

$\partial Q_s/\partial \Delta T = M_a \cdot c_p = 0.202 \cdot 1004 = 202.81$ J/K s

Substitution of the above into equation (B.2.3) yields 103 W. Therefore, from equation (B.2.4), the total sensible heat calculation is precise within 3.56% for 99.7% confidence.

B.4 Precision of the Total Latent Heat Calculation

Following below is the calculation of the precision of the total latent heat calculation and the latent enthalpy.

Precision of the Moist Air Enthalpy Calculation

The moist air enthalpy (h_{fg}) was calculated from the equation representing linear fit of the tabularized air properties.

$$h_{fg} = -2.29 \cdot T + 2499.73 \qquad (B.4.1)$$

The calculated standard deviation of the air temperature was typically σ_a=0.12. Three standard deviations were used in the calculations. The partial derivative of enthalpy with respect to temperature is:

$\partial h_{fg}/\partial T = -2.29$

Substitution of the above in the equation (B.2.3) yields 0.82. Therefore, from equation (B.2.4), the moist air enthalpy is precise within 0.03% for 99.7% confidence.

Precision of the Total Latent Enthalpy Calculation

The total latent enthalpy was calculated from the following equation:

$$Q_l = m_w \cdot h_{fg} \qquad (B.4.2)$$

The following are typical values for component measurements. These values were used in the calculation of the uncertainty of the Q_l calculation.

$m_w = 0.00042 \pm 2.22*10^{-6}$ kg/s

$h_{fg} = 2470 \pm 0.82$ KJ/kg

The partial derivatives necessary to calculate the error in determination of the latent load were:

$\partial Q1/\partial m_w = h_{fg}$ = 2470 kJ/kg

$\partial Q_1/\partial h_{fg} = m_w$ = 0.00042 kg/s

Substitution of the above in the equation (B.2.3) yields 0.0055. Therefore, from equation (B.2.4), the latent heat calculation was precise within 0.001% for 99.7% confidence.

B.5 Precision of the Total Heat Calculation

The total heat transferred is the sum of the sensible and the latent loads. The following are typical values for component measurements. These values are then used in a sample calculation of the uncertainty of the Q calculation.

Q_s = 2684 ± 103 W

Q_l = 1037 ± .0055 W

Calculating the partial derivatives and substituting into equation (B.2.3) results in E_r = ±103 W. Substitution of E_r and Q = 3721 W for N in equation (B.2.4) yields 2.69 %. Therefore, the total heat transferred calculation is precise within ±2.69 % for 99.7 % confidence.

B.6 Precision of the Total Heat Transfer Calculation for One Bank

Following below is the calculation of all component uncertainties for the calculation of the total heat transfer coefficient for one bank. First, the precision of the total heat calculation for one bank is performed followed by the precision of calculation of inside and outside heat transfer coefficient coefficients. Finally, the precision of the total heat transfer coefficient

is determined.

Precision of the Total Heat Calculation for One Bank

The total heat transferred to one bank is also a sum of both the sensible and the latent portions. The following equations apply:

$$Q = Q_s + Q_l \qquad \text{(B.6.1)}$$

$$Q_s = M_a \cdot c_p \cdot \Delta T \qquad \text{(B.6.2)}$$

$$Q_l = m_w \cdot h_{fg} \qquad \text{(B.6.3)}$$

The partial derivatives for each of the heat equation component are:

$\partial Q_s/\partial M_a$ = .24 kJ/kgK 5K =1.2 kJ/kg

$\partial Q_s/\partial \Delta T$ = .24 kJ/kgK 0.202 kg/s = 0.048 kJ/sK

$\partial Q_l/\partial m_w$ = 2470 kJ/kg

$\partial Q_l/\partial h_{fg}$ = -0.00011

Substitution of the above partial derivatives into equation (B.2.3) results in an error of ±0.0246 for sensible and ±.00548 for latent heat calculation. Since for total heat calculation the partial derivatives are unity, the above error values are substituted into equation (B.2.3) to obtain an error of ±0.024. Substitution of this into equation (B.2.4) yields total heat calculation for one bank to be precise within 0.002%.

Precision of the Inside Heat Transfer Coefficient Calculation

Inside heat transfer coefficient was calculated from the following equation:

$$h_i = Q_b/A_{bi} \cdot \Delta T \qquad \text{(B.6.4)}$$

where Q_b is heat transferred to a bank, A_{bi} is the inside heat transfer area of a bank and ΔT is temperature difference between fin and refrigerant. Typical values used in the calculations are:

$Q_b = 944 \pm 0.0246$ W

$A_{bi} = 0.1598$ m^2

$\Delta T = 4.48 \pm 1.38$ K

The uncertainty in the ΔT was obtained from the error analysis of the temperature difference between fin and refrigerant. The inside heat transfer area is assumed to be known exactly. The partial derivatives of the inside heat transfer coefficient are as follows:

$\partial h_i/\partial Q = 1/A_{bi}\ \Delta T = 1/0.1598\ m^2\ 4.48\ K = 1.396\ 1/m^2K$

$\partial h_i/\partial \Delta T = - Q_b/Ab_i \cdot \Delta T^2 = 1204\ W/0.1598\ m^2\ 4.48^2K = 375\ W/m^2K$

Substitution of the above into equation (B.2.3) yields ± 517.5 W/m^2K. Therefore, from equation (B.2.4), the inside heat transfer coefficient calculation is precise within 20.9% for 99.7% confidence.

Precision of the Outside Heat Transfer Coefficient Calculation

The outside heat transfer coefficient is calculated using the same type of the equation as for the inside heat transfer coefficient. A_{bo} is the outside heat transfer area, and ΔT is the temperature difference between air and refrigerant. Similarly, the partial derivatives yield the following values:

$\partial h_o/\partial Q_o = 0.055\ 1/m^2K$

$\partial h_o/\partial \Delta T = 1.36\ W/m^2K$

Substituting the above into equation (B.2.3) yields 1.06 W/m^2K. Therefore, from equation (B.2.4) calculation of the outside heat transfer coefficient is precise within 2.6% for 99.7% confidence.

Precision of the Total Heat Transfer Coefficient Calculation

The following equation is utilized to calculate the total heat transfer coefficient for one bank:

$$h = h_i \cdot R_a \cdot h_o/(h_o+h_i \cdot R_a) \qquad (B.6.5)$$

where R_a is the ratio of the inside heat transfer area to the outside heat transfer area for one bank.

The partial derivatives necessary to calculate the uncertainty are:

$$\partial h/\partial h_i = R_a \cdot h_o^2/(h_o+h_i \cdot R_a)^2 =$$

$$= 0.04388 \cdot 40.21^2\ W/m^2K/(40.21W/m^2K+2465W/m^2K \cdot 0.04388)^2 =$$

$$= 0.00322$$

$$\partial h/\partial h_o = (h_i \cdot R_a)^2/(h_o + h_i \cdot R_a)^2 =$$

$$= (2465W/m^2K \cdot 0.04388)^2/(40.21W/m^2K+2465W/m^2K \cdot 0.04388)^2 =$$

$$= 0.53$$

Substituting the above into equation (B.2.3) yields the error $\pm 1.76\ W/m^2K$.

Therefore, substituting E_r and h = 29.31 W/m^2K into equation (B.2.4) yields 6.% precision for 99.7% confidence.

Appendix B

SIMPLIFIED HEAT EXCHANGER OPERATING WITH NONAZEOTROPIC MIXTURE R22/R114

The purpose of this appendix is to illustrate the use of derived ϵ-NTU relations for a heat exchanger, in which moist air exchanges heat with a refrigerant mixture. A simplified design procedure shows how a heat transfer area of a heat exchanger may be determined if ϵ-NTU curves have already been calculated using equation (4.31). An example calculation is presented for a mixture composition of 46% R22 by mass, typical inlet and outlet air temperatures and mass flow rate. The following information is provided for the design of the heat exchanger:

Air side:

Flow rate: 1502 lbm/h (680 kg/h)

Inlet temperature: 80°F DB/67°F WB

Outlet temperature: 55°F

Refrigerant side:

Flow rate: 190 lbm/h (86.3 kg/h)

Inlet temperature: 46°F (7.8°C)

Outlet temperature: 69°F (20.6°C)

Also known are the geometric parameters for the heat exchanger used in this study:

Fin thickness t=0.01" (0.00025 m)

Fin height y=0.3125" (0.0079 m)

Distance between adjacent fins z=0.066" (0.0017 m)

Tube diameter D_o=0.375" (0.0095 m)

Heat exchanger width W=18" (0.457 m)

Heat exchanger height H=12" (0.305 m)

Modified equation (6.5), disregarding tube wall resistance, is applied to determine the overall heat transfer coefficient:

$$\frac{1}{U_o} = \frac{1}{\eta_o h_o} + \frac{1}{(A_i/A_o)h_i}$$

The equation (6.2) is used to find the outside heat transfer coefficient, h_o:

$$Nu = \frac{h_o \cdot D_o}{k_a} = 0.134\ (Re)^{0.681} \cdot Pr^{.333} \cdot (z/y)^{.2} \cdot (z/t)^{0.1134}$$

where for air inlet conditions, Pr=0.7. Reynolds number is calculated based on the tube diameter and the mass flux across the unobstructed area.

$$Re = \frac{D_o \cdot G}{\mu}$$

The mass flux, G, is determined by dividing the mass flow rate of air by the unobstructed air passage through the evaporator face.

For G=1476 lbm/h·ft^2

A=116 in^2

μ=0.0448 lbm/ft·h

D_o=0.375 in

the Reynolds number is 1030 for this specific case. By substituting the appropriate quantities into equation for Nusselt number, it becomes equal to 13.72.

For D_o=0.375 in

k_a=0.015 Btu/h·ft°F

the air side heat transfer coefficient equals 6.58 Btu/h·ft^2·F. The fin temperature effectiveness can be calculated using equation (6.3).

For h=6.58 Btu/h·ft^2·F

δ=0.01 in

k=100 Btu/h·ft·F

then $m=2\cdot h/k\cdot\delta$, m=12.57

For l=0.3125 in , η_f=0.966

The total surface temperature effectiveness is evaluated with the use of equation (6.4). For a unit ratio of A_f/A=0.8896/0.962 and the above calculated value of fin temperature effectiveness, η_o=0.963.

The inside heat transfer coefficient is calculated with the use of the correlation derived by Jung [4]. This correlation takes into consideration both nucleate and convective boiling. By using average values of refrigerant mixture properties in an evaporator, the inside heat transfer coefficient equals h_i=300 Btu/h·ft^2·F.

The overall heat transfer coefficient may now be calculated and it equals U=4.28. For the given temperatures of air and refrigerant, ϵ=0.735. Going

to Fig. 5.9, for a curve representing 46% R22 by mass, NTU=3.75. From the definition of the NTU, using appropriate values of the air specific heat and mass flow rate, the outside heat transfer area for this heat exchanger equals A=315 ft^2, which is close to the actual value of 312 ft^2. This value represents an estimate of the size of a heat exchanger necessary for the desired temperature effectiveness. To ensure that pressure drops are not excessive, equations (6.7) and (6.8) are applied for refrigerant and air side, respectively. These calculations are omitted in this example. The procedure outlined above, may be used for calculating the size of a heat transfer area of a heat exchanger with a mixture as an operating fluid.

NIST-114A
(REV. 3-89)

U.S. DEPARTMENT OF COMMERCE
NATIONAL INSTITUTE OF STANDARDS AND TECHNOLOGY

BIBLIOGRAPHIC DATA SHEET

1. PUBLICATION OR REPORT NUMBER
NISTIR 4723

2. PERFORMING ORGANIZATION REPORT NUMBER

3. PUBLICATION DATE
NOVEMBER 1991

4. TITLE AND SUBTITLE
Evaporator Performance Investigation for Residential Air-Conditioning Applications Using Mixed Refrigerants

5. AUTHOR(S)
Maciej Chwalowski

6. PERFORMING ORGANIZATION (IF JOINT OR OTHER THAN NIST, SEE INSTRUCTIONS)
U.S. DEPARTMENT OF COMMERCE
NATIONAL INSTITUTE OF STANDARDS AND TECHNOLOGY
GAITHERSBURG, MD 20899

7. CONTRACT/GRANT NUMBER

8. TYPE OF REPORT AND PERIOD COVERED

9. SPONSORING ORGANIZATION NAME AND COMPLETE ADDRESS (STREET, CITY, STATE, ZIP)
Electric Power Research Institute
3412 Hillview Avenue
Palo Alto, CA 94304

10. SUPPLEMENTARY NOTES

[ ] DOCUMENT DESCRIBES A COMPUTER PROGRAM; SF-185, FIPS SOFTWARE SUMMARY, IS ATTACHED.

11. ABSTRACT (A 200-WORD OR LESS FACTUAL SUMMARY OF MOST SIGNIFICANT INFORMATION. IF DOCUMENT INCLUDES A SIGNIFICANT BIBLIOGRAPHY OR LITERATURE SURVEY, MENTION IT HERE.)

The design of the heat exchanger utilizing nonazeotropic refrigerant in an air conditioning application presents unique problems due to the phase change of the moist air and the variable specific heat of the evaporating refrigerant mixture. This study discusses the performance analysis and the design procedure of a cross counterflow heat exchanger working as an evaporator in an experimental system which simulated a residential air conditioning application.

The effect of the change of the mixture composition on heat exchanger performance was evaluated.

The focus of the theoretical study was the development of the effectiveness/NTU (ϵ/NTU) relationships with the use of the experimentally derived quantities for moist air flowing across the heat exchanger. Variable mixture specific heat, air and heat profiles obtained from the experimental results were utilized to obtain the expression for ϵ/NTU. The derived ϵ/NTU relations were verified and found to be in good agreement with test results.

12. KEY WORDS (6 TO 12 ENTRIES; ALPHABETICAL ORDER; CAPITALIZE ONLY PROPER NAMES; AND SEPARATE KEY WORDS BY SEMICOLONS)
air-conditioning; effectiveness; evaporator; mixture; nonazeotropic; NTU; profile; refrigerant

13. AVAILABILITY

[X] UNLIMITED

[ ] FOR OFFICIAL DISTRIBUTION. DO NOT RELEASE TO NATIONAL TECHNICAL INFORMATION SERVICE (NTIS).

[ ] ORDER FROM SUPERINTENDENT OF DOCUMENTS, U.S. GOVERNMENT PRINTING OFFICE, WASHINGTON, DC 20402.

[X] ORDER FROM NATIONAL TECHNICAL INFORMATION SERVICE (NTIS), SPRINGFIELD, VA 22161.

14. NUMBER OF PRINTED PAGES
147

15. PRICE
A07

ELECTRONIC FORM